USE OF AN ALLELIC SERIES IN MOUSE TO STUDY THE ROLE OF EPIDERMAL GROWTH FACTOR RECEPTOR IN PLACENTAL DEVELOPMENT AND PREGNANCY

Jennifer Clore Dackor

A dissertation submitted to the faculty of the University of North Carolina at Chapel Hill in partial fulfillment of the requirements for the degree of Doctor of Philosophy in the Curriculum in Genetics and Molecular Biology.

Chapel Hill
2008

Approved by:

David W. Threadgill

Victoria L. Bautch

Scott Bultman

Kathleen Caron

Steven Young

ABSTRACT

JENNIFER DACKOR: Use of an allelic series in mouse to study the role of epidermal growth factor receptor in placental development and pregnancy
(Under the direction of David W. Threadgill)

Epidermal growth factor receptor (EGFR) is a member of the ERBB family of receptor tyrosine kinases that has been shown to play an important developmental and physiological role in many aspects of pregnancy. Using genetically engineered mice our lab and others have demonstrated that *Egfr*^{tm1Mag} nullizygous placentas exhibit strain-specific defects ranging from mild reductions in spongiotrophoblasts to severe labyrinth dysmorphogenesis that results in mid-gestational embryonic lethality. Experiments included in this dissertation show that *Egfr*^{tm1Mag} nullizygous placentas have reduced numbers of proliferating trophoblast. However, intercrosses with mice deficient for cell cycle checkpoint genes did not rescue *Egfr*^{tm1Mag} embryo viability suggesting that reduced proliferation in the placenta is not a primary cause of embryonic lethality.

We characterized an *Egfr* allelic series on several genetic backgrounds in mice to assess the effects of reduced as well as increased EGFR signaling on placental and embryonic growth. Congenic strains homozygous for the hypomorphic *Egfr*^{wa2} allele exhibited strain-dependent placental and embryonic growth restriction at 15.5 dpc while heterozygotes for the antimorphic *Egfr*^{Wa5} allele had placentas were only slightly reduced in size with no effect on embryonic growth. At the histological level *Egfr*^{wa2} homozygous placentas had a reduced layer of spongiotrophoblast and in some strains spongiotrophoblasts

and glycogen cells were almost completely absent. The placentas of embryos heterozygous or homozygous for the hypermorphic *Egfr*^{Dsk5} allele were enlarged with a more prominent spongiotrophoblast layer and increased expression of glycogen cell-specific genes. There were no effects on growth of *Egfr*^{Dsk5} embryos at 15.5 dpc. We also observed strain-specific sub-fertility in *Egfr*^{Dsk5} heterozygous adult females that may be due deferred embryo implantation beyond the normal window of uterine receptivity.

Our results demonstrate that EGFR plays a fundamental role in development of the placental spongiotrophoblast layer in mice and suggest that reduced proliferation in EGFR-deficient placentas primarily affects the spongiotrophoblast compartment. We have also shown that aberrant levels of EGFR signaling result in an extensive level of genetic background-dependent phenotypic variability and that EGFR expressed in the uterine stroma may function in preparation of the uterus for embryo implantation.

ACKNOWLEDGMENTS

I could not have completed this work without the unwavering support of my parents, my siblings, my husband, my classmates, and my labmates. Since childhood my parents have fostered in me a passion for education and learning in combination with a solid work ethic. I cannot thank them enough for the moral and financial support they have provided me throughout my life as a student. I also want to thank my thoughtful sister for her patience with me as graduate school became difficult. I am so glad that we were able to attend UNC at the same time and I will cherish the memories from those four years we spent in Chapel Hill together. She is the best friend I have ever had and I don't think I could have finished this work without her enthusiastic encouragement. My husband has been the bright spot in every single day for me and no matter how hard or stressful things have become I have always been able to go home and laugh with Ryan. I also owe gratitude to the excellent people in my graduate school class as we held each other up during the good times and bad. And finally I have been so fortunate to be surrounded by the many wonderful people in the Threadgill lab. Working with these folks has been a pleasure everyday.

TABLE OF CONTENTS

LIST OF TABLES

TABLE

LIST OF FIGURES

FIGURE

LIST OF ABBREVIATIONS

Areg	amphiregulin
Btc	betacellulin
BrdU	bromodeoxyuridine
BSA	bovine serum albumin
Ctsq	cathepsin Q
Cx31	connexin 31
Ct	cycle threshold
cdkn	cyclin dependent kinase inhibitor
Dsk5	Darkskin-5
dpc	days post coitus
Dlx3	distal-less homeobox 3
e	embryonic day
EPC	ectoplacental cone
Eomes	Eomesodermin
Egf	epidermal growth factor
Egfr	epidermal growth factor receptor
Epgn	epigen
Ereg	epiregulin
Esrrb	estrogen related receptor beta
Esx1	extraembryonic spermatogenesis homeobox 1
EVT	extravillous trophoblast

Gcm1	glial cells missing 1
Glut3	glucose transporter 3
GT	glycogen trophoblast
Gm52	gene model 52
Gusb	glucuronidase beta
H&E	hematoxylin and eosin
Hbegf	heparin binding EGF-like growth factor
ICM	inner cell mass
IUGR	intra-uterine growth restriction
IP	intraperitoneal
Jz	junctional zone
Lz	labyrinth zone
LE	luminal epithelium
Mash2	achaete-scute complex homolog 2
Mb	Megabase
Nrg	neuregulin
PAS	Periodic acid-Schiff
PBS	phosphate buffered saline
PCR	polymerase chain reaction
Pdch12	protocadherin-12
Pl1	placental lactogen 1
QTL	quantitative trait loci
Rb	retinoblastoma gene

RPA	ribonuclease protection assay
SNP	single nucleotide polymorphism
SpT	spongiotrophoblast
SynT	syncytiotrophoblast
TBST	tris buffered saline with Tween 20
Tcfeb	transcription factor EB
Timp2	tissue inhibitor of metalloproteinase 2
Tgfa	transforming growth factor alpha
TG	trophoblast giant cell
TS	trophoblast stem cell
TUNEL	terminal deoxynucleotidyl transferase mediated dUTP nick end labeling
wa2	waved-2
Wa5	Waved-5
WT	wild-type

CHAPTER I

EPIDERMAL GROWTH FACTOR RECEPTOR SIGNALING IN MOUSE AND HUMAN PLACENTAL DEVELOPMENT

Introduction

Proper formation of a functional placenta is essential for normal growth and development of mammalian embryos. The placenta is composed of highly specialized cells, called trophoblasts that initiate and regulate feto-maternal exchange of nutrients, gas and wastes. In addition, trophoblasts provide the fetus with a barrier to the maternal immune system and modulate maternal response to pregnancy through secretion of various cytokines. The mature mouse placenta consists of three distinct layers including the maternally-derived decidua, which lies in direct contact with the uterus and two embryonically-derived layers, the junctional zone (Jz), composed of trophoblast giant cells and spongiotrophoblast, and the labyrinth zone (Lz). Knock-out and transgenic mice have revealed that a large number of genes are required for normal placental development. To date over 100 mouse models have been reported to exhibit placental abnormalities with many resulting in embryonic lethality or intra-uterine growth restriction (IUGR). Development of both the tetraploid aggregation technique and trophoblast-specific Cre recombinase mouse lines has allowed further delineation of genes required for development of extra-embryonic tissue versus the embryo proper.

Using genetically engineered mice our lab and others have demonstrated that during embryogenesis the prototypical member of the ERBB family of receptor tyrosine kinases, epidermal growth factor receptor (EGFR), is required for establishment of a functional placenta [1-4]. Embryos deficient for EGFR exhibit IUGR and/or mid-gestational lethality due to defects in trophoblast-derived compartments of the placenta [2]. The EGFR nullizygous placenta may be a useful model to study placental insufficiency in humans, however, cellular and molecular origins of the phenotype remain to be determined. This chapter will focus on mouse placental development and highlight the potential roles of ERBB receptors and ligands in both mouse and human placentation.

ERBB Receptors: Mechanisms of Signaling Diversity, Specificity, and Control

During embryonic development cell fate is frequently determined by spatial and temporal cues that originate from adjacent, or in some cases, distant tissue. Under these circumstances cell communication is often facilitated through the use of transmembrane receptors that "sense" stimuli in the external environment and then transduce the signal intracellularly to promote an appropriate biological response. One well-studied family of transmembrane receptors is the ERBB receptor tyrosine kinases comprised of four family members, EGFR (ERBB1), ERBB2 (HER2/Neu), ERBB3 (HER3), and ERBB4 (HER4) [5]. Activation of ERBB receptors is ligand-induced and results in a number of cellular effects including cell survival, growth, proliferation, differentiation, migration, and invasion. Accordingly ERBBs have been shown to be indispensable for the embryonic and postnatal development of a broad array of tissues and involved in progression of several human cancers.

Activated ERBB receptors function as ligand-bound dimers, with EGFR and ERRB4 being autonomous family members that can transduce signals as homodimers and as heterodimers with ERBB2, ERBB3, or each other. Both EGFR and ERBB4 possess an extracellular ligand-binding region consisting of domains I-IV, a single-pass transmembrane domain, as well as a cytoplasmic domain with tyrosine kinase activity and multiple phosphotyrosine docking sites for molecular effectors that initiate downstream signaling events [6]. ERBB2 and ERBB3 exhibit highly conserved sequence and structural similarity to EGFR and ERBB4 but can only function in heterodimeric complexes with other ERBB family members since ERBB2 has no known ligand and ERBB3 has a catalytically inactive kinase domain [7,8].

Eleven distinct ligands have been identified that bind ERBB receptors and they fall into three classes. Epidermal growth factor (EGF), transforming growth factor alpha (TGFA), amphiregulin (AREG), and epigen (EPGN) exclusively bind EGFR [9]. Betacellulin (BTC), heparin binding EGF-like growth factor/diphtheria toxin receptor (HBEGF) and epiregulin (EREG) bind both EGFR and ERBB4 while Neuregulins 1-4, characterized by numerous splice variants, bind ERBB3 and/or ERBB4 [6]. The ligands are present as membrane-bound precursors that undergo metalloprotease-mediated cleavage and ectodomain shedding into a mature form, although receptor activation by membrane-associated ligand has been reported [10,11]. Activation of FZD-, estrogen-, and G-protein-coupled receptors is known to transactivate the ERBBs by stimulating ectodomain shedding of ligands [12,13]. ERBB ligands all share an EGF-like domain that is required, as well as sufficient, for interactions with a binding pocket formed by the extracellular receptor domains I and II [14,15]. Unexpectedly, crystal structures of activated EGFR revealed that

dimerization occurs in a back-to-back orientation resulting in the ligand-binding domains being situated on opposed ends of the complex [16]. This data suggests that ERBB dimers are stabilized through receptor-receptor contacts rather than by interactions between two ligand molecules.

Active and inactive conformations of EGFR are distinguished by intramolecular interactions between extracellular domains I- IV that determine availability of the ligand-binding site [17]. Interactions between domains II and IV hold the receptor in a tethered, inactive position that is unable to bind ligand or dimerize with other receptors [18]. However, an untethered extended conformation of EGFR is able to dimerize and bind ligand resulting in a stabilized active structure [16]. In wildtype cells EGFR exists in equilibrium between its tethered and extended conformations. Equilibrium favors the inactive form so that approximately 95% of total cellular EGFR exists in the tethered conformation, demonstrating the importance of this structural mechanism in regulating EGFR signaling [18]. Interestingly, crystal structures of the ligand-impaired ERBB2 show that it exists primarily in an extended conformation allowing ERBB2 to dimerize much more efficiently than the other ERBBs [19]. This explains observations suggesting that ERBB2 is a potent amplifier of ERBB signaling.

Unlike most other tyrosine kinases, ERBB receptors do not require phosphorylation for kinase activation [20]. Consequently ERBB kinase activity must be tightly controlled by some other mechanism since the kinase itself is in a constitutively "on" state. Similar to inhibitory mechanisms that regulate binding of ligand to the extracellular region of EGFR, the cytoplasmic domain exists primarily in an inactive conformation due to intramolecular interactions between the C-terminal tail and the kinase domain [21]. Upon ligand binding a

rotation of the transmembrane domain occurs and as a result the cytoplasmic domain is reoriented so that the kinase is no longer inhibited by the C-terminus. When the active conformation is stabilized phosphorylation of the receptor's dimerization partner proceeds. Crystallography data indicates that active ERBB dimers are asymmetric due to positioning of the C-terminus of one receptor in proximity of the kinase domain of the other [22]. This structural evidence confirms previous data suggesting that phosphorylation of ERBB dimers occur in trans.

Specificity of downstream signaling is determined primarily by substrate binding to phospho-tyrosine residues on the cytosolic tail of ERBB receptors [23]. Each family member is characterized by its own unique combination of docking sites for adaptor proteins that assemble multi-component signaling complexes as well as sites that directly regulate enzyme activity. EGFR and ERBB4 exhibit similar substrate preference with multiple binding sites for the adaptors SHC and GRB2, both involved in establishing the RAS-MAP kinase cascade. Both receptors have also been shown to bind and activate STAT5. It has been noted that EGFR and ERBB4 are rarely co-expressed, which is not surprising, given the redundancy of their signaling capabilities. EGFR is unique in its binding site for the ubiquitin ligase CBL, which negatively regulates signaling by facilitating lysosomal degradation of the receptor [23,24]. ERBB2, with the fewest phospho-tyrosine residues, contains docking sites for GRB2, SHC, SRC, and a unique site for DOKR, an adaptor shown to negatively regulate MAP kinase signal transduction [25]. ERBB3 is distinct from the other ERBBs in that it is enriched with docking sites for the p85 subunit of phosphoinositide 3-kinase (PI3K) [26]. The PI3K-AKT pathway promotes cell survival through suppression of pro-apoptotic proteins such as Caspase 6, BAD and MDM2 suggesting that ERBB

regulation of cell survival may occur primarily through ERBB3. Ultimately, many factors determine how a cell responds to activation of the ERBB family of receptors. Ligand expression and processing, hetero- or homodimerization of receptors and substrate preference as dictated by both specific phospho-tyrosine docking sites and the milieu of downstream effectors expressed in the cell all influence how ERBB signaling is interpreted.

All four ERBB receptors are essential for mammalian development since mice deficient for any single ERBB do not survive to reproductive age and rarely survive embryogenesis. ERBB2, ERBB3 and ERBB4 are indispensable for embryonic development of the heart and nervous system and in adult animals these family members play a role in mammary gland morphogenesis and lactation [27]. EGFR is also required for development of the nervous system but in contrast to other ERBB knockouts, EGFR null mice display pronounced phenotypes in epithelial structures of the skin, lung, pancreas, kidney, intestine and placenta [1,3,4]. Abnormal placental development results in mid- to late-gestational lethality of EGFR null embryos but the phenotype is strain-dependent. Strains such as 129 and BALB/c die around 11.0 days post-coitus (dpc) and show severe reductions in labyrinth and spongiotrophoblast layers. Some hybrid genetic backgrounds and the outbred stock CD-1 show varying degrees of spongiotrophoblast reduction but embryos survive until birth and succumb to strain-independent neurodegeneration before weaning age [2-4]. Tetraploid aggregation experiments in EGFR-deficient mice have demonstrated that EGFR is required in the extra-embryonic tissue and that embryonic lethality is attributed to failure in developing a functional placenta [2,4].

Placental Development in Mouse

In mouse embryos the first extra-embryonic cells, called trophectoderm, are specified at 3.5 dpc, during the 16-cell stage. At this time the blastocyst segregates into a polarized layer of outer trophectoderm cells surrounding an inner cell mass (ICM), which will eventually give rise to the embryo proper [28]. Further differentiation of the trophoblast lineage ensues at 4.5 dpc when mural trophectoderm, located on the opposite pole from the ICM, differentiates into primary trophoblast giant cells (TG). These polyploid trophoblasts facilitate the process of implantation at 4.5 dpc by invading through maternal luminal epithelium (LE) to establish a secure connection between uterus and embryo. Decidualization of stromal cells surrounding the implantation site, uterine immune cell activity, development of the maternal uterine vasculature, and blood flow to the embryo are all influenced by cytokines and hormonal signals produced by TG cells [29].

Following implantation, differentiation of cells that will form the placenta continues as polar trophectoderm, the trophoblasts in contact with ICM, proliferate and give rise to the extraembryonic ectoderm (ExE) and the ectoplacental cone (EPC) [28]. The ExE contains a pool of pluripotent trophoblast stem cells (TS) that are maintained in a proliferative state by signals from the ICM and eventually it will form the chorion and later labyrinth trophoblasts. The EPC contains progenitors of spongiotrophoblast (SpT) and secondary TG [30]. Concurrent with differentiation of polar trophectoderm the ICM segregates into several lineages, including extraembryonic mesoderm that will form the allantois and give rise to the vascular portion of the Lz [31].

Labyrinth formation is initiated at 8.5 dpc when the allantois and chorion fuse, and folds in the chorion permit penetration of embryonic mesoderm [32]. Extensive branching of

chorionic villi and associated fetal vessels eventually create an elaborate placental vascular network where fetal and maternal exchange occurs. The chorionic villi maintain a diffusional barrier between maternal and fetal blood cells composed of three layers of differentiated trophoblasts and a layer of fetal endothelium [32]. A discontinuous layer of mononuclear trophoblasts lines the maternal sinusoids and two continuous layers of multinucleate syncytiotrophoblasts (SynT) lie between the mononuclear trophoblasts and fetal endothelium. Maternal blood enters the labyrinth via canals entirely lined with trophoblasts rather than maternal endothelium [33]. Maternal spiral arteries that traverse the decidua and converge within the junctional zone supply these canals. The maternal spiral arteries are partially lined by endovascular TG cells and devoid of smooth muscle, allowing extreme dilation for increased blood flow towards the placenta.

From 9.5 to 16.5 dpc, coincident with branching morphogenesis of chorionic villi, the SpT of the junctional zone expand rapidly, providing structural support for the growing labyrinth [30]. Trophoblasts on the outer periphery of the Jz and in contact with maternal decidua differentiate into secondary TG cells while invasive glycogen trophoblasts (GC) arise from the pool of SpT around 10.5 dpc. Glycogen cells migrate through the Jz and invade decidual stroma in the area surrounding maternal arteries. The function of GC is unknown but they may serve as a source of energy for the embryo during late gestation by releasing glucose directly into maternal blood that circulates back into the placenta [34]. An endocrine role of SpT and TG cells has been suggested since they secrete hormones, lactogens and cytokines that potentially mediate various physiological adaptations of pregnancy [29]. In particular, TG cells produce angiogenic factors, VEGF, proliferin and nitric oxide, as well as the vasodilator, adrenomedullin (ADM). Interestingly, SpT express

an anti-angiogenic factor, FLT1, that may limit invasion of maternal vasculature into the placenta. TG and SpT lineages also express lactogenic hormones of the prolactin/placental lactogen family, known to regulate mammary gland development and corpus luteum maintenance [35].

Molecular Control of Trophoblast Differentiation in Mouse

Placental defects identified in transgenic mice and experiments using isolated TS cells in culture have provided significant clues to the molecular control of trophoblast biology and placental development. TS cells derived from mouse blastocysts have been shown to differentiate into all trophoblast cell types identified in the placenta (Figure 1) and can be maintained in culture supplemented with Fibroblast growth factor 4 (FGF4) and either Activin, Nodal, or Transforming growth factor beta (TGFB) ligands [36-38]. *In vivo*, FGF signaling is critical for trophectoderm maintenance since knockouts for both *Fgf4* and fibroblast growth factor 2 receptor (*Fgfr2*) die during the peri-implantation period with a loss of trophoblasts [39,40]. FGF4 is secreted by ICM and FGF2R is present in the trophectoderm supporting a role for the ICM in promoting proliferation in adjacent polar trophectoderm [41,42]. There is evidence of an *in vivo* requirement for Nodal in TS cell pluripotency as well since embryos homozygous for a hypomorphic allele of Nodal die at 9.5 dpc due to a loss of labyrinth and spongiotrophoblast [43]. An *in vivo* role for Activin and/or TGFB in TS cell maintenance has not reported.

Blastocysts null for caudal type homeobox 2 (*Cdx2*), the earliest *in vivo* marker of trophoblast specification, fail to implant due to a block in trophectoderm differentiation [44]. CDX2 has been shown to suppress genes required for maintenance of ICM pluripotency,

including *Oct4,* and over-expression of CDX2 in mouse embryonic stem (ES) cells is sufficient to transform ES cells into trophoblast [45,46]. Similarly, blastocysts null for eomesodermin homolog (*Eomes*), and transcription factor AP-2 gamma (*Tcfap2c*) fail to form trophoblastic outgrowths in culture [47,48]. *In vivo* these embryos implant but die before mid-gestation due to impairment of differentiation and/or proliferation of cells in the ExE. Embryos deficient for estrogen related receptor beta (*Esrrb*), an orphan receptor expressed specifically in the ExE, fail to form labyrinth and spongiotrophoblasts resulting in embryonic lethality at 9.5 dpc [49]. Expression of *Cdx2*, *Eomes* and *Esrrb* is sustained in TS cultures supplemented with FGF4 and Activin, Nodal or TGFB but down-regulated upon TS differentiation supporting their role in TS pluripotency, proliferation and maintenance [36,37]. FGF4 supplementation has also been shown to suppress mammalian achaete scute-like homologue 2 (*Mash2*), a transcription factor required for SpT differentiation [37].

In the developing mouse placenta TS cells reside in the ExE which eventually becomes the chorion and fuses with the allantois to form the labyrinth compartment. Failure of chorio-allantic attachment is a phenotype resulting in embryonic lethality at 8.5 – 10.5 dpc and has been described in a considerable number of transgenic mice including knockouts for alpha 4 integrin (*Itga4*), Cyclin F (*Ccnf)*, and *Wnt7b* [50-52]. An even larger number of genes have been shown to play a role in labyrinth morphogenesis. More than 60 mouse models exhibit a small, under-branched labyrinth compartment but the precise role of most of these genes in trophoblast differentiation and labyrinth formation has not been determined [53]. Broad categories of molecules known to be involved in formation of the labyrinth include the signaling pathways WNT/FRZ, FGF, EGF and HGF, as well as many MAPK signaling cascade components. In addition, nuclear receptor signaling components such as

peroxisome proliferators-activating receptor gamma (PPARG) have been shown to be involved [54].

The transcription factor Glial cells missing-1 (*Gcm1*) is the most well-studied gene required for labyrinth morphogenesis and is one of the first genes required to initiate villi branching and differentiation of labyrinth trophoblasts. *Gcm1* is expressed in clusters of chorionic trophoblasts at sites where the allantois will invade and branch to form the primary villious structures [55]. In *Gcm1* null embryos the chorion remains flat after chorio-allantoic fusion rather than folding to form the primary chorionic villi [55]. Additionally, Gcm1 expression has been found to be necessary for differentiation of cultured TS cells into SynT, although over-expression of *Gcm1* is not sufficient to override FGF signaling and induce differentiation of TS cells into SynT [55,56]. GCM1 may regulate SynT differentiation through transcriptional control of sequences encoding highly fusogenic retroviral envelope proteins known to promote syncytium formation in human trophoblasts [57]. Recently, murine homologs of these retroviral elements, syncytin A and B, were identified and found to be expressed specifically in the labyrinth compartment of the placenta [58]. Binding sites for GCM1 are found in the promoter region of both syncytin genes and *in vitro* experiments showed that functionally these genes are involved in cell-cell fusion [59]. Furthermore, knockdown of syncytin A mRNA in TS cells or treatment of cells with syncytin A antibodies inhibits TS cell fusion and differentation into SynT.

In addition to SynT that compose chorionic villi there are two mononuclear trophoblast lineages present in the labyrinth. Trophoblasts adjacent to the syncytium and lining the maternal sinusoids exhibit characteristics of trophoblast giant cells; they are polyploidy and express placental lactogen 2 (*Pl2*) [60]. However these sinusoidal

trophoblasts seem to represent a distinct lineage of TG cells because they do not arise from *Tbpba*-expressing cells in the EPC and are unique in their expression of cathepsin gene Q (*Cstq*). Clusters of proliferative trophoblasts that express markers of TS cells such as *Eomes* are scattered throughout the labyrinth and may act as a stem cell source for the developing villous structures [61]. Embryos null for retinoblastoma protein (*Rb1*) die by 14.5 dpc due to an expansion of *Eomes*-positive clusters that interfere with morphogenesis of the Lz [61].

Spongiotrophoblasts are another trophoblast cell type frequently affected in knockout mice. The number of genes controlling differentiation and expansion of this compartment is probably many more than reported in the literature since embryo growth and/or viability is not always affected by reductions in SpT. Trophoblast specific protein alpha (*Tpbpa*) is the most commonly used SpT marker since it is expressed specifically and abundantly in EPC and SpT, but the function of TPBPA is unknown [62]. In experiments with knockout mice and cultured TS cells, the basic helix-loop-helix (bHLH) transcription factor MASH2 has consistently been shown to play an essential role in SpT proliferation, differentiation and/or maintenance. *Mash2* is expressed in both chorion and EPC and placentas from *Mash2* null embryos display a complete lack of SpT, an excess of TG cells, as well as a reduced labyrinth layer [63]. Since bHLH transcription factors are known to function as dimers it has been suggested that MASH2 becomes active through dimerization with ALF1 and/or ITF2, two bHLH family members co-expressed in SpT [64]. Two dominant negative bHLH proteins, inhibitor of DNA binding 1 (*Id1*) and *Id2* are expressed in the labyrinth where they may function to inhibit *Mash2* [65]. *Id1* and *Id2* are down-regulated during differentiation of mouse TS cells and the rat Rcho-1 trophoblast stem cell line [36,66].

Further characterization of the *Mash2* null placental phenotype has led to the hypothesis that signals from SpT or their precursors in the EPC are required for proper labyrinth development. In tetraploid aggregation experiments Rosa26-positive/*Mash2* null cells and Rosa26-negative/*Mash2* wildtype cells were used to generate chimeric extra-embryonic tissue [67]. *Mash2* null cells differentiated into TG cells and also contributed to the labyrinth portion of the placenta but were completely absent from the SpT layer. Although standard *Mash2* null embryos exhibit defects in labyrinth morphogenesis, chimeras with a labyrinth composed predominantly of *Mash2* null trophoblast showed normal development of the Lz. This data demonstrates that MASH2 is required cell autonomously in the SpT layer and suggests that development of the Lz may be dependent on SpT formation. An interdependence of these layers during placental development is further supported by the fact that a number mouse models exhibiting reductions in SpT also show defects in labyrinth morphogenesis.

The lineage of glycogen trophoblasts has just recently been elucidated, but the molecular pathways regulating their differentiation are not well understood. GC arise from *Tpbpa*-positive cells in the ectoplacental cone and can be identified by their clear vacuolated-appearing cytoplasm as well as their expression of Protocadherin-12 (*Pcdh12*) that begins as early as 7.5 dpc [68]. Mice that lack expression of the imprinted gene, insulin-like growth factor 2 (*Igf2*), are one of the few models described that exhibit reductions specifically of GC without reduction of SpT [69]. Interestingly, mice deficient in expression of another imprinted gene, cyclin dependent kinase inhibitor $p57^{kip2}$ (*Cdkn1c*), show an expansion of SpT but not GC suggesting that CDNK1C is also involved in differentiation of GC [70].

Trophoblast giant cell fate is considered a "default" trophoblast differentiation pathway since removal of factors required for TS cell pluripotency is sufficient to induce TG formation [36-38,56]. TG cells transiently express markers of the SpT lineage (*Tpbpa, Mash2*) before becoming terminally differentiated, but these transcripts are absent in mature TG cell cultures and *in vivo* TG [63,71]. Several genes have been shown to promote or inhibit TG cell development including suppressor of cytokine signaling 3 (*Socs3)*, leukemia inhibitory factor receptor (*Lifr)*, peroxisome proliferator-activated receptor beta/delta (*Pparb/Ppard*), and a bHLH anatagonist, *Imfa* [72-74]. In addition, treating TS cell cultures with retinoic acid or overexpressing the bHLH transcription factor *Stra13* results in TG transformation [56,75]. The most well-studied gene required for TG differentiation is the bHLH transcription factor, heart and neural crest derivatives expressed transcript 1 (*Hand1*). *Hand1* knock-out embryos die at 7.5 dpc, most likely as a consequence of dramatic reductions in TG cells [76]. Recently, a detailed study of TG markers revealed the existence of at least 4 different polyploid TG cell subtypes, all expressing *Hand1* [60]. TG cells lining spiral arteries were shown to express proliferin (*Plf*), TG cells lining canals in the Jz express *Plf* and *Pl2*, TG cells in the labyrinth (mononuclear trophoblast of the villi) express *Pl2* and *Ctsq*, while the TG cells lining the implantation site express *Plf*, *Pl2*, placental lactogen-1 (*Pl1*). Marker analysis revealed that all four TG subtypes are present in differentiated TS cultures and TS cells from *Hand1* knockouts fail to differentiate into any of the TG lineages [60].

Mouse Versus Human Placentation: Similarities and Disparities

The generation and analysis of transgenic mice has provided an unanticipated wealth of information concerning the genes and pathways involved in placental development that could not have been obtained using human tissue alone. Our understanding of human placentation has arisen mainly from experiments using cultured cells or post-mortem tissue and there have been relatively few studies linking gene mutations or polymorphisms to placental dysfunction. Fortunately, the mouse placenta is an appropriate model for understanding human placentation since human and mouse placentas have comparable structure with analogous cell types shown to express the same or similar molecular markers [77,78].

The human placenta is composed of zones of trophoblasts comparable to the mouse Lz and Jz. The human floating chorionic villi and mouse labyrinth are functionally analogous and both regions contain cell types that express markers of undifferentiated, proliferative trophoblasts as well as differentiated multinucleate SynTs. Langhans cells, also called villous cytotrophoblast, are analogous to chorionic trophoblast in the mouse and similarly express *ID2* and *TCFAP2C* [79,80]. These genes are down-regulated upon cytotrophoblast differentiation. Human and mouse SynT both express the markers transcriptional enhancer factor-5 (*TEF5*), *GLUT1*, and *GCM1* [55,81-83]. SynT fusion in humans is controlled by retroviral envelope proteins syncytin-1 and -2 and homologous fusogenic syncytin proteins are expressed in mouse placenta [58,84,85]. In addition, compound heterozygous mice for null alleles of *Sp1* and *Sp3*, zinc finger transcription factors induced during syncytium formation in humans, exhibit trophoblast defects in the labyrinth [86,87]. In humans a layer of extravillous trophoblast extending from the chorionic villi to

the decidua basalis and traversed by channels of maternal blood plays a structural role similar to the mouse Jz. Called columnar trophoblast or anchoring villi, cells in this layer express *Mash2* homolog, *HASH2*, suggesting that human and mouse counterparts have similar origin and function [83,88].

There are also important differences in the structure and function of human placenta compared to mouse [78]. The overall shape of the placenta in both species is similar but human villous branching is less extensive, terminating in a blunt-ended tree-like pattern, compared to the interconnected maze-like structure of the mouse labyrinth. Human and mouse placentae are both considered haemochorial since feto-maternal exchange occurs by direct contact between maternal blood and fetal chorionic trophoblasts. However, the fetal and maternal interface in human is separated by a single layer of SynTs (monochorial) while the trichorial mouse chorionic villi consists of a single layer of mononuclear trophoblast overlying two layers of SynTs.

Maternal blood in the human placenta is supplied directly to the villous space via a large number of channels originating from over 100 maternal arteries that traverse the placental bed [78]. In contrast, maternal spiral arteries in the mouse decidium converge to form a small number of central canal spaces that traverse the Jz and empty into the labyrinth [33]. The extent of trophoblast invasion through maternal arteries and uterine stroma differs as well. In mouse, endovascular invasion of maternal arteries by TG cells occurs by 10.5 dpc, prior to intersitial invasion of the stroma. Endovascular invasion extends into the decidua only 20 -30 cell diameters from the periphery of the placenta, whereas trophoblast invasion of human maternal arteries extends beyond the deciduas basalis and into the myometrium [33,89]. Interstitial invasion occurs prior to endovascular invasion in humans

and interstitial trophoblasts penetrate deeper than in mouse, extending through the decidua basalis into the inner third of the myometrium [33,90,91]. In humans, interstitial extravillous trophoblast are thought to initiate the loss of smooth muscle surrounding the spiral arteries, while uterine NK-cells mediate this process in mouse.

Based on molecular comparisons of invasive trophoblasts in mouse and human, analogies between cell types remain unclear. Functionally, endovascular extravillous trophoblasts resemble mouse canal and spiral artery-associated TG cells, but molecular similarities between these cell types are not apparent. A subset of invasive cells are polyploid in humans but these cells accumulate 4-8 N DNA content versus the 1000 N+ DNA of mouse TG [92]. Importantly, *HAND1* is not expressed in the human placenta and human giant cells probably originate from cell fusion rather than endoreduplication, suggesting that they are not of the same origin as mouse TG cells [83]. Similar to mouse glycogen cell differentiation from spongiotrophoblast, human extravillous interstitial trophoblast arise from precursors in the proximal region of trophoblast columns [93]. However, pathways that control differentiation and invasion of interstitial trophoblast in humans and glycogen cells in mice have not been described, making it unclear whether these cell types are related.

EGFR in Normal and Abnormal Placental Development

The ERBB family of receptors and their ligands are widely expressed in both human and mouse placenta (summarized in Table 1) [94-108]. Immunostaining of human placental sections and experiments with cultured human trophoblast cell lines indicate that EGFR, in particular, is important for trophoblast growth, differentiation, and function. Interestingly,

only EGFR is expressed in proliferating, undifferentiated populations of trophoblasts, while terminally differentiated trophoblasts (SynT, EVT, TG) express all four ERBBs [95,97,100,101,104,105]. Activating EGFR in cultured trophoblasts by addition of exogenous EGF ligand promotes both trophoblast proliferation as well as differentiation of syncytiotrophoblast and extravillous trophoblast [109-112]. EGF stimulates secretion of PLI in day 7 mouse placenta cultures, suggesting it regulates differentiation of TG cells in mice [112]. The EGFR ligand, TGFA, also induces proliferation of human trophoblasts but, in contrast to EGF, it inhibits secretion of PL1 in mouse placenta cultures [113]. HBEGF, an EGFR/ERBB4 ligand, has been shown to induce differentiation and motility of extravillous trophoblasts as well as inhibit apoptosis in human trophoblasts cultured in low oxygen conditions [114,115]. In low oxygen conditions expression of HBEGF was found to be dependent on ERBB signaling, evidence that a positive feedback loop regulates cell survival in this context [114].

Aberrant EGFR signaling in placental tissue has been associated with several human pregnancy complications. Pre-eclampsia, a hypertensive disorder that can endanger the lives of both mother and fetus, is associated with shallow invasion of trophoblasts into the spiral arteries and HBEGF expression is severely reduced in these placentas [116]. Another condition, placenta accrete, puts a mother at risk for hemorrhage during delivery due to abnormally deep uterine invasion by trophoblast and is associated with reduced levels of ERBB2 but increased EGFR [117,118]. Perhaps most noteworthy are the numerous studies that show lower EGFR expression or phosphorylation in placentas of fetuses affected by IUGR, one of the most common conditions to complicate pregnancy. IUGR affects 4-6% of all pregnancies and is the second leading cause of perinatal death [119-123].

IUGR is most frequently associated with inadequate placental function, resulting in compromised nutrient and oxygen transport from mother to fetus [124]. A recent study of 310 stillborn births found low birth weight represented in 78.7% of the cases and placental alterations were considered to be causative in 45.8% of the intrauterine deaths [125]. IUGR can have serious consequences for the fetus, including impaired development of the lungs, heart, pancreas and brain [126]. Unfortunately, complications associated with IUGR may continue far beyond a newborn's first months of life. At five years of age cognitive ability is more likely to be compromised in children exposed to placental insufficiency *in utero* [127]. As adults their chances of developing type II diabetes, coronary artery disease, hypertension, and stroke are significantly higher than for adults born with a normal birth weight [128-131]. This phenomenon is not well understood, but one hypothesis proposes that these effects are a result of the developmental programming of fetal organs in response to intrauterine stress. Specifically, experimental evidence suggests that reduction in cell number, changes in distribution of cell types, and resetting of hormonal feedback can occur in organs of growth-restricted fetuses [132,133]. Despite the immense impact of IUGR on human health and quality of life, our understanding of the origins of this disease is limited. The significance of EGFR signaling in IUGR has not been determined in humans but studies in the mouse strongly suggest that reduced EGFR activation may be causative of abnormal placental development leading to IUGR.

Although gene-targeting studies have demonstrated that EGFR is essential for normal placental development in the mouse, molecular mechanisms giving rise to the phenotype have not been described. There is no evidence that a single pathway downstream of EGFR regulates placental development. Instead, it is likely that several independent and/or

interacting pathways are involved since placental defects have been reported in knockout mice for a number of molecules known to transduce signals from activated EGFR (Table 2). These include molecular scaffolds, GAB1 and GRB2; the guanine nucleotide exchange factor, SOS1; as well as numerous map kinase cascade molecules and transcriptional activators [86,134-151]. AKT1, a protein kinase in the PI3K pathway that regulates cell cycle progression and apoptosis, is also essential for placental development [152]. Many of these models exhibit placental defects that vary depending on genetic background, similar to the EGFR-deficient mouse. It is not surprising that polymorphic loci can influence a developmental process regulated by such a complex signaling network.

In conclusion, data from studies in both human and mouse underscore the importance of EGFR and the ERBB family of receptors in placentation. However, important questions remain concerning the relationship between EGFR and the etiology of diseases of human pregnancy, such as IUGR. Mouse models have demonstrated that genetic background determines the consequences of EGFR deficiency in placental development suggesting that human placental insufficiency may have a complex genetic origin. An allelic series of EGFR has now been generated in mouse allowing further characterization of placental phenotypes caused by aberrant levels of EGFR signaling that may be relevant to human conditions. Additionally, experiments using TS cell lines derived from EGFR mutant mice will help determine the precise role of EGFR in trophoblast proliferation, differentiation, survival and invasion.

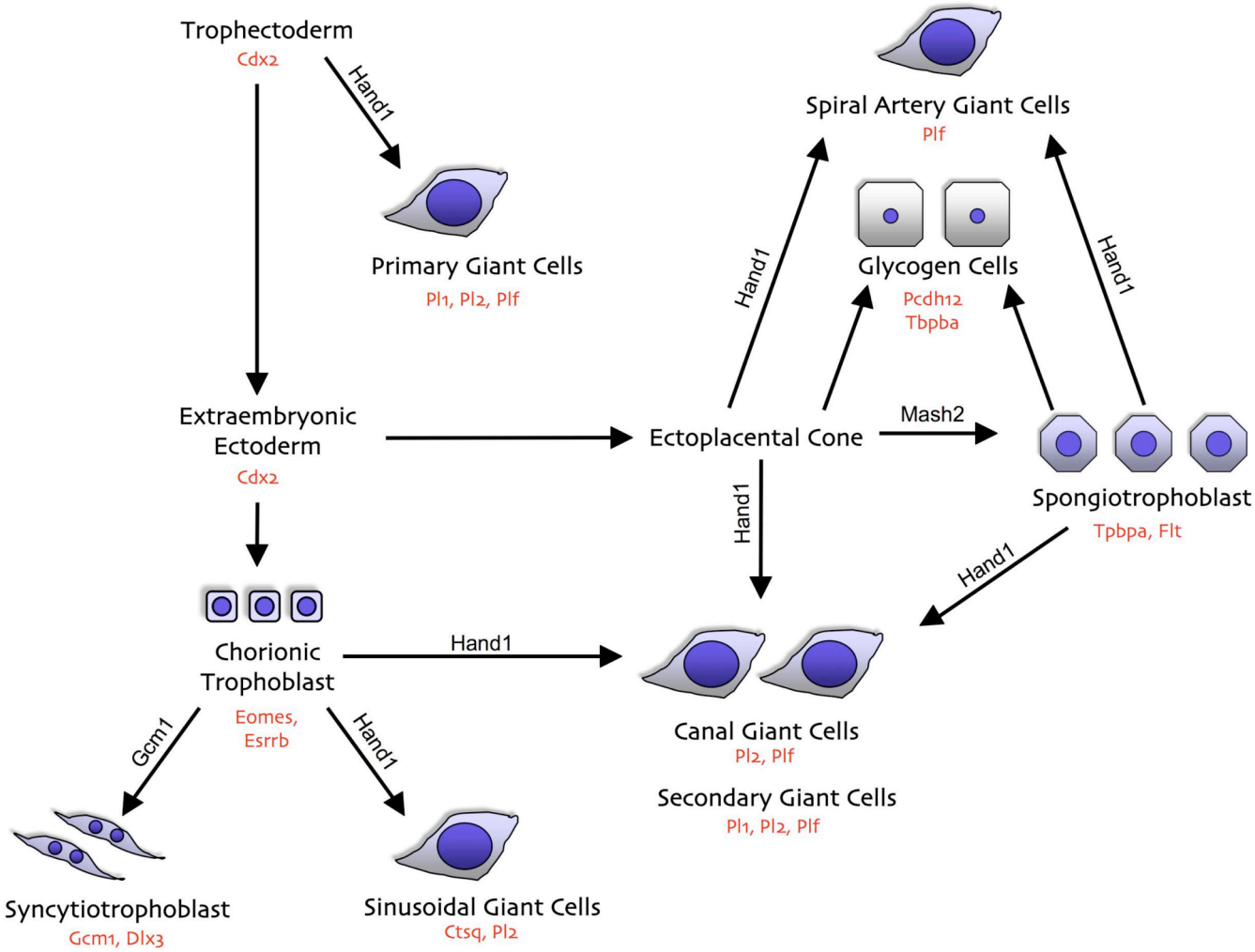

Figure 1. Molecular control of mouse trophoblast cell subtype differentiation. Note the potential of trophoblast stem cell-bearing trophectoderm (upper left) to differentiate into all trophoblast subtypes. Also, five subtypes of *Hand1* expressing trophoblast giant cells are found throughout the mouse placenta.

Table 1. Expression of ERBB receptors and ligands in human and mouse trophoblasts

		HUMAN EXPRESSION	Reference	MOUSE EXPRESSION	Reference
Receptors	EGFR	villous cytotrophoblast, syncytiotrophoblast, extravillous trophoblast: proximal column, placental bed giant cells	Jokhi PP 1994, Muhlhauser J 1993	labyrinth, spongiotrophoblast, trophoblast giant cells	Dackor J 2007
	ERBB2	syncytiotrophoblast, extravillous trophoblast: distal column, endovascular, placental bed giant cells	Jokhi PP 1994, Muhlhauser J 1993	primary trophoblast giant cells (mRNA)	Lim H 1997
	ERBB3	placenta (mRNA only)	Lee H 1998	trophoblast giant cells	Dackor J 2007
	ERBB4	syncytiotrophoblast, extravillous trophoblast	Tanimura K 2004	trophoblast giant cells	Dackor J 2007
Ligands	AREG	syncytiotrophoblast	Lysiak JJ 1995	no data	
	BTC	syncytiotrophoblast, extravillous trophoblast	Tanimura K 2004	no data	
	EGF	villous cytotrophoblast, syncytiotrophoblast	Hoffman GE 1991	secondary giant cells	Cai L 2003
	EPGN	no data		no data	
	EREG	placenta (mRNA)	Toyoda H 1997	placenta (low numbers positive cells)	Lee D 2004
	HBEGF	villous cytotrophoblast, synctytiotrophoblast, extravillous trophoblast	Leach RE 1999, Yoo HJ 1997	labyrinth (mRNA)	David Lee (unpublished data)
	TGFα	villous cytotrophoblast, synctytiotrophoblast, extravillous trophoblast	Lysiak JJ 1993	9.0 dpc placenta (mRNA)	Wilcox JN 1988
	NRG1	no data		no data	
	NRG2	no data		no data	
	NRG3	no data		no data	
	NRG4	no data		no data	

Table 2. Mouse models deficient for EGFR signaling pathway components that exhibit placental phenotypes

Gene	Function	Placental phenotype(s)	Lethality	Strain effect?	Rescue?	Reference
Grb2 (hypomorph/null)	adaptor	chorioallantoic fusion, labyrinth branching	11.5 dpc			Saxton TM 2001
Gab1	adaptor	labyrinth small	13.5 - 17.5 dpc	possible genetic background effect		Itoh M 2000
Nck1/Nck2 (double KO)	adaptor	chorioallantioic fusion	9.5 - 11.0 dpc			Bladt F 2003
Sos1	Ras-specific exchange factor	small poorly developed labyrinth, reduced spongiotrophoblast	9.0 - 11.0 dpc	possible genetic background effect		Qian X 2000
Shp2	phosphatase	increased apoptosis results in no TS cells, reduced TG cells	6.0 - 7.5 dpc			Yang W
Akt1	kinase	growth restriction, reduced numbers of glycogen cells, decidua, spongio, labyrinth all smaller, labyrinth disorganized	postnatal			Yang ZZ 2003
craf1	MAPKKK	reduction in spongiotrophoblast, small labyrinth	10.5 -12.5 dpc in 129/b6. 11.5-13.5 in B6.129 mix 12.5 dpc to Postnatal in CD-1	yes	Mox2 cre: die of liver apoptosis at 16.5 dpc	Wojnowski L 1998, Mikula M 2001, Galabova-Kovacs G 2006

Table 2. Continued

Gene	Function	Placental phenotype(s)	Lethality	Strain effect?	Rescue?	Reference
braf	MAPKKK	labyrinth morphogenesis/apotosis, abnormal VEGF signaling	11.0 - 12.0 dpc		Mox2 cre	Galabova-Kovacs G 2006
Map3k3	MAPKKK	reduced numbr of fetal vessels in labyrinth at 9.5 dpc	11.0 dpc			Yang J 2000
Map2k1	MAPKK	labyrinth branching blocked, decreased proliferation, increased apoptosis at 9.5 and 10.5 dpc	10.5 dpc		tetraploid aggregation	Bissonauth V 2006
ERK2	MAPK	labyrinth morphogenesis, spongiotrophoblast, loss of extraembryonic ectoderm, ectoplacental cone	10.5-11.5 dpc; 7.5 - 8.5 dpc		tetraploid aggregation (Hatano)	Hatano N 2003, Saba-El-Leil MK 2003
Mapk14	MAPK	labyrinth morphogenesis, labyrinth apoptosis at 10.5 dpc, reduced spongiotrophoblast	10.5-16.5 dpc	C57BL6J correlates with reduced survival (Tumara K 2000)	tetraploic aggregation (Adams RH 2000)	Mudgett JS 2000, Tamura K 2000, Adams RH 2000
ERK5	MAPK	labyrinth morphogenesis, labyrinth apoptosis at 10.5 dpc	10.5 - 11.0 dpc	several backgrounds showed similar phenotype		Yan L 2003
sp1/sp3 (compound het)	transcription factor	glycogen cell number reduction, spongiotrophoblast shape, reduction; labyrinth size, morphogenesis	16.5 dpc - 18.5 dpc	possible genetic background effect		Kruger I 2007
sp3	transcription factor	glycogen cell number reduction, spongiotrophoblast shape, reduction; labyrinth size, morphogenesis	16.5 dpc - 18.5 dpc	possible genetic background effect		Kruger I 2007

Table 2. Continued

Gene	Function	Placental phenotype(s)	Lethality	Strain effect?	Rescue?	Reference
Ets2	transcription factor	chorion, EPC proliferation defects	8.0 dpc		tetraplod aggregation	Yamamoto H 1998
JunB	transcription factor	TG cells distributed at antimesometrial pole, labyrinth morphogenesis	8.5 - 10.0 dpc		tetraploid aggregation	Schorpp-Kistner M 1999
C-fos	transcription factor	reduced fetal and placental weight at 15.5 dpc	birth and postnatal	possible genetic background effect		Johnson RS 1992

References

[1] Miettinen PJ, Berger JE, Meneses J, Phung Y, Pedersen RA, Werb Z, Derynck R. Epithelial immaturity and multiorgan failure in mice lacking epidermal growth factor receptor. Nature 1995; 376:337-341.

[2] Sibilia M, Steinbach JP, Stingl L, Aguzzi A, Wagner EF. A strain-independent postnatal neurodegeneration in mice lacking the EGF receptor. Embo J 1998; 17:719-731.

[3] Sibilia M, Wagner EF. Strain-dependent epithelial defects in mice lacking the EGF receptor. Science 1995; 269:234-238.

[4] Threadgill DW, Dlugosz AA, Hansen LA, Tennenbaum T, Lichti U, Yee D, LaMantia C, Mourton T, Herrup K, Harris RC, et al. Targeted disruption of mouse EGF receptor: effect of genetic background on mutant phenotype. Science 1995; 269:230-234.

[5] Yarden Y. The EGFR family and its ligands in human cancer. signalling mechanisms and therapeutic opportunities. Eur J Cancer 2001; 37 Suppl 4:S3-8.

[6] Olayioye MA, Neve RM, Lane HA, Hynes NE. The ErbB signaling network: receptor heterodimerization in development and cancer. Embo J 2000; 19:3159-3167.

[7] Guy PM, Platko JV, Cantley LC, Cerione RA, Carraway KL, 3rd. Insect cell-expressed p180erbB3 possesses an impaired tyrosine kinase activity. Proc Natl Acad Sci U S A 1994; 91:8132-8136.

[8] Klapper LN, Glathe S, Vaisman N, Hynes NE, Andrews GC, Sela M, Yarden Y. The ErbB-2/HER2 oncoprotein of human carcinomas may function solely as a shared coreceptor for multiple stroma-derived growth factors. Proc Natl Acad Sci U S A 1999; 96:4995-5000.

[9] Harris RC, Chung E, Coffey RJ. EGF receptor ligands. Exp Cell Res 2003; 284:2-13.

[10] Sunnarborg SW, Hinkle CL, Stevenson M, Russell WE, Raska CS, Peschon JJ, Castner BJ, Gerhart MJ, Paxton RJ, Black RA, Lee DC. Tumor necrosis factor-alpha converting enzyme (TACE) regulates epidermal growth factor receptor ligand availability. J Biol Chem 2002; 277:12838-12845.

[11] Takemura T, Kondo S, Homma T, Sakai M, Harris RC. The membrane-bound form of heparin-binding epidermal growth factor-like growth factor promotes survival of cultured renal epithelial cells. J Biol Chem 1997; 272:31036-31042.

[12] Levin ER. Bidirectional signaling between the estrogen receptor and the epidermal growth factor receptor. Mol Endocrinol 2003; 17:309-317.

[13] Normanno N, De Luca A, Bianco C, Strizzi L, Mancino M, Maiello MR, Carotenuto A, De Feo G, Caponigro F, Salomon DS. Epidermal growth factor receptor (EGFR) signaling in cancer. Gene 2006; 366:2-16.

[14] Barbacci EG, Guarino BC, Stroh JG, Singleton DH, Rosnack KJ, Moyer JD, Andrews GC. The structural basis for the specificity of epidermal growth factor and heregulin binding. J Biol Chem 1995; 270:9585-9589.

[15] Warren CM, Landgraf R. Signaling through ERBB receptors: multiple layers of diversity and control. Cell Signal 2006; 18:923-933.

[16] Ogiso H, Ishitani R, Nureki O, Fukai S, Yamanaka M, Kim JH, Saito K, Sakamoto A, Inoue M, Shirouzu M, Yokoyama S. Crystal structure of the complex of human epidermal growth factor and receptor extracellular domains. Cell 2002; 110:775-787.

[17] Landau M, Ben-Tal N. Dynamic equilibrium between multiple active and inactive conformations explains regulation and oncogenic mutations in ErbB receptors. Biochim Biophys Acta 2008; 1785:12-31.

[18] Ferguson KM, Berger MB, Mendrola JM, Cho HS, Leahy DJ, Lemmon MA. EGF activates its receptor by removing interactions that autoinhibit ectodomain dimerization. Mol Cell 2003; 11:507-517.

[19] Garrett TP, McKern NM, Lou M, Elleman TC, Adams TE, Lovrecz GO, Kofler M, Jorissen RN, Nice EC, Burgess AW, Ward CW. The crystal structure of a truncated ErbB2 ectodomain reveals an active conformation, poised to interact with other ErbB receptors. Mol Cell 2003; 11:495-505.

[20] Gotoh N, Tojo A, Hino M, Yazaki Y, Shibuya M. A highly conserved tyrosine residue at codon 845 within the kinase domain is not required for the transforming activity of human epidermal growth factor receptor. Biochem Biophys Res Commun 1992; 186:768-774.

[21] Landau M, Fleishman SJ, Ben-Tal N. A putative mechanism for downregulation of the catalytic activity of the EGF receptor via direct contact between its kinase and C-terminal domains. Structure 2004; 12:2265-2275.

[22] Zhang X, Gureasko J, Shen K, Cole PA, Kuriyan J. An allosteric mechanism for activation of the kinase domain of epidermal growth factor receptor. Cell 2006; 125:1137-1149.

[23] Yarden Y, Sliwkowski MX. Untangling the ErbB signalling network. Nat Rev Mol Cell Biol 2001; 2:127-137.

[24] Levkowitz G, Klapper LN, Tzahar E, Freywald A, Sela M, Yarden Y. Coupling of the c-Cbl protooncogene product to ErbB-1/EGF-receptor but not to other ErbB proteins. Oncogene 1996; 12:1117-1125.

[25] Dankort D, Jeyabalan N, Jones N, Dumont DJ, Muller WJ. Multiple ErbB-2/Neu Phosphorylation Sites Mediate Transformation through Distinct Effector Proteins. J Biol Chem 2001; 276:38921-38928.

[26] Fedi P, Pierce JH, di Fiore PP, Kraus MH. Efficient coupling with phosphatidylinositol 3-kinase, but not phospholipase C gamma or GTPase-activating protein, distinguishes ErbB-3 signaling from that of other ErbB/EGFR family members. Mol Cell Biol 1994; 14:492-500.

[27] Casalini P, Iorio MV, Galmozzi E, Menard S. Role of HER receptors family in development and differentiation. J Cell Physiol 2004; 200:343-350.

[28] Rossant J, Cross JC. Placental development: lessons from mouse mutants. Nat Rev Genet 2001; 2:538-548.

[29] Cross JC, Hemberger M, Lu Y, Nozaki T, Whiteley K, Masutani M, Adamson SL. Trophoblast functions, angiogenesis and remodeling of the maternal vasculature in the placenta. Mol Cell Endocrinol 2002; 187:207-212.

[30] Simmons DG, Cross JC. Determinants of trophoblast lineage and cell subtype specification in the mouse placenta. Dev Biol 2005; 284:12-24.

[31] Cross JC. Formation of the placenta and extraembryonic membranes. Ann N Y Acad Sci 1998; 857:23-32.

[32] Cross JC, Nakano H, Natale DR, Simmons DG, Watson ED. Branching morphogenesis during development of placental villi. Differentiation 2006; 74:393-401.

[33] Adamson SL, Lu Y, Whiteley KJ, Holmyard D, Hemberger M, Pfarrer C, Cross JC. Interactions between trophoblast cells and the maternal and fetal circulation in the mouse placenta. Dev Biol 2002; 250:358-373.

[34] Coan PM, Conroy N, Burton GJ, Ferguson-Smith AC. Origin and characteristics of glycogen cells in the developing murine placenta. Dev Dyn 2006; 235:3280-3294.

[35] Linzer DI, Fisher SJ. The placenta and the prolactin family of hormones: regulation of the physiology of pregnancy. Mol Endocrinol 1999; 13:837-840.

[36] Erlebacher A, Price KA, Glimcher LH. Maintenance of mouse trophoblast stem cell proliferation by TGF-beta/activin. Dev Biol 2004; 275:158-169.

[37] Guzman-Ayala M, Ben-Haim N, Beck S, Constam DB. Nodal protein processing and fibroblast growth factor 4 synergize to maintain a trophoblast stem cell microenvironment. Proc Natl Acad Sci U S A 2004; 101:15656-15660.

[38] Tanaka S, Kunath T, Hadjantonakis AK, Nagy A, Rossant J. Promotion of trophoblast stem cell proliferation by FGF4. Science 1998; 282:2072-2075.

[39] Arman E, Haffner-Krausz R, Chen Y, Heath JK, Lonai P. Targeted disruption of fibroblast growth factor (FGF) receptor 2 suggests a role for FGF signaling in pregastrulation mammalian development. Proc Natl Acad Sci U S A 1998; 95:5082-5087.

[40] Goldin SN, Papaioannou VE. Paracrine action of FGF4 during periimplantation development maintains trophectoderm and primitive endoderm. Genesis 2003; 36:40-47.

[41] Haffner-Krausz R, Gorivodsky M, Chen Y, Lonai P. Expression of Fgfr2 in the early mouse embryo indicates its involvement in preimplantation development. Mech Dev 1999; 85:167-172.

[42] Niswander L, Martin GR. Fgf-4 expression during gastrulation, myogenesis, limb and tooth development in the mouse. Development 1992; 114:755-768.

[43] Ma GT, Soloveva V, Tzeng SJ, Lowe LA, Pfendler KC, Iannaccone PM, Kuehn MR, Linzer DI. Nodal regulates trophoblast differentiation and placental development. Dev Biol 2001; 236:124-135.

[44] Kunath T, Strumpf D, Rossant J. Early trophoblast determination and stem cell maintenance in the mouse--a review. Placenta 2004; 25 Suppl A:S32-38.

[45] Strumpf D, Mao CA, Yamanaka Y, Ralston A, Chawengsaksophak K, Beck F, Rossant J. Cdx2 is required for correct cell fate specification and differentiation of trophectoderm in the mouse blastocyst. Development 2005; 132:2093-2102.

[46] Tolkunova E, Cavaleri F, Eckardt S, Reinbold R, Christenson LK, Scholer HR, Tomilin A. The caudal-related protein cdx2 promotes trophoblast differentiation of mouse embryonic stem cells. Stem Cells 2006; 24:139-144.

[47] Auman HJ, Nottoli T, Lakiza O, Winger Q, Donaldson S, Williams T. Transcription factor AP-2gamma is essential in the extra-embryonic lineages for early postimplantation development. Development 2002; 129:2733-2747.

[48] Russ AP, Wattler S, Colledge WH, Aparicio SA, Carlton MB, Pearce JJ, Barton SC, Surani MA, Ryan K, Nehls MC, Wilson V, Evans MJ. Eomesodermin is required for mouse trophoblast development and mesoderm formation. Nature 2000; 404:95-99.

[49] Luo J, Sladek R, Bader JA, Matthyssen A, Rossant J, Giguere V. Placental abnormalities in mouse embryos lacking the orphan nuclear receptor ERR-beta. Nature 1997; 388:778-782.

[50] Parr BA, Cornish VA, Cybulsky MI, McMahon AP. Wnt7b regulates placental development in mice. Dev Biol 2001; 237:324-332.

[51] Tetzlaff MT, Bai C, Finegold M, Wilson J, Harper JW, Mahon KA, Elledge SJ. Cyclin F disruption compromises placental development and affects normal cell cycle execution. Mol Cell Biol 2004; 24:2487-2498.

[52] Yang JT, Rayburn H, Hynes RO. Cell adhesion events mediated by alpha 4 integrins are essential in placental and cardiac development. Development 1995; 121:549-560.

[53] Watson ED, Cross JC. Development of structures and transport functions in the mouse placenta. Physiology (Bethesda) 2005; 20:180-193.

[54] Barak Y, Nelson MC, Ong ES, Jones YZ, Ruiz-Lozano P, Chien KR, Koder A, Evans RM. PPAR gamma is required for placental, cardiac, and adipose tissue development. Mol Cell 1999; 4:585-595.

[55] Anson-Cartwright L, Dawson K, Holmyard D, Fisher SJ, Lazzarini RA, Cross JC. The glial cells missing-1 protein is essential for branching morphogenesis in the chorioallantoic placenta. Nat Genet 2000; 25:311-314.

[56] Hughes M, Dobric N, Scott IC, Su L, Starovic M, St-Pierre B, Egan SE, Kingdom JC, Cross JC. The Hand1, Stra13 and Gcm1 transcription factors override FGF signaling to promote terminal differentiation of trophoblast stem cells. Dev Biol 2004; 271:26-37.

[57] Yu C, Shen K, Lin M, Chen P, Lin C, Chang GD, Chen H. GCMa regulates the syncytin-mediated trophoblastic fusion. J Biol Chem 2002; 277:50062-50068.

[58] Dupressoir A, Marceau G, Vernochet C, Benit L, Kanellopoulos C, Sapin V, Heidmann T. Syncytin-A and syncytin-B, two fusogenic placenta-specific murine envelope genes of retroviral origin conserved in Muridae. Proc Natl Acad Sci U S A 2005; 102:725-730.

[59] Gong R, Huang L, Shi J, Luo K, Qiu G, Feng H, Tien P, Xiao G. Syncytin-A mediates the formation of syncytiotrophoblast involved in mouse placental development. Cell Physiol Biochem 2007; 20:517-526.

[60] Simmons DG, Fortier AL, Cross JC. Diverse subtypes and developmental origins of trophoblast giant cells in the mouse placenta. Dev Biol 2007; 304:567-578.

[61] Wu L, de Bruin A, Saavedra HI, Starovic M, Trimboli A, Yang Y, Opavska J, Wilson P, Thompson JC, Ostrowski MC, Rosol TJ, Woollett LA, Weinstein M, Cross JC, Robinson ML, Leone G. Extra-embryonic function of Rb is essential for embryonic development and viability. Nature 2003; 421:942-947.

[62] Lescisin KR, Varmuza S, Rossant J. Isolation and characterization of a novel trophoblast-specific cDNA in the mouse. Genes Dev 1988; 2:1639-1646.

[63] Guillemot F, Nagy A, Auerbach A, Rossant J, Joyner AL. Essential role of Mash-2 in extraembryonic development. Nature 1994; 371:333-336.

[64] Scott IC, Anson-Cartwright L, Riley P, Reda D, Cross JC. The HAND1 basic helix-loop-helix transcription factor regulates trophoblast differentiation via multiple mechanisms. Mol Cell Biol 2000; 20:530-541.

[65] Jen Y, Manova K, Benezra R. Each member of the Id gene family exhibits a unique expression pattern in mouse gastrulation and neurogenesis. Dev Dyn 1997; 208:92-106.

[66] Cross JC, Flannery ML, Blanar MA, Steingrimsson E, Jenkins NA, Copeland NG, Rutter WJ, Werb Z. Hxt encodes a basic helix-loop-helix transcription factor that regulates trophoblast cell development. Development 1995; 121:2513-2523.

[67] Tanaka M, Gertsenstein M, Rossant J, Nagy A. Mash2 acts cell autonomously in mouse spongiotrophoblast development. Dev Biol 1997; 190:55-65.

[68] Bouillot S, Rampon C, Tillet E, Huber P. Tracing the glycogen cells with protocadherin 12 during mouse placenta development. Placenta 2006; 27:882-888.

[69] Lopez MF, Dikkes P, Zurakowski D, Villa-Komaroff L. Insulin-like growth factor II affects the appearance and glycogen content of glycogen cells in the murine placenta. Endocrinology 1996; 137:2100-2108.

[70] Takahashi K, Kobayashi T, Kanayama N. p57(Kip2) regulates the proper development of labyrinthine and spongiotrophoblasts. Mol Hum Reprod 2000; 6:1019-1025.

[71] Carney EW, Prideaux V, Lye SJ, Rossant J. Progressive expression of trophoblast-specific genes during formation of mouse trophoblast giant cells in vitro. Mol Reprod Dev 1993; 34:357-368.

[72] Kraut N, Snider L, Chen CM, Tapscott SJ, Groudine M. Requirement of the mouse I-mfa gene for placental development and skeletal patterning. Embo J 1998; 17:6276-6288.

[73] Nadra K, Anghel SI, Joye E, Tan NS, Basu-Modak S, Trono D, Wahli W, Desvergne B. Differentiation of trophoblast giant cells and their metabolic functions are dependent on peroxisome proliferator-activated receptor beta/delta. Mol Cell Biol 2006; 26:3266-3281.

[74] Takahashi Y, Carpino N, Cross JC, Torres M, Parganas E, Ihle JN. SOCS3: an essential regulator of LIF receptor signaling in trophoblast giant cell differentiation. Embo J 2003; 22:372-384.

[75] Yan J, Tanaka S, Oda M, Makino T, Ohgane J, Shiota K. Retinoic acid promotes differentiation of trophoblast stem cells to a giant cell fate. Dev Biol 2001; 235:422-432.

[76] Riley P, Anson-Cartwright L, Cross JC. The Hand1 bHLH transcription factor is essential for placentation and cardiac morphogenesis. Nat Genet 1998; 18:271-275.

[77] Cross JC, Baczyk D, Dobric N, Hemberger M, Hughes M, Simmons DG, Yamamoto H, Kingdom JC. Genes, development and evolution of the placenta. Placenta 2003; 24:123-130.

[78] Georgiades P, Ferguson-Smith AC, Burton GJ. Comparative developmental anatomy of the murine and human definitive placentae. Placenta 2002; 23:3-19.

[79] Janatpour MJ, McMaster MT, Genbacev O, Zhou Y, Dong J, Cross JC, Israel MA, Fisher SJ. Id-2 regulates critical aspects of human cytotrophoblast differentiation, invasion and migration. Development 2000; 127:549-558.

[80] Richardson BD, Cheng YH, Langland RA, Handwerger S. Differential expression of AP-2gamma and AP-2alpha during human trophoblast differentiation. Life Sci 2001; 69:2157-2165.

[81] Hahn T, Barth S, Graf R, Engelmann M, Beslagic D, Reul JM, Holsboer F, Dohr G, Desoye G. Placental glucose transporter expression is regulated by glucocorticoids. J Clin Endocrinol Metab 1999; 84:1445-1452.

[82] Jacquemin P, Sapin V, Alsat E, Evain-Brion D, Dolle P, Davidson I. Differential expression of the TEF family of transcription factors in the murine placenta and during differentiation of primary human trophoblasts in vitro. Dev Dyn 1998; 212:423-436.

[83] Janatpour MJ, Utset MF, Cross JC, Rossant J, Dong J, Israel MA, Fisher SJ. A repertoire of differentially expressed transcription factors that offers insight into mechanisms of human cytotrophoblast differentiation. Dev Genet 1999; 25:146-157.

[84] Blaise S, de Parseval N, Benit L, Heidmann T. Genomewide screening for fusogenic human endogenous retrovirus envelopes identifies syncytin 2, a gene conserved on primate evolution. Proc Natl Acad Sci U S A 2003; 100:13013-13018.

[85] Mi S, Lee X, Li X, Veldman GM, Finnerty H, Racie L, LaVallie E, Tang XY, Edouard P, Howes S, Keith JC, Jr., McCoy JM. Syncytin is a captive retroviral envelope protein involved in human placental morphogenesis. Nature 2000; 403:785-789.

[86] Kruger I, Vollmer M, Simmons DG, Elsasser HP, Philipsen S, Suske G. Sp1/Sp3 compound heterozygous mice are not viable: impaired erythropoiesis and severe placental defects. Dev Dyn 2007; 236:2235-2244.

[87] Loregger T, Pollheimer J, Knofler M. Regulatory transcription factors controlling function and differentiation of human trophoblast--a review. Placenta 2003; 24 Suppl A:S104-110.

[88] Alders M, Hodges M, Hadjantonakis AK, Postmus J, van Wijk I, Bliek J, de Meulemeester M, Westerveld A, Guillemot F, Oudejans C, Little P, Mannens M. The human Achaete-Scute homologue 2 (ASCL2,HASH2) maps to chromosome 11p15.5, close to IGF2 and is expressed in extravillus trophoblasts. Hum Mol Genet 1997; 6:859-867.

[89] Pijnenborg R, Robertson WB, Brosens I, Dixon G. Review article: trophoblast invasion and the establishment of haemochorial placentation in man and laboratory animals. Placenta 1981; 2:71-91.

[90] Kam EP, Gardner L, Loke YW, King A. The role of trophoblast in the physiological change in decidual spiral arteries. Hum Reprod 1999; 14:2131-2138.

[91] Leonard S, Murrant C, Tayade C, van den Heuvel M, Watering R, Croy BA. Mechanisms regulating immune cell contributions to spiral artery modification -- facts and hypotheses -- a review. Placenta 2006; 27 Suppl A:S40-46.

[92] Zybina EV, Zybina TG. Polytene chromosomes in mammalian cells. Int Rev Cytol 1996; 165:53-119.

[93] Redline RW, Chernicky CL, Tan HQ, Ilan J, Ilan J. Differential expression of insulin-like growth factor-II in specific regions of the late (post day 9.5) murine placenta. Mol Reprod Dev 1993; 36:121-129.

[94] Cai L, Zhang J, Duan E. Dynamic distribution of epidermal growth factor during mouse embryo peri-implantation. Cytokine 2003; 23:170-178.

[95] Dackor J, Strunk KE, Wehmeyer MM, Threadgill DW. Altered trophoblast proliferation is insufficient to account for placental dysfunction in Egfr null embryos. Placenta 2007; 28:1211-1218.

[96] Hofmann GE, Scott RT, Jr., Bergh PA, Deligdisch L. Immunohistochemical localization of epidermal growth factor in human endometrium, decidua, and placenta. J Clin Endocrinol Metab 1991; 73:882-887.

[97] Jokhi PP, King A, Loke YW. Reciprocal expression of epidermal growth factor receptor (EGF-R) and c-erbB2 by non-invasive and invasive human trophoblast populations. Cytokine 1994; 6:433-442.

[98] Leach RE, Khalifa R, Ramirez ND, Das SK, Wang J, Dey SK, Romero R, Armant DR. Multiple roles for heparin-binding epidermal growth factor-like growth factor are suggested by its cell-specific expression during the human endometrial cycle and early placentation. J Clin Endocrinol Metab 1999; 84:3355-3363.

[99] Lee D, Pearsall RS, Das S, Dey SK, Godfrey VL, Threadgill DW. Epiregulin is not essential for development of intestinal tumors but is required for protection from intestinal damage. Mol Cell Biol 2004; 24:8907-8916.

[100] Lee H, Maihle NJ. Isolation and characterization of four alternate c-erbB3 transcripts expressed in ovarian carcinoma-derived cell lines and normal human tissues. Oncogene 1998; 16:3243-3252.

[101] Lim H, Dey SK, Das SK. Differential expression of the erbB2 gene in the periimplantation mouse uterus: potential mediator of signaling by epidermal growth factor-like growth factors. Endocrinology 1997; 138:1328-1337.

[102] Lysiak JJ, Han VK, Lala PK. Localization of transforming growth factor alpha in the human placenta and decidua: role in trophoblast growth. Biol Reprod 1993; 49:885-894.

[103] Lysiak JJ, Johnson GR, Lala PK. Localization of amphiregulin in the human placenta and decidua throughout gestation: role in trophoblast growth. Placenta 1995; 16:359-366.

[104] Muhlhauser J, Crescimanno C, Kaufmann P, Hofler H, Zaccheo D, Castellucci M. Differentiation and proliferation patterns in human trophoblast revealed by c-erbB-2 oncogene product and EGF-R. J Histochem Cytochem 1993; 41:165-173.

[105] Tanimura K, Nakago S, Murakoshi H, Takekida S, Moriyama T, Matsuo H, Hashimoto K, Maruo T. Changes in the expression and cytological localization of betacellulin and its receptors (ErbB-1 and ErbB-4) in the trophoblasts in human placenta over the course of pregnancy. Eur J Endocrinol 2004; 151:93-101.

[106] Toyoda H, Komurasaki T, Uchida D, Morimoto S. Distribution of mRNA for human epiregulin, a differentially expressed member of the epidermal growth factor family. Biochem J 1997; 326 (Pt 1):69-75.

[107] Wilcox JN, Derynck R. Developmental expression of transforming growth factors alpha and beta in mouse fetus. Mol Cell Biol 1988; 8:3415-3422.

[108] Yoo HJ, Barlow DH, Mardon HJ. Temporal and spatial regulation of expression of heparin-binding epidermal growth factor-like growth factor in the human endometrium: a possible role in blastocyst implantation. Dev Genet 1997; 21:102-108.

[109] Amemiya K, Kurachi H, Adachi H, Morishige KI, Adachi K, Imai T, Miyake A. Involvement of epidermal growth factor (EGF)/EGF receptor autocrine and paracrine mechanism in human trophoblast cells: functional differentiation in vitro. J Endocrinol 1994; 143:291-301.

[110] Filla MS, Zhang CX, Kaul KL. A potential transforming growth factor alpha/epidermal growth factor receptor autocrine circuit in placental cytotrophoblasts. Cell Growth Differ 1993; 4:387-393.

[111] Peters TJ, Chapman BM, Wolfe MW, Soares MJ. Placental lactogen-I gene activation in differentiating trophoblast cells: extrinsic and intrinsic regulation involving mitogen-activated protein kinase signaling pathways. J Endocrinol 2000; 165:443-456.

[112] Yamaguchi M, Ogren L, Endo H, Thordarson G, Kensinger R, Talamantes F. Epidermal growth factor stimulates mouse placental lactogen I but inhibits mouse placental lactogen II secretion in vitro. Proc Natl Acad Sci U S A 1992; 89:11396-11400.

[113] Yamaguchi M, Ogren L, Kurachi H, Hirota K, Imai T, Talamantes F. Opposite effects of transforming growth factor alpha and epidermal growth factor on mouse placental lactogen I secretion. Proc Natl Acad Sci U S A 1995; 92:2830-2834.

[114] Armant DR, Kilburn BA, Petkova A, Edwin SS, Duniec-Dmuchowski ZM, Edwards HJ, Romero R, Leach RE. Human trophoblast survival at low oxygen concentrations requires metalloproteinase-mediated shedding of heparin-binding EGF-like growth factor. Development 2006; 133:751-759.

[115] Leach RE, Kilburn B, Wang J, Liu Z, Romero R, Armant DR. Heparin-binding EGF-like growth factor regulates human extravillous cytotrophoblast development during conversion to the invasive phenotype. Dev Biol 2004; 266:223-237.

[116] Leach RE, Romero R, Kim YM, Chaiworapongsa T, Kilburn B, Das SK, Dey SK, Johnson A, Qureshi F, Jacques S, Armant DR. Pre-eclampsia and expression of heparin-binding EGF-like growth factor. Lancet 2002; 360:1215-1219.

[117] Tseng JJ, Chou MM. Differential expression of growth-, angiogenesis- and invasion-related factors in the development of placenta accreta. Taiwan J Obstet Gynecol 2006; 45:100-106.

[118] Tseng JJ, Hsu SL, Wen MC, Ho ES, Chou MM. Expression of epidermal growth factor receptor and c-erbB-2 oncoprotein in trophoblast populations of placenta accreta. Am J Obstet Gynecol 2004; 191:2106-2113.

[119] Calvo MT, Romo A, Gutierrez JJ, Relano E, Barrio E, Ferrandez Longas A. Study of genetic expression of intrauterine growth factors IGF-I and EGFR in placental tissue from pregnancies with intrauterine growth retardation. J Pediatr Endocrinol Metab 2004; 17 Suppl 3:445-450.

[120] Faxen M, Nasiell J, Blanck A, Nisell H, Lunell NO. Altered mRNA expression pattern of placental epidermal growth factor receptor (EGFR) in pregnancies complicated by preeclampsia and/or intrauterine growth retardation. Am J Perinatol 1998; 15:9-13.

[121] Fondacci C, Alsat E, Gabriel R, Blot P, Nessmann C, Evain-Brion D. Alterations of human placental epidermal growth factor receptor in intrauterine growth retardation. J Clin Invest 1994; 93:1149-1155.

[122] Fujita Y, Kurachi H, Morishige K, Amemiya K, Terakawa N, Miyake A, Tanizawa O. Decrease in epidermal growth factor receptor and its messenger ribonucleic acid levels in intrauterine growth-retarded and diabetes mellitus-complicated pregnancies. J Clin Endocrinol Metab 1991; 72:1340-1345.

[123] Gabriel R, Alsat E, Evain-Brion D. Alteration of epidermal growth factor receptor in placental membranes of smokers: relationship with intrauterine growth retardation. Am J Obstet Gynecol 1994; 170:1238-1243.

[124] Ghidini A. Idiopathic fetal growth restriction: a pathophysiologic approach. Obstet Gynecol Surv 1996; 51:376-382.

[125] Horn LC, Langner A, Stiehl P, Wittekind C, Faber R. Identification of the causes of intrauterine death during 310 consecutive autopsies. Eur J Obstet Gynecol Reprod Biol 2004; 113:134-138.

[126] Gagnon R. Placental insufficiency and its consequences. Eur J Obstet Gynecol Reprod Biol 2003; 110 Suppl 1:S99-107.

[127] Scherjon S, Briet J, Oosting H, Kok J. The discrepancy between maturation of visual-evoked potentials and cognitive outcome at five years in very preterm infants with and without hemodynamic signs of fetal brain-sparing. Pediatrics 2000; 105:385-391.

[128] Barker DJ, Eriksson JG, Forsen T, Osmond C. Fetal origins of adult disease: strength of effects and biological basis. Int J Epidemiol 2002; 31:1235-1239.

[129] Martyn CN, Barker DJ, Osmond C. Mothers' pelvic size, fetal growth, and death from stroke and coronary heart disease in men in the UK. Lancet 1996; 348:1264-1268.

[130] Painter RC, de Rooij SR, Bossuyt PM, Simmers TA, Osmond C, Barker DJ, Bleker OP, Roseboom TJ. Early onset of coronary artery disease after prenatal exposure to the Dutch famine. Am J Clin Nutr 2006; 84:322-327; quiz 466-327.

[131] Syddall HE, Sayer AA, Simmonds SJ, Osmond C, Cox V, Dennison EM, Barker DJ, Cooper C. Birth weight, infant weight gain, and cause-specific mortality: the Hertfordshire Cohort Study. Am J Epidemiol 2005; 161:1074-1080.

[132] Gluckman PD, Hanson MA. The developmental origins of the metabolic syndrome. Trends Endocrinol Metab 2004; 15:183-187.

[133] Langley-Evans SC. Developmental programming of health and disease. Proc Nutr Soc 2006; 65:97-105.

[134] Adams RH, Porras A, Alonso G, Jones M, Vintersten K, Panelli S, Valladares A, Perez L, Klein R, Nebreda AR. Essential role of p38alpha MAP kinase in placental but not embryonic cardiovascular development. Mol Cell 2000; 6:109-116.

[135] Bissonauth V, Roy S, Gravel M, Guillemette S, Charron J. Requirement for Map2k1 (Mek1) in extra-embryonic ectoderm during placentogenesis. Development 2006; 133:3429-3440.

[136] Bladt F, Aippersbach E, Gelkop S, Strasser GA, Nash P, Tafuri A, Gertler FB, Pawson T. The murine Nck SH2/SH3 adaptors are important for the development of mesoderm-derived embryonic structures and for regulating the cellular actin network. Mol Cell Biol 2003; 23:4586-4597.

[137] Giroux S, Tremblay M, Bernard D, Cardin-Girard JF, Aubry S, Larouche L, Rousseau S, Huot J, Landry J, Jeannotte L, Charron J. Embryonic death of Mek1-deficient mice reveals a role for this kinase in angiogenesis in the labyrinthine region of the placenta. Curr Biol 1999; 9:369-372.

[138] Hatano N, Mori Y, Oh-hora M, Kosugi A, Fujikawa T, Nakai N, Niwa H, Miyazaki J, Hamaoka T, Ogata M. Essential role for ERK2 mitogen-activated protein kinase in placental development. Genes Cells 2003; 8:847-856.

[139] Itoh M, Yoshida Y, Nishida K, Narimatsu M, Hibi M, Hirano T. Role of Gab1 in heart, placenta, and skin development and growth factor- and cytokine-induced extracellular signal-regulated kinase mitogen-activated protein kinase activation. Mol Cell Biol 2000; 20:3695-3704.

[140] Johnson RS, Spiegelman BM, Papaioannou V. Pleiotropic effects of a null mutation in the c-fos proto-oncogene. Cell 1992; 71:577-586.

[141] Man AK, Young LJ, Tynan JA, Lesperance J, Egeblad M, Werb Z, Hauser CA, Muller WJ, Cardiff RD, Oshima RG. Ets2-dependent stromal regulation of mouse mammary tumors. Mol Cell Biol 2003; 23:8614-8625.

[142] Mikula M, Schreiber M, Husak Z, Kucerova L, Ruth J, Wieser R, Zatloukal K, Beug H, Wagner EF, Baccarini M. Embryonic lethality and fetal liver apoptosis in mice lacking the c-raf-1 gene. Embo J 2001; 20:1952-1962.

[143] Mudgett JS, Ding J, Guh-Siesel L, Chartrain NA, Yang L, Gopal S, Shen MM. Essential role for p38alpha mitogen-activated protein kinase in placental angiogenesis. Proc Natl Acad Sci U S A 2000; 97:10454-10459.

[144] Qian X, Esteban L, Vass WC, Upadhyaya C, Papageorge AG, Yienger K, Ward JM, Lowy DR, Santos E. The Sos1 and Sos2 Ras-specific exchange factors: differences in placental expression and signaling properties. Embo J 2000; 19:642-654.

[145] Saba-El-Leil MK, Vella FD, Vernay B, Voisin L, Chen L, Labrecque N, Ang SL, Meloche S. An essential function of the mitogen-activated protein kinase Erk2 in mouse trophoblast development. EMBO Rep 2003; 4:964-968.

[146] Saxton TM, Cheng AM, Ong SH, Lu Y, Sakai R, Cross JC, Pawson T. Gene dosage-dependent functions for phosphotyrosine-Grb2 signaling during mammalian tissue morphogenesis. Curr Biol 2001; 11:662-670.

[147] Schorpp-Kistner M, Wang ZQ, Angel P, Wagner EF. JunB is essential for mammalian placentation. Embo J 1999; 18:934-948.

[148] Wojnowski L, Stancato LF, Zimmer AM, Hahn H, Beck TW, Larner AC, Rapp UR, Zimmer A. Craf-1 protein kinase is essential for mouse development. Mech Dev 1998; 76:141-149.

[149] Yamamoto H, Flannery ML, Kupriyanov S, Pearce J, McKercher SR, Henkel GW, Maki RA, Werb Z, Oshima RG. Defective trophoblast function in mice with a targeted mutation of Ets2. Genes Dev 1998; 12:1315-1326.

[150] Yang J, Boerm M, McCarty M, Bucana C, Fidler IJ, Zhuang Y, Su B. Mekk3 is essential for early embryonic cardiovascular development. Nat Genet 2000; 24:309-313.

[151] Yang W, Klaman LD, Chen B, Araki T, Harada H, Thomas SM, George EL, Neel BG. An Shp2/SFK/Ras/Erk signaling pathway controls trophoblast stem cell survival. Dev Cell 2006; 10:317-327.

[152] Yang ZZ, Tschopp O, Hemmings-Mieszczak M, Feng J, Brodbeck D, Perentes E, Hemmings BA. Protein kinase B alpha/Akt1 regulates placental development and fetal growth. J Biol Chem 2003; 278:32124-32131.

CHAPTER II

ALTERED TROPHOBLAST PROLIFERATION IS INSUFFICIENT TO ACCOUNT FOR PLACENTAL DYSFUNCTION IN *EGFR* NULL EMBRYOS

Preface

This work was previously published in the journal PLACENTA as a first co-author manuscript between Karen Strunk and myself. Karen Strunk performed the RPAs, western blots, and immunohistochemistry as well as the BrdU and TUNEL experiments. I set up crosses between the cell cycle knockout and *Egfr*^{tm1Mag} mice and analyzed data from the timed pregnancies. I also collected samples for and performed the quantitative PCR analysis of markers for proliferation and cell cycle arrest. Karen Strunk and I were both equally involved in preparing the manuscript.

Jennifer Dackor, Karen E. Strunk, Meggan M. Wehmeyer, David W. Threadgill. Altered trophoblast proliferation is insufficient to account for placental dysfunction in *Egfr* null embryos. Placenta 2007; 28:1211-8.

Abstract

Homozygosity for the *Egfr*^{tm1Mag} null allele in mice leads to genetic background dependent placental abnormalities and embryonic lethality. Molecular mechanisms or genetic modifiers that differentiate strains with surviving versus non-surviving *Egfr* nullizygous embryos have yet to be identified. *Egfr* transcript in wildtype placenta was quantified by ribonuclease protection assay (RPA) and the lowest level of *Egfr* mRNA expression was found to coincide with *Egfr*^{tm1Mag} homozygous lethality. Immunohistochemical analysis of ERBB family receptors, ERBB2, ERBB3, and ERBB4, showed similar expression between *Egfr* wildtype and null placentas indicating that *Egfr* null trophoblast do not up-regulate these receptors to compensate for EGFR deficiency. Significantly fewer numbers of bromodeoxyuridine (BrdU) positive trophoblast were observed in *Egfr* nullizygous placentas and *cdc25A* and *cMyc*, genes associated with proliferation, were significantly down-regulated in null placentas, as measured by real-time PCR. However, strains with both mild and severe placental phenotypes exhibit reduced proliferation suggesting that this defect alone does not account for strain-specific embryonic lethality. Consistent with this hypothesis, intercrosses generating null mice for cell cycle checkpoint components (*p53*, *pRb*, *p21*^{Cip1}, *p27*^{Kip1} or *p18*^{INK4c}) in combination with *Egfr* deficiency did not increase survival of *Egfr* nullizygous embryos. Since complete development of the spongiotrophoblast compartment is not required for survival of *Egfr* nullizygous embryos, reduction of this layer that is commonly observed in *Egfr* nullizygous placentas likely accounts for the decrease in proliferation.

Introduction

EGFR is the prototypical member of a family of related receptor tyrosine kinases (RTKs) that includes ERBB2, ERBB3, and ERBB4. The broadly expressed mouse *Egfr* gives rise to multiple alternatively spliced and polyadenylated transcripts [1]. A null allele of the *Egfr* was previously generated in mice and phenotypic analysis revealed that homozygous *Egfr* null mutants exhibit peri-implantation to post-natal lethality, depending on the genetic background of the mouse [2,3]. *Egfr* homozygous null embryos on a 129/Sv background die around 11.5 days post-coitus (dpc) due to abnormal placental development, with a reduced spongiotrophoblast layer and severe disorganization of the labyrinth layer [4]. On an outbred CD-1 stock the spongiotrophoblast layer is similarly reduced, but there is rescue of the disorganized labyrinthine layer allowing *Egfr* null embryos to survive to birth. A more comprehensive characterization of *Egfr* null embryonic lethality on many genetic backgrounds revealed that the timing of lethality varies widely between strains [5]. Several Swiss-derived strains, on either a congenic FVB/NJ or hybrid ICR/HaROS.129 background exhibit lethality prior to 10.5 dpc. Similar to the 129/Sv strain labyrinth defects are observed beginning at 11.5 dpc in many strains which do not support embryonic survival, including congenic BALB/cJ and BTBR T^{+} *tf*/J. Some backgrounds, such as hybrid ALR.129 and to a lesser extent hybrid FVB.129 and BALB.129, support robust survival of *Egfr* null embryos past midgestation although null placentas are smaller than those from wildtype embryos. The existence of placental phenotypes that are strain specific suggests the effects of EGFR deficiency on normal growth and differentiation of placenta are mediated by background-specific modifiers.

Thus far no loci have been identified that modify placental development in *Egfr* nullizygous mice. Two separate mapping crosses have failed to yield significant quantitative trait loci (QTL) associated with survival of *Egfr* nullizygous embryos suggesting the existence of many modifiers with complex relationships [5]. In addition, the molecular mechanism contributing to the *Egfr* null placental phenotype has yet to be elucidated. Placental defects have been reported in animals deficient for a number of signaling molecules downstream of EGFR. Mice deficient for the adaptor proteins GRB2 and GAB1, Ras-specific guanine nucleotide exchange factor, SOS1 and its target KRAS, components of MAPK cascades including RAF1, MAPK2K1, ERK2 and MAPK14 (p38), and downstream transcription factors JUNB, ETS2, and FOS all exhibit labyrinth defects and embryonic lethality at midgestation [6-16]. Together these data are consistent with MAPK signaling being required for normal placental development and suggests that *Egfr* null strains surviving past midgestation probably use alternate pathways in the trophoblasts to activate MAPK signaling and/or achieve the downstream effects of cellular proliferation, migration, and differentiation. Consistent with the importance of EGFR signaling for normal placental development, EGFR is expressed in human placenta and altered expression has been associated with intrauterine growth restriction (IUGR), preeclampsia, and placenta accreta [17-22].

In this study, we have further characterized strain-dependent *Egfr* nullizygous placental defects to investigate the mechanism responsible for differential survival in the absence of EGFR signaling. RNase protection assays were used to analyze expression of alternatively-spliced *Egfr* transcripts in the developing embryo and placenta. We tested the hypothesis that ERBB family member receptors, ERBB2, ERBB2, or ERBB4 can be up-

regulated in the placenta to compensate for the loss of EGFR in strains supporting survival of *Egfr* nullizygous embryos. We have also measured rates of proliferation and apoptosis in EGFR-deficient placentas to address the cellular mechanism contributing to *Egfr* nullizygous placental defects. Lastly, mice double mutant for *Egfr* and either *Trp53* (*p53*), *Rb*, *Cdkn1a* ($p21^{Cip1}$), *Cdkn1b* ($p27^{Kip1}$) or *Cdkn2c* ($p18^{INK4c}$) were generated to determine if elimination of cell cycle checkpoints rescues *Egfr* null placental defects.

Materials and methods

Mice and genetic crosses

A null allele for *Egfr* ($Egfr^{tm1Mag}$) on outbred CD-1 stock or inbred 129/Sv, ALR/LtJ, FVB/NJ, C57BL/6J, and BALB/cJ strains have been previously described [5]. 129S1/SvImJ and 129S6/SvEvTAC strains were used interchangably due to their highly similarity [23]. Males heterozygous for the $Egfr^{tm1Mag}$ mutation, on either an ALR/LtJ, FVB/NJ, C57BL/6J, or BALB/cJ genetic background, were mated to heterozygous 129/Sv females to generate hybrid F1 embryos and $Egfr^{tm1Mag}$ heterozygous F1 adults. The ALR.129 heterozygous F1 adults were backcrossed to 129/Sv $Egfr^{tm1Mag}$ heterozygotes to obtain N2 backcross embryos. Adult mice and embryos were genotyped using 1 *u*L of a lysed tissue sample (prepared by incubating ear punches at 95°C in 100 *u*L of 25mM NaOH/0.2mM EDTA for 20 minutes and then neutralizing with 100 *u*L 40mM TrisHCl pH 5.0) per PCR reaction. The following primers were used for amplification of the wildtype and $Egfr^{tm1Mag}$ alleles: EgfrCommon, 5'-GCCCTGCCTTTCCCACCATA-3' and EgfrWT, 5'- ATCAACTTTGGGAGCCACAC-3' and EgfrKO, 5'-AACGTCGTGACTGGGAAAAC-3' (Qiagen). PCR conditions included 40 cycles of denaturing at 94°C, primer annealing at 55°C and extension at 72°C. PCR products

were run on a 2.5% agarose gel to separate a 350-bp product corresponding to wildtype *Egfr* and a 450-bp product corresponding to the *Egfr*^{tm1Mag} allele.

Noon on the day that copulation plugs were observed was designated as 0.5 days post-coitus (dpc). Pregnant females were euthanized by CO_2 asphyxiation and embryos and placentas dissected from the uterine horns on the morning of 9.5 through 18.5 dpc into phosphate buffered saline (PBS). The placenta and extra-embryonic tissues were separated from the embryo by mechanical dissection and either whole embryos before 10.5 dpc or tail biopsies after 10.5 dpc were collected for DNA extraction to determine the genotype of each individual embryo. Placentas were either flash frozen or preserved in RNAlater (Ambion) for extraction of RNA or fixed in 10% NBF (neutral buffered formalin) for histological analysis.

For cell cycle crosses *Egfr*^{tm1Mag} heterozygous mice on a 129/Sv genetic background were intercrossed with mice heterozygous for *Trp53*^{tm1Tyj}, *Rb*^{tm1Tyj}, *Cdkn1a*^{tm1Tyj}, or *Cdkn1b*^{tm1Mlf} null alleles maintained on a similar 129/Sv background. *Egfr*^{tm1Mag} heterozygous mice from a BALB/cJ background were intercrossed with mice heterozygous for *Trp53*^{tm1Tyj}, *Rb*^{tm1Tyj}, or *Cdkn2c*^{tm1Yxi} null alleles, also on a BALB/cJ background. Double heterozygous mice were intercrossed and embryos with placentas were collected and genotyped at 13.5 dpc (Table 4). To increase numbers of double homozygous embryos, some *Trp53*^{tm1Tyj} and *Cdkn1a*^{tm1Tyj} crosses were set up by intercrossing animals homozygous for *Trp53*^{tm1Tyj} or *Cdkn1a*^{tm1Tyj}, and heterozygous for *Egfr*^{tm1Mag} (Table 4). *Trp53*^{tm1Tyj}, *Rb*^{tm1Tyj}, *Cdkn1a*^{tm1Tyj}, *Cdkn1b*^{tm1Mlf} and *Cdkn2c*^{tm1Yxi} null alleles were amplified by PCR and detected as previously described [24-27].

Mice were fed Purina Mills Lab Diet 5058 or 5010 and water *ad libitum* under specific pathogen free conditions in an American Association for the Accreditation of Lab

Animal Care approved facility. All experiments were approved by an Institutional Animal Care and Use Committee.

Ribonuclease protection assay

Wildtype samples were collected at 9.5, 10.5, 11.5, 12.5, 13.5, 14.5, 15.5, and 16.5 dpc from CD-1 females mated to CD-1 males. Embryos were dissected from extraembryonic tissue in PBS and total RNA was isolated from the embryo or placenta by homogenizing tissue in 1-2 mls of Tri-reagent (Molecular Research Center). A *Pvu* II-*Sst* I restriction fragment generated from the region spanning exons 15-18 of the *Egfr* was subcloned into pBSK+ for use as a probe. The plasmid was linearized with *Xho* I and a 440 bp antisense probe was generated and radiolabeled with T3 polymerase and dUTP-P^{32} using the MAXIscript *in vitro* transcription kit (Ambion). The riboprobe was quantified by scintillation counting and 10 μg of total RNA from each embryonic or placental time point was incubated with 6 X 10^5 CPM (250-300 ng) labeled riboprobe. Ribonuclease protection assays (RPAs) were carried out using the RPA Kit II (Ambion), and analyzed using a phosphoimager system (Molecular Dynamics). The radioactivity of each fragment was quantified, normalized to a glyceraldehyde-3-phosphate dehydrogenase (*Gapdh*) probe, and expressed as normalized counts. Each RPA was repeated three times for each time point and each experiment included a 20 μg sample of total liver RNA to demonstrate that the probe was in excess of RNA in the reaction. The *Gapdh* probe was a 280-bp *Hind* III-*Pst* I fragment from mouse *Gapdh* that was linearized with *Bam* HI and antisense probe was generated using SP6 polymerase as described above. Error is expressed as the standard error of the mean for three independent RPAs for the embryonic and placental timepoints.

Immunohistochemistry and Western blots

FVB.129 F_1 and BALB.129 F_1 placentas at 18.5 dpc were collected and fixed in 10% neutral buffered formalin (NBF) at 4^{o}C overnight. Samples were then floated in 30% sucrose, embedded in Tissue Tek (Fisher Scientific), and cryosectioned. Slides were post fixed in 10% NBF for 10 minutes, endogenous peroxidases quenched using 3% hydrogen peroxide in MeOH, and subjected to heat-induced epitope retrieval in 10mM citrate buffer pH 6.0. Non-specific sites were blocked using blocking solution (0.1 mM Tris pH 8.0, 0.1% Tween-20, 1% BSA) incubated with sheep-anti-mouse-EGFR (1:100; Maine Biotechnologies) or rabbit-anti-human-ERBB2 (sc284, 1:100), rabbit-anti-human-ERBB3 (sc285, 1:100), or rabbit-anti-human-ERBB4 (sc283, 1:100; Santa Cruz Biotechnologies). Samples exposed to anti-EGFR were incubated in species-specific anti-sheep secondary antibody conjugated to HRP at 1:100, while the other anti-ERBB samples were incubated in goat anti-rabbit-HRP secondary antibody (Jackson Immunologics). Antigen was colormetrically detected by reaction with 3-3'-diaminobenzidine (DAB) and counterstained with hematoxalin. Slides were viewed using a DMRE microscope (Leica) and photographed at 200X with a CCD digital camera (SPOT Diagnostics). Levels of immunoreactivity were determined qualitatively.

For western analysis placentas were collected at 10.5 dpc from C57B6.129 F_1, 13.5 dpc from ALR.129 F_1, and 18.5 dpc from FVB.129 F_1 crosses. Tissues were mechanically homogenized on ice in protein lysis buffer (40mM HEPES pH 7.4, 10mM EDTA pH 8.0, 4mM EGTA pH7.5, 2% Triton X-100, 20 ng/mL aprotinin, 20 ng/mL leupeptin, 1mM sodium vanadate, 1mM PMSF) based on 10% weight/volume. Proteins were separated using 6% stacking and 10% resolving SDS-polyacrylamide gel electrophoresis in 1X Laemelli running buffer then transferred to nitrocellulose membrane. Membranes were washed in

TBST (10mM Tris pH7.5, 150mM NaCl, 0.1% Tween 20), blocked with 5% powdered milk in TBST, and incubated with the following primary antibodies Egfr (1:500), ErbB3 (1:500), or mouse-anti-rat-beta tubulin (Sigma T5201, 1:500), washed and incubated with secondary antibody to either rabbit anti-sheep, goat anti-rabbit or rabbit-anti-mouse conjugated to HRP (Jackson Immuno) and antigen detected using ECL detection (Amersham cat # RPN 2106).

Proliferation assays

Placentas, from N2 embryos generated by backcrossing ALR.129F$_1$ *Egfr*^{tm1Mag} heterozygous mice to 129/Sv *Egfr*^{tm1Mag} heterozygous mice, were collected two hours after maternal intraperitoneal injection with 10 µl per gram of body weight of 25 mg/ml bromodeoxyuridine (BrdU) in PBS. Timed pregnancies were collected at 10.5, 13.5 and 18.5 dpc, the placenta washed in PBS, bisected, and fixed in 10% neutral buffered formalin at 4°C overnight. Tissue was then washed in PBS and 0.9% saline, dehydrated in ethanols and xylenes then embedded in paraffin. Seven-micron sections were cut using a RM2165 microtome (Leica). A BrdU staining kit (Zymed Laboratories) was used to determine proliferation rates in *Egfr*^{tm1Mag} homozygous null and wildtype placentas per manufacturer's protocol. Colorometric reaction was detected using DAB-tetrahydrochloride horseradish peroxidase substrate, counterstained with hematoxylin, dehydrated in a series of ethanols, and mounted using Permount (Fisher Scientific). Samples were photographed on a DMRE microscope (Leica) at a magnification of 400X using a CCD digital camera (SPOT Diagnostics). BrdU positive nuclei were counted in one field of view for 5-10 independent placenta from 3-4 BrdU injected pregnant females per time point. Percentages are expressed as the number of BrdU positive nuclei over total number of nuclei in a field of view.

Real-time PCR

Total RNA was prepared from 129/Sv and BALB/c 10.5 dpc placentas using Trizol reagent and purified using an RNAeasy mini kit according to the manufacturer's protocol (Qiagen). One microgram of each RNA sample was reverse transcribed with the High Capacity cDNA Archive Kit (Applied Biosystems) and equivalent amounts of cDNA were used in a real-time PCR reaction to measure transcript levels of *Cdkn1a*, *Cdkn1b*, *Myc,* and *Cdc25a*. Levels were normalized relative to expression of *Gusb* in each sample and fold change in gene expression was calculated using the $2^{(-\Delta\Delta Ct)}$ method [28]. Primer and probe sets for *Cdkn1a*, *Cdkn1b*, *Myc*, *Cdc25a*, and *Gusb* were Assays-On-Demand (Applied Biosysems) and used according to the manufacturer's protocol with a Mx3000P real-time PCR machine (Stratagene).

Statistical analysis

For BrdU experiments samples were collected from 2-5 independently injected females, with 2-10 placentas collected per gestational time. Error bars are expressed as the standard error of the mean (SEM). Significance was determined by the Mann-Whitney test with $p < 0.05$ being significant. For real-time PCR data *p*-values were determined by student's T-test with $p < 0.05$ being significant.

Results

Egfr transcripts are dynamically expressed in the developing mouse placenta

Three major transcripts of *Egfr* have been detected in rodent tissue by northern blot analysis; 10 and 6.5-Kb transcripts that encode the full-length 170 kD receptor and a 2.8-Kb transcript that encodes a secreted 95 kD protein corresponding to the extracellular ligand-binding domain of EGFR [29-31]. A quantitative RPA distinguishing the full-length and

truncated receptor transcripts revealed a dynamic expression pattern during gestation. Full-length *Egfr* transcripts are expressed at very low levels in the embryo from 8.5 to 10.5 dpc with expression increasing steadily from 11.5 dpc to 14.5 dpc and then decreasing after 14.5 dpc (Fig. 2A). No truncated *Egfr* transcripts are detectable during embryogenesis.

In contrast to the embryonic expression pattern, full-length and truncated *Egfr* transcripts are detectable at all stages of placental development. Expression of the full-length transcripts decrease from 9.5 to 11.5 dpc and then increase from 12.5 to 16.5 dpc, where the highest levels of expression are observed (Fig. 2B). Interestingly, the lowest level of expression occurs around 11.5 dpc, coincident with abnormal development of the *Egfr* nullizygous placenta and embryonic lethality on many genetic backgrounds [2,3,5]. The highest level of truncated receptor transcript is observed at 9.5 dpc. When compared to levels of full-length transcript at the same time points, truncated transcripts in the placenta decrease from 81% at 9.5 dpc to 17% at 13.5 dpc of the total *Egfr* transcripts.

ERBB receptor expression is unaltered in EGFR deficient placenta

Since individual members of the ERBB family can activate similar signaling pathways, it is possible that other ERBB family members compensate for the loss of EGFR during placental development in strains with a less severe phenotype. To address this possibility, localization of EGFR, ERBB2, ERBB3, and ERBB4 in 18.5 dpc wildtype and $Egfr^{tm1Mag}$ null placenta was determined by immunohistochemistry.

EGFR was detected primarily in the decidua, trophoblast giant and spongiotrophoblast cells, with low levels detected in the labyrinthine layer (Fig. 3A). The EGFR was not detected in the *Egfr* null placenta at 18.5 dpc (Fig. 3B). The only ERBB family member not detected in the wildtype or *Egfr* null placenta was ERBB2 (Fig. 3C and

D), suggesting that in the 18.5 dpc mouse placenta this receptor is expressed at undetectable levels or is not involved in normal placental formation. Up-regulation of ERBB2 was not detected in response to a lack of EGFR signaling. Both ERBB3 and ERBB4 were detected in the maternal decidua and in the trophoblast giant cells of wildtype and *Egfr* null placentas (Fig. 3E - H). Since dysregulation of ERBB2, ERBB3 or ERBB4 was not detected in the *Egfr* null placenta, it is unlikely that these ERBB receptors contribute to compensatory mechanisms supporting embryonic survival in the absence of EGFR.

Levels of the ERBB3 and EGFR were confirmed by western blot at 18.5 dpc, as well as at 10.5 and 13.5 dpc. No EGFR immunoreactivity was detected in homozygous *Egfr* null placenta, while a normal 170 kD EGFR protein was detected in corresponding wildtype samples (Fig. 4). Higher levels of ERBB3 were detected at 18.5 dpc compared to 10.5 and 13.5 dpc in wildtype placentas, with no significant differences noted between wildtype and *Egfr* null samples. Weak bands observed in 10.5 and 13.5 dpc samples likely reflect contribution from the deciduas, since EGFR, ERBB3 and ERBB4 are all highly expressed in the decidua.

Reduced trophoblast proliferation in EGFR deficient placentas

Differences in cellular proliferation in wildtype and *Egfr* null placenta were assessed by incorporation of the thymidine analog BrdU into cells that are in the S-phase of the cell cycle. Based on immunohistochemical analysis, the number of BrdU-positive nuclei appeared reduced in 10.5 dpc *Egfr* null placentas from 129/Sv, a strain exhibiting abnormal labyrinth and spongiotrophoblast development and embryonic lethality by 11.5 dpc (Table 3). At 10.5 dpc a 60% decrease in proliferation in the *Egfr* null placenta was detected compared to wildtype placenta, suggesting that there is a significant reduction in proliferating

trophoblast cells without EGFR. To determine whether the reduction in proliferation contributes to mid-gestation lethality of *Egfr* null embryos, BrdU incorporation was determined at 10.5 dpc in the ALR.129 mixed genetic background, which has a functional labyrinth but reduced spongiotrophoblast layer and supports embryo survival through late gestation. Similar to that observed in the 129/Sv background, EGFR deficiency on the ALR.129 background resulted in a 56% reduction in BrdU positive cells. These data suggest that proliferation does not contribute to differential survival of *Egfr* null embryos.

Interestingly at 13.5 dpc of gestation, there was no longer a statistically significant difference in BrdU incorporation between the ALR.129 wildtype and *Egfr* null placentas (Table 3). We also did not observe differences in proliferation rates in specific trophoblast layers when the amount of BrdU incorporation was analyzed specifically in the spongiotrophoblast or labyrinthine layer at 13.5 dpc (data not shown). By 18.5 dpc few cells are actively replicating (Table 3). Additionally there was no significant difference in the number of trophoblast cells undergoing apoptosis when comparing ALR.129 wildtype and *Egfr* null placentas at 10.5, 13.5 or 18.5 dpc using a TUNEL assay (Table 3). We observed few TUNEL-positive trophoblasts across gestation, consistent with previous reports characterizing apoptosis in mouse placental tissue [7,32].

To confirm the BrdU data, markers of proliferation and cell cycle arrest were measured by real-time PCR in 10.5 dpc *Egfr* wildtype and null placentas. Expression of *Cdc25a* and *Myc*, two genes known to be transcriptionally up-regulated in proliferating cells [33,34], were significantly higher in wildtype (n = 11) versus *Egfr* null (n = 12) placentas (Fig. 5). *Myc* expression in *Egfr* null placentas was 74% of wildtype levels ($p = 0.01$), while *Cdc25a* expression was 61% of wildtype levels ($p < 0.02$) (Fig. 5). *Cdkn1a* and *Cdkn1b* are

known to be transcriptionally up-regulated in cells arresting in the cell cycle at G1-S [33]. We found no significant changes in *Cdkn1a expression*, but *Cdkn1b* transcripts were significantly higher (117% compared to wildtype) in *Egfr* null placentas ($p < 0.05$) (Figure 5). These data are consistent with a greater number of *Egfr* nullizygous trophoblast cells undergoing cell cycle arrest.

Placental defects are not rescued by genetic reduction of cell cycle checkpoint regulators

Although genetic backgrounds showing disparite survival of *Egfr* null embryos have equivalent reductions in trophoblast proliferation at 10.5 dpc, it is possible that the ALR.129 strain overcomes the 10.5 dpc proliferation defect and continues to develop a functioning placenta while the 129/Sv strain does not. To investigate this, we intercrossed $Egfr^{tm1Mag}$ heterozygous mice with mice carrying null alleles of various cell cycle checkpoint genes that regulate the G1 to S transition [33,35], including three cyclin dependent kinase inhibitiors (CKIs), *Cdkn1a* ($p21^{Cip1}$), *Cdkn1b* ($p27^{Kip1}$), and *Cdkn2c* ($p18^{INK4c}$), as well as two tumor suppressors, *Trp53* (*p53*), and *Rb*. *Trp53* and *Cdkn1a* also regulate the G2 to M checkpoint [36]. Genetic ablation of these cell cycle checkpoint molecules would be expected to increase cellular proliferation and, if this contributed to the mid-gestation lethality observed on the 129/Sv background, increase survival of *Egfr* null embryos.

The 129/Sv background was used for $Trp53^{tm1Ty}$, Rb^{tm1Tyj}, $Cdkn1a^{tm1Tyj}$, and $Cdkn1b^{tm1Mlf}$ null allele crosses while the BALB/cJ background, which has a phenotype similar to 129/Sv, was used for $Trp53^{tm1Ty}$, $Cdkn2c^{tm1Yxi}$ and Rb^{tm1Tyj} null allele crosses. Surviving $Egfr^{tm1Mag}$ homozygous embryos were not detected at 13.5 dpc irrespective of $Trp53^{tm1Tyj}$ (n = 120), Rb^{tm1Tyj} (n = 108), or $Cdkn1b^{tm1Mlf}$ (n = 102) genotype (Table 4). At 13.5 dpc a low number of viable embryos from the $Cdkn2c^{tm1Yxi}$ cross were found to be

homozygous for *Egfr*^{tm1Mag} (2 out of 119). However, one of these two embryos was wildtype for *Cdkn2c*. Similarly 12 out of 257 total embryos from the *Cdkn1a*^{tm1Tyj} cross were found to be *Egfr*^{tm1Mag} homozygous and viable at 13.5 dpc. Data from *Cdkn1a*^{tm1Tyj}, *Egfr*^{tm1Mag} heterozygous intercrosses revealed that 3 of the 5 surviving *Egfr* nullizygous embryos carried wildtype *Cdkn1a* alleles. Because genotypes of *Cdkn1a*^{tm1Tyj} or *Cdkn2c*^{tm1Yxi} did not correlate with embryonic survival it is likely that *Cdkn1a*^{tm1Tyj} and *Cdkn2c*^{tm1Yxi} congenic lines were not pure 129/Sv or BALB/cJ and were probably segregating unknown genetic background modifiers of the *Egfr*^{tm1Mag} phenotype. In composite, these data indicate that removing negative regulators of the cell cycle is not sufficient to support survival of *Egfr* null embryos.

Discussion

EGFR transcripts and protein are abundantly detected in human placenta and aberrant expression of the receptor has been associated with IUGR, preeclampsia, and placenta accreta [17-22]. Interestingly, alternative transcripts from the *Egfr* locus that encode a secreted 60 kD protein corresponding to the extracellular ligand binding domain of EGFR have been reported in both human and mouse placenta [1,21,37]. It has been suggested that these secreted EGFRs play a role in negatively regulating ERBB signaling by sequestering ligand or binding cell membrane-associated ERBB receptors to prevent receptor phosphorylation and activation of downstream pathways [38]. Using RPA we demonstrated dynamic expression of the full-length and truncated *Egfr* transcript during mouse embryo and placental development. Truncated *Egfr* transcripts were not detected in the developing embryo, but low levels detected throughout placental development raise the possibility that secreted, ligand-binding EGFR may negatively regulate EGFR signaling in extra-embryonic

tissue. In addition, we observed up-regulation of full-length *Egfr* transcripts after 11.5 dpc suggesting that EGFR is actively being turned-over around the time that the placental labyrinth develops and begins to function. Since RPA provides no information on the localization of *Egfr* transcripts the dynamic expression patterns observed may reflect differences in the composition of the placenta related to gestational age rather than changes in *Egfr* expression. By immunohistochemistry EGFR has been detected in all layers of the developing mouse placenta, however, the antibody used does not distinguish between the full length and truncated receptor forms.

One potential explanation for strain-specificity of the *Egfr* nullizygous placental phenotype is that surviving strains may developmentally compensate for a lack of *Egfr* signaling by up-regulating expression of other ERBB family members. For example, strain-specific developmental compensation has been demonstrated in the *Ptgs2* (Cox2) null mouse uterus where up-regulation of *Ptgs1* (Cox1) allows partial rescue of fertility defects in CD-1 females [39]. We compared expression of ERBB2, ERBB3, and ERBB4 in wildtype and *Egfr* null placentas from two hybrid strains that survive until late gestation. ERBB2 was not detected, and although ERBB3 and ERBB4 were detected in the decidua and trophoblast giant cells at late gestation, there was no difference in expression or localization between *Egfr* wildtype and null placentas. In fact, EGFR-deficient strains that survive past mid-gestation probably utilize a mechanism other than ERBB compensation since ERBB2, ERBB3, and ERBB4 are not expressed at detectable levels in the spongiotrophoblasts or labyrinth trophoblasts, where defects in the *Egfr* nullizygous placenta are primarily observed.

EGFR plays an important role in regulating cellular proliferation and cell survival [40]. EGFR signaling has been shown to promote cell cycle progression through the G1-S,

as well as G2-M checkpoints, and it is possible that the strain-specific placental phenotype observed in *Egfr* null mice could result from surviving strains using alternate pathways to enhance cell cycle progression in trophoblasts [41]. We found that *Egfr* null placentas on 129/Sv and ALR.129 genetic backgrounds have fewer BrdU-positive trophoblasts than wildtype at 10.5 dpc. However, proliferation defects in the *Egfr* nullizygous placentas do not correlate with embryonic lethality since *Egfr* null embryos on ALR.129 survive to late gestation despite having equivalently reduced trophoblast proliferation compared to embryos on a 129/Sv background at 10.5 dpc,. This result does not exclude the possibility that the ALR.129, but not the 129/Sv genetic background, harbors modifiers allowing the strain to overcome proliferation defects at 10.5 dpc and develop a functioning placenta. We tested this hypothesis by genetically reducing negative cell cycle regulators downstream of EGFR, thus potentially permitting cell cycle progression in the absence of EGFR on backgrounds that do not support survival of *Egfr* null embryos past mid-gestation. Hyper-proliferation of labyrinth trophoblasts has been observed in mouse RB-deficient placentas and in placentas deficient for both CDKN1B and CDKN1C [42-44]. We surmised that eliminating these and other cell cycle checkpoint components would rescue *Egfr* nullizygous placental development by increasing trophoblast proliferation. We intercrossed $Egfr^{tm1Mag}$ heterozygotes with mice segregating $Trp53^{tm1Tyj}$, Rb^{tm1Tyj}, $Cdkn1a^{tm1Tyj}$, $Cdkn1b^{tm1Mlf}$ or $Cdkn2c^{tm1Yxi}$ null alleles carried on 129/Sv and BALB/cJ backgrounds. Results from the intercrosses indicated that genetic reduction of negative cell cycle checkpoint components does not rescue the embryonic lethality of EGFR deficient embryos.

Together our data indicates that proliferation defects observed in 10.5 dpc $Egfr^{tm1Mag}$ nullizygous placentas do not contribute to the midgestation embryonic lethality since the

phenotype is observed in both surviving (ALR.129) and non-surviving (129/Sv) strains. At 10.5 dpc the spongiotrophoblast is likely the primary lineage affected by the proliferation defect because both ALR.129 and 129/Sv show dramatic reduction of this trophoblast compartment. Consequently, a decrease in the spongiotrophoblast population probably does not contribute to placental insufficiency in *Egfr* nullizygous embryos. Rather, survival of embryos beyond 11.5 dpc is prevented by an abnormal labyrinth phenotype in strains such as 129/Sv. Additional experiments utilizing markers for trophoblast sub-type progenitors are necessary to evaluate differences in early labyrinth cell populations that may distinguish surviving and non-surviving strains.

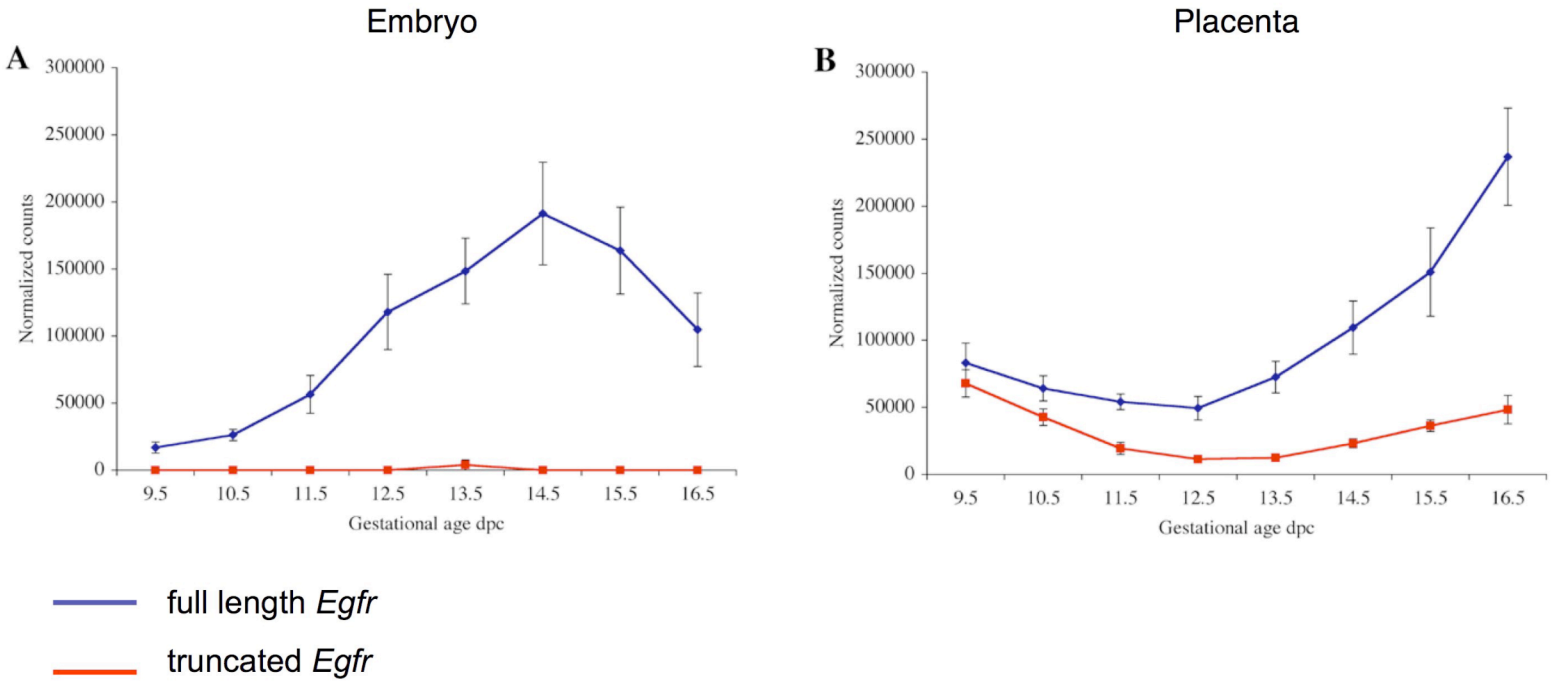

Figure 2. Expression profile of *Egfr* during development. Graphs of normalized counts from (A) embryonic and (B) placental RNase protection assays at gestational time points 9.5 to 16.5 dpc. Transcript levels were quantitated by phosphoimager analysis, normalized to *Gapdh* expression and expressed as normalized counts on the Y-axis. Blue lines represent full-length *Egfr* transcript levels and red lines represent truncated *Egfr* levels. Error is represented as the SEM. (Strunk)

Figure 3. Immunohistochemistry for ERBB family members on late gestation placentas. Immunohistochemistry was done using FVB.129 or BALB.129 N_2 placentas at 18.5 dpc. Panels (A, C, E, G) are wildtype samples, while (B, D, F, H) are *Egfr*^{tm1Mag} null samples. (A, B) Protein localization for an EGFR specific antibody. In wildtype sample EGFR is localized to both the spongiotrophoblast and labyrinthine layers. Note loss of localization of EGFR in the *Egfr*^{tm1Mag} null placenta, although there is some immunoreactivity in the maternally derived decidual layer. Also note the loss of the spongiotrophoblast cell layer. (C, D) ERBB2 is not detected in either wildtype or null samples. (E, F) Localization of ERBB3 protein to the TGC layer and the maternal decidua. Levels of protein appear equivalent in both the wildtype and *Egfr*^{tm1Mag} null placenta. (G, H) Protein levels of ERBB4 appear unaltered between the wildtype and *Egfr*^{tm1Mag} null samples, with localization observed in the TGC and maternal decidua. Abbreviations: SP:spongiotrophoblast layer; LT:labyrinthine trophoblast layer; De:decidua; TGC:trophoblast giant cells. Arrowheads indicate TGC, scale bars 50μm. (Strunk)

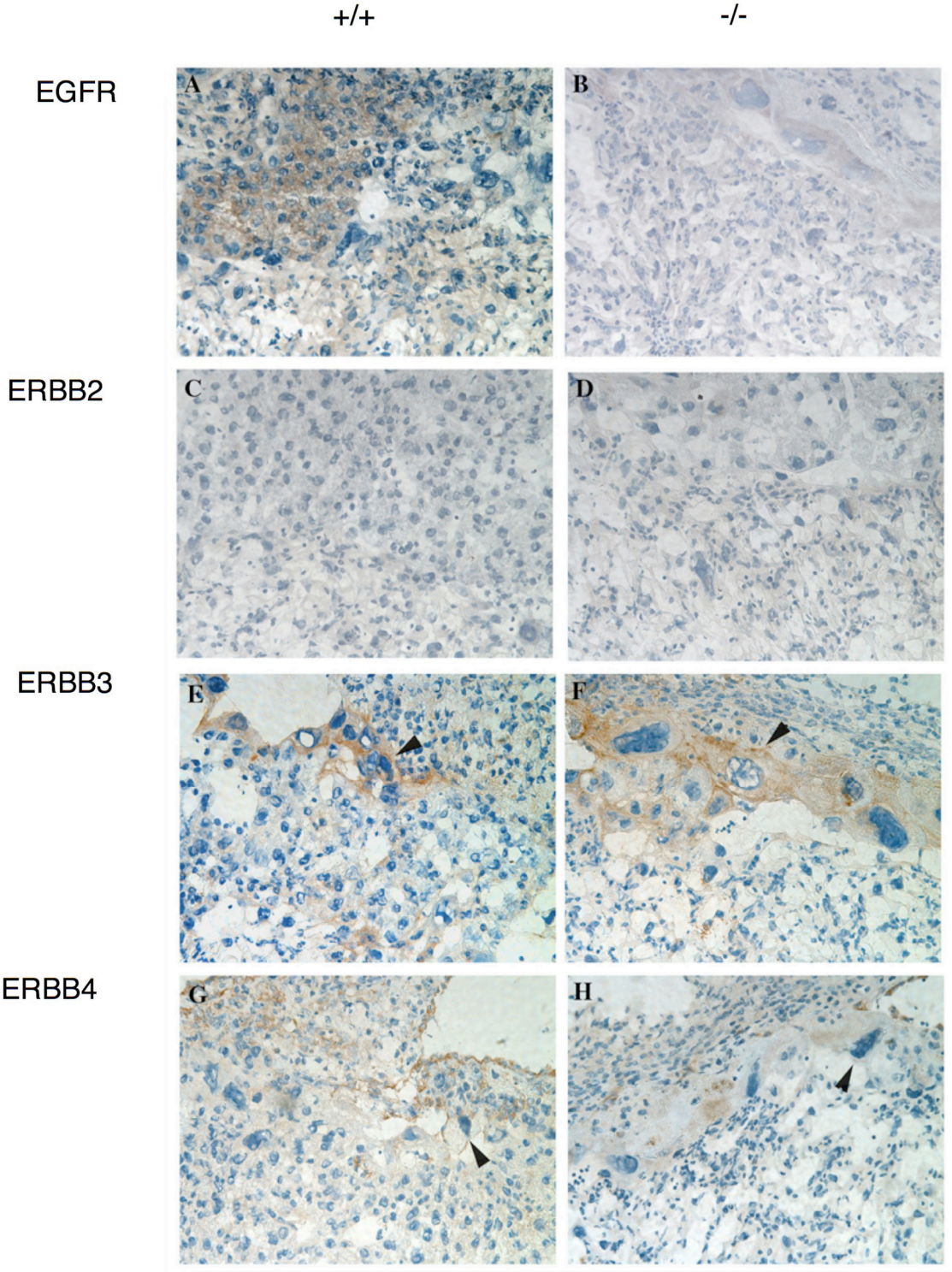
+/+
-/-
EGFR
ERBB2
ERBB3
ERBB4
A
B
C
D
E
F
G
H

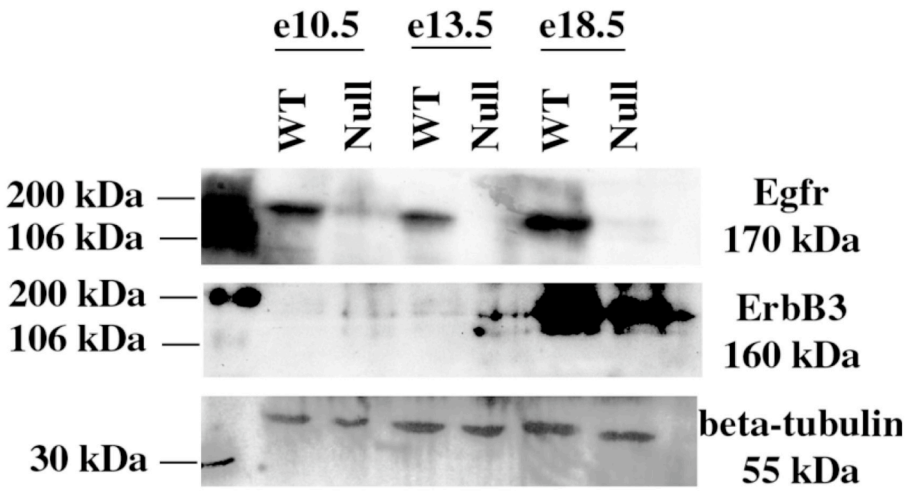

Figure 4. Western blot analysis of EGFR, ERBB3 and TUBB1 (beta-tubulin) during placental development. Protein lysates are from *Egfr* wildtype or null placentas isolated at the indicated time points. Beta tubulin represents loading control. (Strunk)

Table 3. Percentage of BrdU or TUNEL positive nuclei in placentas

	10.5 dpc	13.5 dpc	18.5 dpc
BrdU-129/Sv			
Wildtype	45.3 ± 5.0% (n = 5)	ND	ND
Egfr null	27.0 ± 12.5% (n = 7)	ND	ND
BrdU-ALR.129			
Wildtype	38.3 ± 6.2% (n = 7)	9.3 ± 1.8% (n = 4)	0.71 ± 0.55% (n = 8)
Egfr null	21.5 ± 11.8% (n = 10)	10.1 ± 1.6% (n = 2)	0.06±0.067% (n = 6)
TUNEL-ALR.129			
Wildtype	1.1 ± 0.6% (n = 6)	0.5 ± 0.5% (n = 6)	1.96 ± 1.3% (n = 5)
Egfr null	0.83 ± 0.4% (n = 7)	0.48 ± 0.48% (n = 5)	0.0% (n = 3)

ND, not determined

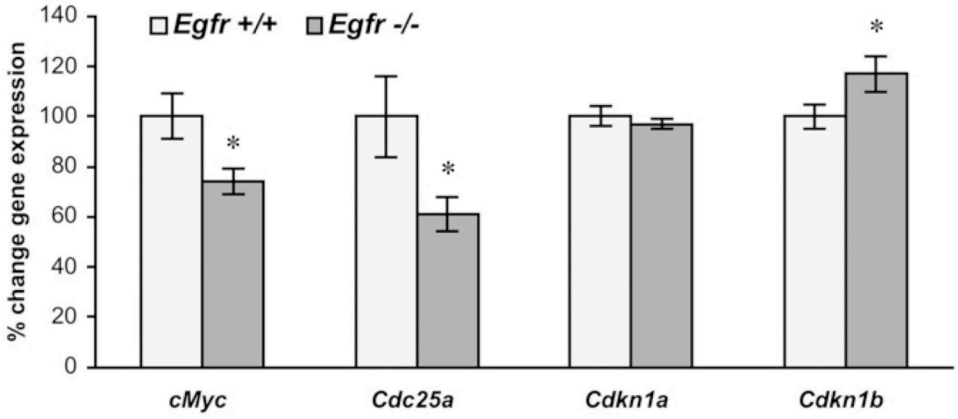

Figure 5. Real-time PCR expression analysis of proliferation and cell cycle arrest markers. RNA from 10.5 dpc placenta are identified by open bars, *Egfr* wildtype and gray bars, *Egfr* null. Y-axis represents the percent change in gene expression compared to the average expression in wildtype samples adjusted to 100%. Expression of proliferation, *Myc* and *Cdc25a*, and cell cycle arrest, *Cdkn1a* and *Cdkn1b*, markers are presented.

Table 4. Viable *Egfr* null embryos observed at 13.5 dpc in intercrosses with cell cycle checkpoint deficient strains

Intercross	Strain(s)	Total Embryos	Viable *Egfr* -/-
Trp53 +/-, *Egfr* +/-	129/Sv, Balb/cJ	92	0
Trp53 -/-, *Egfr* +/-	Balb/cJ	28	0
Rb +/-, *Egfr* +/-	129/Sv, Balb/cJ	108	0
Cdkn1a +/-, *Egfr* +/-	129/Sv	103	5[A]
Cdkn1a -/-, *Egfr* +/-	129/Sv	154	7
Cdkn1b +/-, *Egfr* +/-	129/Sv	102	0
Cdkn2c +/-, *Egfr* +/-	Balb/cJ	119	2[B]

[A] 3 out of 5 *Egfr* -/- embryos were *Cdkn1a* +/+ or +/-

[B] 1 out of 2 *Egfr* -/- embryos was *Cdkn2c* +/+

References

[1] Reiter JL, Threadgill DW, Eley GD, Strunk KE, Danielsen AJ, Sinclair CS, Pearsall RS, Green PJ, Yee D, Lampland AL, Balasubramaniam S, Crossley TD, Magnuson TR, James CD, Maihle NJ. Comparative genomic sequence analysis and isolation of human and mouse alternative EGFR transcripts encoding truncated receptor isoforms. Genomics 2001; 71:1-20.

[2] Sibilia M, Wagner EF. Strain-dependent epithelial defects in mice lacking the EGF receptor. Science 1995; 269:234-238.

[3] Threadgill DW, Dlugosz AA, Hansen LA, Tennenbaum T, Lichti U, Yee D, LaMantia C, Mourton T, Herrup K, Harris RC, et al. Targeted disruption of mouse EGF receptor: effect of genetic background on mutant phenotype. Science 1995; 269:230-234.

[4] Sibilia M, Steinbach JP, Stingl L, Aguzzi A, Wagner EF. A strain-independent postnatal neurodegeneration in mice lacking the EGF receptor. Embo J 1998; 17:719-731.

[5] Strunk KE, Amann V, Threadgill DW. Phenotypic variation resulting from a deficiency of epidermal growth factor receptor in mice is caused by extensive genetic heterogeneity that can be genetically and molecularly partitioned. Genetics 2004; 167:1821-1832.

[6] Adams RH, Porras A, Alonso G, Jones M, Vintersten K, Panelli S, Valladares A, Perez L, Klein R, Nebreda AR. Essential role of p38alpha MAP kinase in placental but not embryonic cardiovascular development. Mol Cell 2000; 6:109-116.

[7] Bissonauth V, Roy S, Gravel M, Guillemette S, Charron J. Requirement for Map2k1 (Mek1) in extra-embryonic ectoderm during placentogenesis. Development 2006; 133:3429-3440.

[8] Hatano N, Mori Y, Oh-hora M, Kosugi A, Fujikawa T, Nakai N, Niwa H, Miyazaki J, Hamaoka T, Ogata M. Essential role for ERK2 mitogen-activated protein kinase in placental development. Genes Cells 2003; 8:847-856.

[9] Itoh M, Yoshida Y, Nishida K, Narimatsu M, Hibi M, Hirano T. Role of Gab1 in heart, placenta, and skin development and growth factor- and cytokine-induced extracellular signal-regulated kinase mitogen-activated protein kinase activation. Mol Cell Biol 2000; 20:3695-3704.

[10] Johnson RS, Spiegelman BM, Papaioannou V. Pleiotropic effects of a null mutation in the c-fos proto-oncogene. Cell 1992; 71:577-586.

[11] Man AK, Young LJ, Tynan JA, Lesperance J, Egeblad M, Werb Z, Hauser CA, Muller WJ, Cardiff RD, Oshima RG. Ets2-dependent stromal regulation of mouse mammary tumors. Mol Cell Biol 2003; 23:8614-8625.

[12] Mikula M, Schreiber M, Husak Z, Kucerova L, Ruth J, Wieser R, Zatloukal K, Beug H, Wagner EF, Baccarini M. Embryonic lethality and fetal liver apoptosis in mice lacking the c-raf-1 gene. Embo J 2001; 20:1952-1962.

[13] Qian X, Esteban L, Vass WC, Upadhyaya C, Papageorge AG, Yienger K, Ward JM, Lowy DR, Santos E. The Sos1 and Sos2 Ras-specific exchange factors: differences in placental expression and signaling properties. Embo J 2000; 19:642-654.

[14] Saxton TM, Cheng AM, Ong SH, Lu Y, Sakai R, Cross JC, Pawson T. Gene dosage-dependent functions for phosphotyrosine-Grb2 signaling during mammalian tissue morphogenesis. Curr Biol 2001; 11:662-670.

[15] Schorpp-Kistner M, Wang ZQ, Angel P, Wagner EF. JunB is essential for mammalian placentation. Embo J 1999; 18:934-948.

[16] Shaw AT, Meissner A, Dowdle JA, Crowley D, Magendantz M, Ouyang C, Parisi T, Rajagopal J, Blank LJ, Bronson RT, Stone JR, Tuveson DA, Jaenisch R, Jacks T. Sprouty-2 regulates oncogenic K-ras in lung development and tumorigenesis. Genes Dev 2007; 21:694-707.

[17] Faxen M, Nasiell J, Blanck A, Nisell H, Lunell NO. Altered mRNA expression pattern of placental epidermal growth factor receptor (EGFR) in pregnancies complicated by preeclampsia and/or intrauterine growth retardation. Am J Perinatol 1998; 15:9-13.

[18] Ferrandina G, Lanzone A, Scambia G, Caruso A, Panici PB, Mancuso S. Epidermal growth factor receptors in placentae and fetal membranes from hypertension-complicated pregnancies. Hum Reprod 1995; 10:1845-1849.

[19] Fondacci C, Alsat E, Gabriel R, Blot P, Nessmann C, Evain-Brion D. Alterations of human placental epidermal growth factor receptor in intrauterine growth retardation. J Clin Invest 1994; 93:1149-1155.

[20] Hofmann GE, Drews MR, Scott RT, Jr., Navot D, Heller D, Deligdisch L. Epidermal growth factor and its receptor in human implantation trophoblast: immunohistochemical evidence for autocrine/paracrine function. J Clin Endocrinol Metab 1992; 74:981-988.

[21] Reiter JL, Maihle NJ. Characterization and expression of novel 60-kDa and 110-kDa EGFR isoforms in human placenta. Ann N Y Acad Sci 2003; 995:39-47.

[22] Tseng JJ, Hsu SL, Wen MC, Ho ES, Chou MM. Expression of epidermal growth factor receptor and c-erbB-2 oncoprotein in trophoblast populations of placenta accreta. Am J Obstet Gynecol 2004; 191:2106-2113.

[23] Threadgill DW, Yee D, Matin A, Nadeau JH, Magnuson T. Genealogy of the 129 inbred strains: 129/SvJ is a contaminated inbred strain. Mamm Genome 1997; 8:390-393.

[24] Franklin DS, Godfrey VL, Lee H, Kovalev GI, Schoonhoven R, Chen-Kiang S, Su L, Xiong Y. CDK inhibitors p18(INK4c) and p27(Kip1) mediate two separate pathways to collaboratively suppress pituitary tumorigenesis. Genes Dev 1998; 12:2899-2911.

[25] Jacks T, Fazeli A, Schmitt EM, Bronson RT, Goodell MA, Weinberg RA. Effects of an Rb mutation in the mouse. Nature 1992; 359:295-300.

[26] Jacks T, Remington L, Williams BO, Schmitt EM, Halachmi S, Bronson RT, Weinberg RA. Tumor spectrum analysis in p53-mutant mice. Curr Biol 1994; 4:1-7.

[27] Jackson RJ, Adnane J, Coppola D, Cantor A, Sebti SM, Pledger WJ. Loss of the cell cycle inhibitors p21(Cip1) and p27(Kip1) enhances tumorigenesis in knockout mouse models. Oncogene 2002; 21:8486-8497.

[28] Livak KJ, Schmittgen TD. Analysis of relative gene expression data using real-time quantitative PCR and the 2(-Delta Delta C(T)) Method. Methods 2001; 25:402-408.

[29] Das SK, Tsukamura H, Paria BC, Andrews GK, Dey SK. Differential expression of epidermal growth factor receptor (EGF-R) gene and regulation of EGF-R bioactivity by progesterone and estrogen in the adult mouse uterus. Endocrinology 1994; 134:971-981.

[30] Petch LA, Harris J, Raymond VW, Blasband A, Lee DC, Earp HS. A truncated, secreted form of the epidermal growth factor receptor is encoded by an alternatively spliced transcript in normal rat tissue. Mol Cell Biol 1990; 10:2973-2982.

[31] Tong BJ, Das SK, Threadgill D, Magnuson T, Dey SK. Differential expression of the full-length and truncated forms of the epidermal growth factor receptor in the preimplantation mouse uterus and blastocyst. Endocrinology 1996; 137:1492-1496.

[32] Nakamura Y, Hamada Y, Fujiwara T, Enomoto H, Hiroe T, Tanaka S, Nose M, Nakahara M, Yoshida N, Takenawa T, Fukami K. Phospholipase C-delta1 and -delta3 are essential in the trophoblast for placental development. Mol Cell Biol 2005; 25:10979-10988.

[33] Blagosklonny MV, Pardee AB. The restriction point of the cell cycle. Cell cycle (Georgetown, Tex 2002; 1:103-110.

[34] Jinno S, Suto K, Nagata A, Igarashi M, Kanaoka Y, Nojima H, Okayama H. Cdc25A is a novel phosphatase functioning early in the cell cycle. Embo J 1994; 13:1549-1556.

[35] Roussel MF. The INK4 family of cell cycle inhibitors in cancer. Oncogene 1999; 18:5311-5317.

[36] Taylor WR, Stark GR. Regulation of the G2/M transition by p53. Oncogene 2001; 20:1803-1815.

[37] Ilekis JV, Stark BC, Scoccia B. Possible role of variant RNA transcripts in the regulation of epidermal growth factor receptor expression in human placenta. Mol Reprod Dev 1995; 41:149-156.

[38] Basu A, Raghunath M, Bishayee S, Das M. Inhibition of tyrosine kinase activity of the epidermal growth factor (EGF) receptor by a truncated receptor form that binds to EGF: role for interreceptor interaction in kinase regulation. Mol Cell Biol 1989; 9:671-677.

[39] Wang H, Ma WG, Tejada L, Zhang H, Morrow JD, Das SK, Dey SK. Rescue of female infertility from the loss of cyclooxygenase-2 by compensatory up-regulation of cyclooxygenase-1 is a function of genetic makeup. J Biol Chem 2004; 279:10649-10658.

[40] Grant S, Qiao L, Dent P. Roles of ERBB family receptor tyrosine kinases, and downstream signaling pathways, in the control of cell growth and survival. Front Biosci 2002; 7:d376-389.

[41] Baker NE, Yu SY. The EGF receptor defines domains of cell cycle progression and survival to regulate cell number in the developing Drosophila eye. Cell 2001; 104:699-708.

[42] Wenzel PL, Wu L, de Bruin A, Chong JL, Chen WY, Dureska G, Sites E, Pan T, Sharma A, Huang K, Ridgway R, Mosaliganti K, Sharp R, Machiraju R, Saltz J, Yamamoto H, Cross JC, Robinson ML, Leone G. Rb is critical in a mammalian tissue stem cell population. Genes Dev 2007; 21:85-97.

[43] Wu L, de Bruin A, Saavedra HI, Starovic M, Trimboli A, Yang Y, Opavska J, Wilson P, Thompson JC, Ostrowski MC, Rosol TJ, Woollett LA, Weinstein M, Cross JC, Robinson ML, Leone G. Extra-embryonic function of Rb is essential for embryonic development and viability. Nature 2003; 421:942-947.

[44] Zhang P, Wong C, DePinho RA, Harper JW, Elledge SJ. Cooperation between the Cdk inhibitors p27(KIP1) and p57(KIP2) in the control of tissue growth and development. Genes Dev 1998; 12:3162-3167.

CHAPTER III

PLACENTAL AND EMBRYONIC GROWTH PHENOTYPES IN MICE WITH REDUCED FUNCTION OF EPIDERMAL GROWTH FACTOR RECEPTOR

Abstract

Epidermal growth factor receptor (EGFR) is an ERBB family receptor tyrosine kinase essential for a wide range of developmental and physiological processes. Although characterization of knockout mice has revealed some redundant functions for the four ERBB receptors only EGFR is required for development of the placenta. *Egfr*^{tm1Mag} nullizygous placentas exhibit strain-specific defects that range from mild reductions in spongiotrophoblasts to severe labyrinth dysmorphogenesis that results in mid-gestational embryonic lethality. The aim of the current study was to characterize placental development in several congenic strains homozygous for the hypomorphic *Egfr*^{wa2} allele or heterozygous for the antimorphic *Egfr*^{Wa5} allele. *Egfr*^{wa2} homozygous embryos and placentas exhibited strain-dependent growth restriction at 15.5 dpc while *Egfr*^{Wa5} heterozygous placentas were only slightly reduced in size with no effect on embryonic growth. A panel of genes expressed specifically in the various trophoblast cell subtypes of the placenta was used to quantify changes in differentiated trophoblasts. *Egfr*^{wa2} homozygous and *Egfr*^{Wa5} heterozygous placentas exhibited reduced expression of spongiotrophoblast and glycogen cell markers with *Egfr*^{wa2} homozygotes having the most pronounced changes. At the histological level *Egfr*^{wa2} homozygous placentas had a reduced layer of spongiotrophoblast and in some strains spongiotrophoblasts and glycogen cells were almost completely absent.

Our results demonstrate that more EGFR signaling occurs in *Egfr*^{Wa5} heterozygotes versus *Egfr*^{wa2} homozygotes and suggest that *Egfr*^{wa2} homozygous embryos may be useful models for studying intrauterine growth restriction (IUGR). During our study we also consistently observed differences between strains in wildtype placenta and embryo size as well as in expression of trophoblast cell subtype markers. Strain-dependent placental trophoblast composition and gene expression may contribute to phenotypic variability observed in knockouts for *Egfr* and other genes.

Introduction

Epidermal growth factor receptor (EGFR) is the prototypical member of the ERBB family of receptor tyrosine kinases and is known to regulate many aspects of cellular biology including cell proliferation, survival, differentiation and migration. Eleven known ligands bind the extra-cellular region of ERBB-family receptors, and activation of the tyrosine kinase domain occurs following receptor homo- or heterodimerization. The resulting biological responses are dependent upon specific signaling cascades initiated by ERBBs and can be influenced by the particular ligand – ERBB combination [1]. Studies using cultured cells have underscored the importance of EGFR in modulating various cellular processes but animal models have been able to demonstrate that EGFR is required for numerous developmental and physiological processes [2]. *In vivo* studies have shown that EGFR is particularly important for normal placental development in mice; placentas from *Egfr* nullizygous ($Egfr^{tm1Mag/tm1Mag}$) embryos exhibit strain-specific defects that result in differential embryonic lethality [3,4]. Two additional *Egfr* alleles result in reduced EGFR signaling in mice, the recessive hypomorphic $Egfr^{wa2}$ (*waved-2*) and dominant antimorphic $Egfr^{Wa5}$ (*Waved-5*) alleles [5-8]. These alleles can provide insight into the level of EGFR signaling required for normal placental development.

$Egfr^{wa2}$ is a classical spontaneous mutation that arose in 1935, and causes a distinct wavy coat phenotype in the homozygote (Figure 6). This recessive mutation was subsequently found to be a single nucleotide transversion resulting in a Valine → Glycine substitution in the highly conserved kinase domain of EGFR [6,8]. Since mice homozygous for the $Egfr^{tm1mag}$ null allele die before or shortly after birth, the hypomorphic $Egfr^{wa2}$ allele has been the primary model used to study the effect of attenuated EGFR signaling in a

variety of adult physiological and disease states. In addition to eye and hair phenotypes the adult *Egfr*^{wa2} homozygous mouse exhibits delayed onset of puberty, abnormal ovulation, enlarged aortic valves and cardiac hypertrophy, decreased body size, defects in mammary gland development and lactation, increased susceptibility to colitis, and impaired intestinal adaptation following small bowel resection [6,9-14]. *Egfr*^{wa2} homozygosity reduces tumor number in several mouse models of cancer including the *Apc*^{min} intestinal tumorigenesis, the *Nf1*$^{+/-}$, *p53*$^{+/-}$ neurofibromatosis-related peripheral nerve tumorigenesis, the transgenic SOS-F skin tumor and the MMTV-ErbB2 mammary tumor models suggesting that EGFR plays a role in the development and/or progression of many types of cancer [15-18]. Similarly *Egfr*^{wa2} homozygosity significantly reduces the number of renal cysts in the *orpk* model of autosomal recessive polycystic kidney disease [19].

There have been some limitations in using *Egfr*^{wa2} homozygous mice to clearly define the physiological roles of EGFR. *Egfr*^{wa2} has traditionally been maintained in cis with the tightly linked mutant *Wnt3a* allele, *Wnt3a* ^{Vt} (*Vestigal tail*), making phenotypic analysis of reduced EGFR signaling by itself difficult. In addition, *Egfr*^{wa2} has typically been bred on a mixed background and since the *Egfr* nullizygous phenotype is influenced by genetic modifiers a mixed background could mask phenotypes that become evident when *Egfr*^{wa2} mice are inbred.

The *Egfr*^{Wa5} allele arose in a large, genome-wide ethylnitrosourea (ENU) mutagenesis screen for dominant visible mutations in the mouse. *Egfr*^{Wa5} heterozygous mice were first identified by their open eyelids at birth and development of a wavy coat, similar to the phenotype of *Egfr*^{wa2} homozygous mice (Figure 6). *Egfr*^{Wa5} failed to complement the *Egfr*^{tm1mag} null allele and was shown to function as an antimorph since *Egfr*^{Wa5}, but not

Egfr^{tm1mag} heterozygotes, exhibit a phenotype [7]. Although *Egfr*^{Wa5} heterozygotes are viable, *Egfr*^{Wa5} homozygotes die prenatally and exhibit placental defects identical to those of *Egfr*^{tm1mag} homozygous null embryos. Placentas from *Egfr*^{Wa5} heterozygotes on a mixed background show variable reduction in the spongiotrophoblast layer and some abnormalities in the labyrinth region, but there are no significant effects on embryo survival.

A single nucleotide missense mutation was found in the *Egfr*^{Wa5} allele that results in an Asp → Gly substitution in the highly conserved DFG domain of the EGFR kinase catalytic loop [5,7]. The Asp833 residue is involved in coordination of ATP and Mg^{2+} and is essential for the phospho-transfer reaction of the kinase. Results from *in vitro* studies with *Egfr*^{Wa5} suggest that it encodes a kinase-dead EGFR since no phosphorylation of WA5 is detected following stimulation with ligands. In agreement with the genetic data showing that *Egfr*^{Wa5}is an antimorph, in vitro studies have also demonstrated that WA5 receptor can inhibit phosphorylation of wildtype EGFR and MAPK in a dose-dependent manner. In CHO cells transfected with equal amount of wildtype EGFR and the WA5 receptor less than 10% of wildtype phosphorylation levels were observed by western blot [7]. There have been no studies that report the effect of WA5 on phosphorylation of other ERBB family members.

To have an EGFR allelic series available in the mouse is a phenomenal resource since EGFR is involved in a multitude of developmental processes and human diseases. Although both *Egfr*^{wa2} and *Egfr*^{Wa5} alleles result in reduced EGFR signaling, the activity and phenotypic consequences of *Egfr*^{wa2} homozygosity has not been compared to that of *Egfr*^{Wa5} heterozygosity in mice on the same genetic background. *Egfr*^{Wa5} heterozygous mice appear highly similar to *Egfr*^{wa2} homozygotes. As adults both genotypes exhibit a wavy coat and curly or broken whiskers and during embryogenesis delayed eyelid closure is incompletely

penetrant. The only functional studies that have shown a difference in phenotype between the *Egfr*^{wa2} homozygote and the *Egfr*^{Wa5} heterozygote are crosses with the *Apc*^{Min} intestinal tumor model [7,17]. A more substantial reduction in tumor number occurs when the *Apc*^{Min} mutation is bred onto the *Egfr*^{wa2} homozygous background than onto the *Egfr*^{Wa5} heterozygous background suggesting that the *Egfr*^{Wa5} heterozygous mice retain higher levels of EGFR activity than *Egfr*^{wa2} homozygous mice. However the data is confounded by the fact that previous crosses were performed on different mixed genetic backgrounds.

Recently we bred the *Egfr*^{wa2} and *Egfr*^{Wa5} alleles to congenicity on several genetic backgrounds. This study reports the effects of reduced EGFR signaling on placental development and embryonic growth for three genetic backgrounds, C57BL/6J (B6), 129S1/SvImJ (129), and BTBR/J-T+, tf/tf (BTBR). Wildtype placenta weight, embryo weight, and mRNA levels of genes selected for their trophoblast-specific expression were found to be highly strain-dependent. *Egfr*^{wa2} homozygous placentas are reduced in size in all three strains and a proportion of the 129-*Egfr*^{wa2} homozygotes die before 15.5dpc. *Egfr*^{wa2} homozygous embryos also display background-dependent growth restriction in late gestation, which is most severe on 129 and BTBR backgrounds. *Egfr*^{Wa5} heterozygous placentas exhibit minor reduction in size on all three backgrounds with no impact on embryonic growth. These results suggest that reduced levels of EGFR signaling can interfere with normal placental development. In addition, our data clearly shows that the level of EGFR signaling in *Egfr*^{Wa5} heterozygous mice is higher than in *Egfr*^{wa2} homozygotes.

Materials and Methods

Mice and genetic crosses

Congenic *Egfr*^{wa2} lines were generated by backcrossing outbred C57BL/6JEiC3H-a/A-*Egfr*$^{wa2/wa2}$ *Wnt3a*$^{vt/vt}$ mice obtained from The Jackson Laboratory (Bar Harbor, ME) to B6, 129 and BTBR wildtype inbred strains for 10 or more generations. Removal of the linked *Wnt3a*^{vt} allele, 20 cM distal to *Egfr* on chromosome 11, was verified by PCR-based genotyping (Figure 7). Congenic *Egfr*^{wa2} heterozygous mice were then intercrossed to produce litters from each background containing wildtype, *Egfr*^{wa2} heterozygous and homozygous congenic embryos and pups (Figure 8A).

Congenic *Egfr*^{Wa5} mice were generated by backcrossing heterozygous *Egfr*^{Wa5} mice from a mixed genetic background to inbred B6, 129 and BTBR strains for 10 or more generations. Congenic heterozygous mice were then crossed to wildtype animals of the same strain to produce litters containing wildtype and *Egfr*^{wa5} heterozygous congenic embryos and pups (Figure 8B).

Mice were fed Purina Mills Lab Diet 5058 or 5010 and water *ad libitum* under specific pathogen free conditions in an American Association for the Accreditation of Lab Animal Care approved facility. All experiments were approved by an Institutional Animal Care and Use Committee.

Genotyping

DNA was extracted from adult ear punches or embryo tail biopsies for genotyping by incubating at 95°C in 100 *u*L of 25mM NaOH/0.2mM EDTA for 20 minutes and then neutralizing with 100 *u*L 40mM TrisHCl pH 5.0. For the subsequent genotyping reactions, 1 *u*L of lysed tissue sample was used per reaction.

The *Egfr*^{wa2} allele was amplified by PCR with the following primers: Wa2F, 5'-TACCCAGAAAGGGATATGCG-3' and Wa2R, 5'- GGAGCCAATGTTGTCCTTGT-3' (Qiagen). PCR conditions were 30 cycles at 94°C for 30 sec, 60°C for 60 sec and 72°C for 60 sec. PCR products were digested for 3 hours at 37°C with *Fok* I and Restriction Enzyme Buffer 2 (NEB) and run on a 3% agarose gel to separate a 230-bp product corresponding to wildtype *Egfr* and a 130 and 100-bp set of products corresponding to the digested *Egfr*^{wa2} allele.

Egfr^{Wa5} allele was detected by real-time PCR with primers WA5F, 5'-GTGAAGACACCACAGCATGTC-3' and WA5R, 5'-CTCTTCAGCACCAAGCAGTTTG-3' along with 5' VIC-labeled probe WA5V1, 5'-AAGATCACAGATTTTGG-3' to detect wildtype *Egfr* and 5' FAM-labeled probe WA5M1, 5'-AGATCACAGGTTTTGG-3' to detect *Egfr*^{Wa5} (ABI). Genotyping was performed on an MXP-3000 Real-time PCR instrument (Stratagene) with 2X Taqman Universal PCR Master Mix (Applied Biosystems) and 20X mix primers and probes. PCR conditions were 95°C for 10 minutes followed by 40 cycles of 92°C for 15 seconds and 60°C for 1 minute. Amplification of the wildtype allele was detected by comparative quantification of VIC-labeled PCR products and amplification of the *Egfr*^{Wa5} allele was detected by comparative quantification of FAM-labeled PCR products with positive and negative *Egfr*^{Wa5} adult tissue used as reference sample.

Collection of placenta samples

Noon on the day that copulation plugs were observed was designated as 0.5 days post-coitus (dpc). Pregnant females were euthanized by exposure to a lethal dose of isoflourane and embryos with their corresponding placentas dissected from the uterine horns on the morning of 15.5 dpc or 18.5 dpc into phosphate buffered saline (PBS). The placenta

and extra-embryonic tissues were separated from the embryo by mechanical dissection and a tail biopsy collected for DNA extraction to determine the genotype of each embryo. Wet weights of embryos and placentas were recorded at the time of dissection. Placentas were preserved in RNAlater (Ambion) for extraction of RNA or fixed in 10% NBF (neutral buffered formalin) for histological analysis.

Histology

After fixing placentas in 10% neutral buffered formalin overnight, tissues were washed in PBS, dehydrated in ethanols and xylenes, and embedded in paraffin. Seven-micron sections were cut using a Leica RM2165 microtome. Sections were deparaffinized, rehydrated in a graded series of ethanols, and stained with hematoxylin and eosin (H&E) or Periodic acid-Schiff (PAS). Stained sections were dehydrated in a series of ethanols and mounted using permount. Representative histological images were photographed on a Nikon FXA microscope at a magnification of 1.25X, 10X, or 12 X using a CCD digital camera.

Real-time PCR

Placentas were homogenized in 1.2 mL Trizol using a bead mill (Eppendorf) and RNA was isolated according to manufacturer's protocol (Invitrogen). For each sample, 15 ug of RNA was DNAse-treated, followed by a phenol-chloroform extraction. RNA was quantified (Nanodrop) and 1 ug of each sample was reverse transcribed using the cDNA Archive kit (Applied Biosystems). The amount of cDNA corresponding to 20 ng of RNA was used for each 20 uL real-time PCR reaction on an MXP-3000 instrument (Stratagene). Primer and probe sets for *Gusb*, *Eomes*, *Esrrb*, *Esx1*, *Dlx3*, *Gm52*, *Tcfeb*, *Ctsq*, *Timp2*, *Glut3*, *Cx31* and *Pdch12* were run according to manufacturer's protocol with 2X Taqman Universal Mastermix (ABI). Probes for *4311*, *Gcm1* and *Pl1* were designed and manufactured in-house

(Dr. Kathleen Caron, UNC). *Gusb* was used as an endogenous control and fold change of each gene of interest was calculated using the ΔΔCt method [20]. The average ΔCt of wildtype animals for each strain/allele combination was used as the control value to calculate ΔΔCt values for samples of the same strain and allele. Fold-change values were computed from the ΔΔCt for each sample and converted to a percent increase over the wildtype average fold change for $Egfr^{Wa5}$ heterozygous and $Egfr^{wa2}$ heterozygous and homozygous samples.

For cluster analysis, ΔCt values for each sample and probe were uploaded into Cluster and median-centered. Data was visualized using TreeView.

Statistical Analysis

All placenta and embryo weights were analyzed using the Mann Whitney test. A χ^2 goodness of fit test performed to determine if the genotype distribution deviated from expected Mendelian ratios. Real-time fold change values were analyzed using the student's T-test.

Results

$Egfr^{wa2}$ homozygous placentas are reduced in size on all genetic backgrounds.

To determine the effect of the $Egfr^{wa2}$ allele on placental development, placentas were collected at 15.5 dpc and 18.5 dpc from each of the three congenic strains by intercrossing respective $Egfr^{wa2}$ heterozygous mice (Figure 9A). At 15.5 dpc, placenta weight was reduced 24% in B6-$Egfr^{wa2}$ homozygous versus wildtype ($p < 0.001$) and heterozygous ($p < 0.001$) littermates (Figure 9A). Placenta weight was similarly affected at 18.5 dpc with a 24% weight reduction in B6-$Egfr^{wa2}$ homozygous versus wildtype ($p < 0.01$) and heterozygous (p

< 0.05) littermates (Figure 9B). Wildtype and *Egfr*^{wa2} heterozygous placenta weights did not differ at either timepoint.

In the 129 congenic strain, *Egfr*^{wa2} homozygous placenta weight was reduced 19% compared to wildtype ($p < 0.001$) and heterozygous ($p < 0.001$) littermates at 15.5 dpc (Figure 9A). Although at 15.5 dpc, 129 had the least affected placental weight of the three strains, by 18.5 dpc the 129 congenic strain had the most severe reduction in placenta weight. At 18.5 dpc, 129-*Egfr*^{wa2} homozygous placentas weighed 37% less than wildtype ($p < 0.01$) and heterozygous ($p < 0.01$) littermates (Figure 9B). There were no significant differences between 129 wildtype and *Egfr*^{wa2} heterozygous placentas at either timepoint.

The BTBR congenic line showed the most severe placental weight reduction at 15.5 dpc. BTBR-*Egfr*^{wa2} homozygous placentas weighed 39% less than wildtype ($p < 0.01$) and heterozygous ($p < 0.001$) littermates (Figure 9A). By 18.5 dpc, placental growth had increased in the BTBR-*Egfr*^{wa2} homozygotes since the organ weighed 28% less than wildtype ($p < 0.01$) and heterozygous ($p < 0.01$) littermates (Figure 9B). Like the B6 and 129 strains there were no differences in placental weight between wildtype and *Egfr*^{wa2} heterozygous placentas for BTBR at either timepoint.

Egfr^{wa2} *homozygous embryos display strain-dependent intrauterine growth restriction.*

To assess the effect of *Egfr*^{wa2} on embryonic growth, wildtype, *Egfr*^{wa2} heterozygous and homozygous embryos were collected at 15.5 dpc and 18.5 dpc for each strain. At 15.5 and 18.5 dpc there were no significant differences in B6 embryo weight between the genotypes (Figure 10). At 18.5 dpc, there was a slight, but not statistically significant, *Egfr*^{wa2} dose-dependent effect on embryo weight for the B6 background (Figure 10B).

At 15.5 dpc, 129-*Egfr*^{wa2} homozygous embryos did not weigh significantly different from wildtype embryos but heterozygous embryos weighed 12% more than wildtype ($p < 0.01$) and *Egfr*^{wa2} homozygotes ($p < 0.05$) (Figure 10A). In contrast, at 18.5 dpc growth restriction was observed in 129-*Egfr*^{wa2} homozygotes with *Egfr*^{wa2} homozygous embryos weighing 34% less than wildtype ($p < 0.01$) and heterozygous ($p < 0.001$) littermates (Figure 10B and 10C). At 18.5 dpc there were no differences in embryo weight between 129 wildtype and *Egfr*^{wa2} heterozygous embryos (Figure 10B).

At 15.5 dpc, BTBR-*Egfr*^{wa2} homozygous embryos weighed 18% less than wildtype ($p < 0.05$) and heterozygous ($p < 0.01$) littermates (Figure 10A). By 18.5 dpc an even more severe embryonic growth restriction was observed in BTBR, with *Egfr*^{wa2} homozygous embryos weighing 32% less than wildtype ($p < 0.01$) and heterozygous ($p < 0.001$) littermates (Figure 10B). There were no differences in embryo weight between BTBR wildtype and *Egfr*^{wa2} heterozygous embryos at either timepoint. We found that embryo and placenta weights were highly correlated in 18.5 dpc BTBR-*Egfr*^{wa2} homozygous embryos ($R^2 = 0.78$) and to some extent in 129 *Egfr*^{wa2} homozygotes ($R^2 = 0.45$), suggesting that fetal growth restriction was caused by the placental phenotype (Figure 10D).

129-Egfr^{wa2} *homozygous embryo survival is reduced at 15.5 dpc*

To determine the effect of *Egfr*^{wa2} on embryo survival, viable 15.5 dpc embryos were genotyped for each strain and evaluated for deviation from expected Mendelian ratios (Table 5). For B6, 32% of 75 viable embryos were *Egfr*^{wa2} homozygous, which was not significantly different than the expected 25%. However, a significant deviation from Mendelian ratios was observed on the 129 background as only 14% of 86 viable embryos

were *Egfr*^{wa2} homozygous at 15.5 dpc ($p < 0.01$); a similar percentage of homozygotes were also observed at weaning (Table 5). This result suggests that a significant number of *Egfr*^{wa2} homozygous embryos die prior to 15.5 dpc. Only a few BTBR litters were analyzed and survival was statistically similar to B6. Nevertheless, three BTBR embryos were found dead at 15.5 dpc and all three were *Egfr*^{wa2} homozygous suggesting that there may be some loss of *Egfr*^{wa2} homozygotes prior to 15.5 dpc on the BTBR background. There were also fewer than expected numbers of BTBR-*Egfr*^{wa2} homozygous weanlings observed in the breeding colony (data not shown).

Egfr^{Wa5} *heterozygous embryos have a small reduction in placental size but no change in embryo weight*

To measure the effect of the *Egfr*^{Wa5} allele on growth of the placenta and embryo, litters were collected from crosses between *Egfr*^{Wa5} heterozygous and wildtype mice for the same three strains. Placenta weight at 15.5 dpc was reduced by 9% in B6-*Egfr*^{Wa5} heterozygous versus wildtype littermates ($p< 0.001$). (Figure 11A), but embryo weight was not affected (Figure 11B). A similar reduction in placenta weight was observed in 129-*Egfr*^{Wa5} heterozygous embryos compared to wildtype littermates ($p < 0.001$; Figure 11A), with embryo weight being identical to wildtype littermates (Figure 11B). At 18.5 dpc, placenta and embryo weights were unchanged between 129-*Egfr*^{Wa5} and wildtype littermates (Figure 11C). BTBR-*Egfr*^{Wa5} heterozygous placentas were more modestly affected, showing only a 5% reduction in placenta weight and no difference in embryo weight at 15.5 dpc when compared to wildtype littermates ($p < 0.05$; Figure 11A and 11B).

Viable embryos were genotyped for each strain to determine if the genotype distributions deviated from expected Mendelian ratios (Table 6). For B6 and 129, 53% and 51% of viable embryos, respectively, were *Egfr*^{Wa5} heterozygotes. Although the BTBR strain exhibited the smallest change in placental weight, only 40% of viable embryos were *Egfr*^{Wa5} heterozygotes ($p < 0.05$).

129 and BTBR Egfr^{wa2} *homozygous placentas have very few spongiotrophoblasts*

Placentas from 18.5 dpc embryos were stained with H and E for general morphological characterization and with PAS to identify glycogen-containing cells (stain magenta in color) of the spongiotrophoblast layer. The PAS-stained sections were particularly useful in visualizing the thickness of the spongiotrophoblast layer since this layer stained magenta and a darker purple compared to the labyrinth. The wildtype B6 placenta had a very thick layer of spongiotrophoblast with numerous protrusions into the labyrinth region (Figure 12A). The B6 *Egfr*^{wa2} homozygous placentas exhibited a reduction in spongiotrophoblasts compared to wildtype (Figure 12B) but there were many glycogen-positive cells present (Figure 12C). Overall the B6 strain showed very intense PAS staining of the spongiotrophoblast indicating an abundance of glycogen-storing cells in this layer. BTBR and 129 wildtype placentas (Figure 12D and 12G, respectively) exhibited a less substantial layer of spongiotrophoblast than B6 but the layer was well-developed and stained strongly for PAS in all wildtype placentas examined. In contrast, there were only a few small clusters of spongiotrophoblasts in the BTBR and 129 *Egfr*^{wa2} homozygous placentas (Figure 12E and 12H, respectively). Closer examination of these clusters revealed some PAS staining (Figure 12F and 12I, arrowheads).

There was no obvious reduction in the the spongiotrophoblast layer of 129 *Egfr*^{Wa5} heterozygous placentas (Figure 12J) compared to wildtype (Figure 12G). There were no detectable differences in the structure of the labyrinth region between 129 wildtype and *Egfr*^{wa2} homozygous 18.5 dpc placentas (Figure 12K, L).

Expression of markers for specific trophoblast cell subtypes differed in Egfr^{wa2} *homozygous versus wildtype placentas*

The relative expression of trophoblast cell subtype markers *Gcm1*, *Dlx3, Tcfeb, Esx1, Esrrb*, *Eomes*, *Gm52*, *Ctsq*, *4311, Pdch12, Pl1*, *Timp2*, *Glut3* and *Cx31* were measured by quantitative PCR (Table 7) and compared to an endogenous control, *Gusb*, in *Egfr*^{wa2} heterozygous, *Egfr*^{wa2} homozygous, *Egfr*^{Wa5} heterozygous and wildtype placentas from 15.5 dpc embryos. Significant differences between *Egfr*^{wa2} homozygous and wildtype placentas were found in the expression of several placental genes (Table 8). In B6 several labyrinth expressed genes were significantly higher in *Egfr*^{wa2} homozygous placentas compared to control littermates (n = 10). *Gcm1, Dlx3* and *Tcfeb* were 129 %, 141% and 143% of wildtype levels, respectively ($p < 0.001$ to 0.05). *4311*, a marker of spongiotrophoblast was 58% of wildtype levels ($p = 0.001$), while *Pdch12*, a marker of glycogen cells was 71% of wildtype levels ($p < 0.01$). Levels of a decidua marker, *Timp2* were 74% of wildtype levels ($p < 0.01$) and the expression of a gap junction protein expressed in glycogen trophoblast, *Cx31*, was 64% of wildtype levels ($p < 0.001$). There were no significant changes in expression between B6 *Egfr*^{wa2} heterozygous (n = 10) and wildtype placentas (n = 5). In 129-*Egfr*^{wa2} homozygous placentas (n = 7) labyrinth gene expression was also increased, *Gcm1* was 142 % ($p = 0.01$), *Dlx3* was 143% ($p = 0.001$), *Tcfeb* was 134 % ($p < 0.05$) and *Gm52* was 164%

of wildtype levels ($p < 0.01$). For spongiotrophoblast, *4311* was 17% of wildtype levels ($p < 0.001$) and *Pdch12* was 84% of wildtype levels ($p < 0.05$). Expression of a marker of sinusoidal labyrinth giant cells, *Ctsq*, was 78% of wildtype levels ($p < 0.01$). The only significant change in expression between the 129-*Egfr*^{wa2} heterozygous (n = 10) and wildtype (n = 6) was in the trophoblast giant cell marker *Pl1* which was expressed at 175% of wildtype levels in *Egfr*^{wa2} heterozygous placenta. Changes in *Esx1*, *Esrrb1*, *Eomes*, and *Glut3* were not significant for either strain.

ΔCT values for genes that were significantly different between *Egfr*^{wa2} homozygous and wildtype placentas clustered by genotype for the 129 background with the *Egfr*^{wa2} homozygous samples showing high expression of labyrinth specific genes and low expression of spongiotrophoblast specific genes (Figure 13). The B6 samples showed some genotype-specific clustering but not as strongly as for 129. Overall, the *Egfr*^{wa2} samples clustered strongly by strain for the probes analyzed.

Compared to the *Egfr*^{wa2} homozygotes, there were fewer differences observed in expression between *Egfr*^{Wa5} heterozygous and wildtype placentas (Table 8). For the B6 background, the *Egfr*^{Wa5} heterozygous (n = 7) expression of *Gcm1* was 125% of wildtype ($p < 0.01$, n = 9), *Dlx3* was 120% of wildtype ($p <0.05$) and *Esx1* was 121% of wildtype ($p < 0.05$). There were no significant changes in expression for the 129 background between *Egfr*^{Wa5} heterozygous (n = 8) and wildtype (n = 8) placentas. BTBR-*Egfr*^{Wa5} heterozygotes (n = 8) expressed *Gm52* at 133% of wildtype ($p < 0.05$, n = 8). ΔCT values for *Egfr*^{Wa5} samples clustered strongly by strain but not by genotype (Figure 14).

Wildtype placenta weights, embryo weights, and expression of trophoblast markers are strain-dependent.

Wildtype placenta and embryo weights from the *Egfr*^{Wa5} crosses were compared at 15.5 dpc for the three strains (Figure 15). B6 placentas and embryos were the largest of the three strains at 15.5 dpc with an average weight of 98.3 mg and 385 mg for the placenta and embryo, respectively. 129 placentas and embryos were the smallest with an average of 73.9 mg for placenta and 318.6 mg for embryos. The BTBR placentas had an average weight of 82.3 mg and the embryos an average of 332.5 mg. Placenta and embryo weights were significantly different in all strain comparisons ($p < 0.001$).

ΔCT values of all genes analyzed for *Egfr*^{Wa5} samples were clustered by sample and gene (Figure 14). This included a larger set of probes than for the *Egfr*^{wa2} samples since genes were included that were not significantly different between *Egfr*^{Wa5} heterozygous and wildtype samples. BTBR samples were not included in the cluster analysis because the endogenous control was expressed at a different level for this strain. The genes clustered into two main groups with the labyrinth genes *Tcfeb*, *Dlx3*, *Gm52*, *Gcm1* and *Esx1* in one group and the spongiotrophoblast genes, *4311* and *Pdch12* in the other group.

Clustering the ΔCT values of the *Egfr*^{Wa5} data set by sample revealed interesting strain-specific differences in wildtype placenta. The 129 background showed high expression of the labyrinth-specific genes *Tcfeb*, *Dlx3*, *Gm52*, *Gcm1*, *Esx1*, and *Ctsq* compared to B6. B6 showed higher expression of *Eomes*, *4311*, *Glut3, Pl1*, *Esrrb* and *Pdch12* than 129.

Discussion

Numerous studies have provided evidence that EGFR and its ligands are important for normal growth of the placenta and embryo. Over-expression of the EGFR ligand, EGF, has been found to reduce fetal growth in both humans and mice. In humans, a polymorphism in the 5' untranslated region of EGF that results in increased EGF expression has been associated with lower birth weight and fetal growth restriction in pregnant women from western Europe [21]. In addition transgenic mice that over-express EGF are born at half the weight of their littermates and have lower levels of serum IGFBP3 [22]. Interestingly, reduced EGF and EGFR phosphorylation have also been associated with low birth weight. Several groups have found associations between intrauterine growth restriction (IUGR) and diminished placental EGFR expression and/or activation in human pregnancies [23-27]. In pregnant mice, reduction of maternal EGF by sialoadenectomy results in growth restriction of embryos [28]. Also, EGFR-deficient mouse embryos exhibit placental defects that are dependent on strain and result in embryonic growth restriction and lethality [3,4]. The effects of genetically reduced, but not abolished, EGFR signaling on placental development and embryo growth has not been reported. In this study we measured the strain-specific effects of two reduced-function alleles of *Egfr* on placental and embryonic growth, and expression of trophoblast cell subtype markers in the placenta.

Attenuated EGFR signaling leads to growth restriction of placenta and embryo.

Our data shows that mice homozygous for the classical hypomorphic allele of *Egfr*, $Egfr^{wa2}$, exhibit smaller placentas than wildtype littermates on three inbred strains examined at 15.5 dpc (Figure 9A). The largest effect was seen on the BTBR background where $Egfr^{wa2}$

homozygous placental weight was reduced by almost 40%. The smallest effect on placental weight at 15.5 dpc occurred on the 129 background, where *Egfr*^{wa2} homozygous placental weights were reduced by 18%. BTBR was also the only background to show a reduction in embryo weight at 15.5 dpc with the weight of *Egfr*^{wa2} homozygous embryos being reduced 18% compared to wildtype littermates (Figure 10A).

The structure of the mouse placenta is fully developed by 15.5 dpc and its size does not change significantly for the remainder of gestation. However, the embryo undergoes its most dramatic change in size during this time period, with a 300% or greater increase in weight. The growth of *Egfr*^{wa2} homozygous placentas and embryos during late gestation differed by strain (summarized in Figure 16). Of the three strains, growth of the 129-*Egfr*^{wa2} homozygous placenta and embryo slowed the most during this time period. At 15.5 dpc the 129-*Egfr*^{wa2} homozygous placenta was the least affected of the three strains but by 18.5 dpc, it showed the most severe phenotype, reduced in weight by almost 40% compared to wildtype littermates (Figure 9). The 129-*Egfr*^{wa2} homozygous embryos also showed severe growth restriction at 18.5 dpc, a phenotype not observed at 15.5 dpc (Figure 10). The BTBR-*Egfr*^{wa2} homozygous placenta grew more than *Egfr*^{wa2} homozygotes on other backgrounds between 15.5 dpc and 18.5 dpc. Placental weight was reduced 28% at 18.5 dpc compared to 39% at 15.5 dpc (Figure 9). In contrast the BTBR-*Egfr*^{wa2} homozygous embryo became more affected by 18.5 dpc with a weight reduction of 32% compared to 18% at 15.5 dpc (Figure 10). No changes were observed in the growth rate of B6-*Egfr*^{wa2} homozygous placentas and embryos across late gestation. The B6-*Egfr*^{wa2} homozygous placenta was reduced by 24% at 15.5 dpc and 18.5 dpc compared to wildtype, and the embryo weight was not significantly different than wildtype (Figure 9, 10).

We also observed strain-specific embryonic lethality prior to 15.5 dpc (Table 5). Only 14% of viable embryos on the 129 background were *Egfr*^{wa2} homozygotes suggesting that some *Egfr*^{wa2} homozygotes die earlier in gestation, possibly due to placental defects as previously described for the *Egfr*^{tm1Mag} null allele. Most likely there is also lethality of some BTBR-*Egfr*^{wa2} homozygous embryos since all three dead embryos in the crosses were *Egfr*^{wa2} homozygous.

Egfr^{Wa5} *heterozygous embryos exhibit less severe phenotypes than Egfr*^{wa2} homozygotes

We observed small, but significant differences in placental weight between *Egfr*^{Wa5} heterozygotes and wildtype littermates. Heterozygosity for *Egfr*^{Wa5} on the B6 and 129 backgrounds had an approximately 10% reduction in placental weight, while the BTBR background had a 5% reduction in placental weight (Figure 11A). There was no effect on embryonic weight for any of the genetic backgrounds at 15.5 dpc (Figure 11B). Embryos on the 129 background were also examined at 18.5 dpc and although there was a trend towards lower placental and embryonic weights in the *Egfr*^{Wa5} heterozygotes, the differences were not significant (Figure 11C). Unlike the *Egfr*^{wa2} homozygotes, there was no embryonic lethality of 129-*Egfr*^{Wa5} heterozygotes prior to 15.5 dpc. Interestingly we did observe significantly fewer *Egfr*^{Wa5} heterozygotes than expected for the BTBR background but the reason remains to be determined (Table 6).

To estimate cellular, as well as molecular, differences in mutant and wildtype placenta, we measured transcripts of 14 genes expressed specifically in different placental layers and trophoblast cell types (Table 7) [29-41]. The overall gene expression changes observed at 15.5 dpc in *Egfr*^{wa2} homozygotes and *Egfr*^{Wa5} heterozygotes mirrored the gross

observations. There were more significant changes between *Egfr*^{wa2} homozygotes and their wildtype littermates versus *Egfr*^{Wa5} heterozygotes and wildtype littermates. Overall, expression of genes specific to spongiotrophoblasts and glycogen cells were reduced in *Egfr*^{wa2} homozygotes and expression of markers specific for labyrinth trophoblasts were increased (Table 8). The histology was consistent with these findings since 18.5 dpc *Egfr*^{wa2} homozygous placentas had a reduction of spongiotrophoblast and glycogen cells that was particularly severe in the 129 and BTBR backgrounds (Figure 12). The placenta of 129 and BTBR-*Egfr*^{wa2} homozygotes almost completely lacked the spongiotrophoblast layer and consisted primarily of labyrinth trophoblasts which explains the increased abundance of labyrinth transcripts observed. Interestingly, expression of *Esrrb*, a marker of trophoblast stem cells and *Ctsq*, a marker for sinusoidal trophoblast giant cells were decreased in *Egfr*^{wa2} homozygotes, even though both of these cell types reside in the labyrinth, suggesting that these particular trophoblasts cells may be reduced in number in the *Egfr*^{wa2} homozygous placenta [36,39]. We also observed unique down-regulation of *Cx31* and *Timp2* in B6-*Egfr*^{wa2} homozygotes (Table 8).

Although the data was less significant and the changes occurred to a lesser extent, the *Egfr*^{Wa5} heterozygotes also showed up-regulation of labyrinth specific transcripts and down-regulation of spongiotrophoblast-specific genes (Table 8). Embryos on the BTBR background showed a significant increase in the labyrinth-specific *Gm52* transcript although the spongiotrophoblast markers were marginally affected, suggesting that the *Gm52* increase may be from a true mis-regulation of the gene rather than a disproportionate number of labyrinth trophoblasts.

Together our placenta and embryo weight measurements, histology and gene expression data show that the *Egfr*^{Wa5} heterozygous phenotype is less severe than the *Egfr*^{wa2} homozygous phenotype. Recent reports provide evidence for an asymmetric dimer model of EGFR activation [42]. Studies have shown that in an ERBB dimer, one of the receptors, the activator, acts to hold the other, the activated receptor, in a conformation that promotes its activation and subsequent auto-phosphorylation. The N-lobe of the activated receptor makes critical contacts with the C-lobe of the activator and mutations that disrupt this interaction generally result in reduced or abolished phosphorylation. A kinase-dead EGFR, such as from the *Egfr*^{Wa5} allele, is capable of acting as the activator but not the activated receptor . According to this model, EGFR signaling in the *Egfr*^{Wa5} heterozygote would occur normally through the wildtype dimer, to some extent through the WA5/wildtype dimer, and not at all through the WA5 dimer. However, in vitro experiments have shown that WA5 acts as a dominant negative and has a more severe effect on wildtype EGFR phosphorylation than a kinase-dead receptor. EGFR phosphorylation is reduced by approximately 90% when cells express equal amounts of EGFR and WA5 [7]. Thus, the *Egfr*^{Wa5} mutation not only renders the receptor kinase-dead but also affects receptor activation through an additional mechanism, perhaps by modifying conformation of the receptor it encodes.

Estimates of WA2 receptor signaling capabilities have varied from 10% to almost wildtype levels of activity depending on the cell type analyzed and the experimental approach. The *Egfr*^{wa2} mutation lies upstream of *Egfr*^{Wa5} in an alpha-helix portion of the receptor N-lobe [6,8]. The effect of *Egfr*^{wa2} on EGFR phosphorylation is not well understood but it is possible that the mutation compromises contact with the C-lobe portion of the activator directly or indirectly by altering conformation of the activated receptor. Du and

colleagues proposed that *Egfr*^{wa2} homozygotes and *Egfr*^{Wa5} heterozygotes have approximately the same reduction in EGFR signaling [5]. Based on the more severe phenotype observed in *Egfr*^{wa2} homozygous placentas, we propose that the following levels of EGFR signaling occur in the *Egfr* allelic series:

$$Egfr^{+}/Egfr^{+} > Egfr^{+}/Egfr^{tm1Mag} = Egfr^{+}/Egfr^{wa2} > Egfr^{+}/Egfr^{Wa5} > Egfr^{wa2}/Egfr^{wa2} = Egfr^{wa2}/Egfr^{tm1Mag} > Egfr^{wa2}/Egfr^{Wa5} > Egfr^{Wa5}/Egfr^{Wa5} = Egfr^{Wa5}/Egfr^{tm1Mag} = Egfr^{tm1Mag}/Egfr^{tm1Mag}$$

Our data also demonstrate that tissue-specific requirements for EGFR signaling can be determined using the allelic series. We have shown that normal development of the placenta requires less EGFR activity than morphogenesis of hair follicles since the *Egfr*^{wa2} and *Egfr*^{Wa5} mouse share the same wavy coat phenotype but not the same degree of placental defects.

Wildtype placenta show strain-specific characteristics

Although our study set out to examine placental and embryonic growth in several mouse strains with reduced EGFR signaling, we also observed strain-dependent differences in growth of wildtype placentas and embryos. Our data show that there are significant differences in placental and embryo weights between the B6, 129 and BTBR strains (Figure 15). The B6 strain exhibited the largest placentas at 98.3 mg and the largest embryos at 385.0 mg, while the 129 strain exhibited the smallest placentas at 73.9 mg and the smallest embryos at 318.6 mg. Real-time PCR data comparing expression of trophoblast cell subtype specific genes in 129 and B6 suggests that, in addition to a difference in size, placentas from the strains may consists of different proportions of trophoblast layers and/or the level of gene

expression may vary. Histological comparison of wildtype placentas from the three strains showed that the numbers of spongiotrophoblast and intensity of PAS-stained varied by strain (Figure 12).

Clustering the ΔCT values revealed that even with *Egfr* alleles that affect placental composition, the data still clustered most strongly by strain rather than genotype (Figure 14). Placentas from 129 embryos showed relatively high expression of a set of labyrinth-specific genes while B6 exhibited the highest expression of a separate set of genes that included *Eomes*, *4311*, *Pl1*, and *Glut3*. The relatively high expression of *Glut3* in B6 is interesting considering the role of this protein in embryonic growth. Embryos heterozygous for a null allele of *Glut3* display late gestational IUGR and placental *Glut3* expression is reduced in growth-restricted embryos from EGF-deficient sialoadenectomized dams [28,33]. Elevated expression of *Glut3* in B6 placentas may allow $Egfr^{wa2}$ homozygous embryos to escape the severe growth restriction observed on the 129 and BTBR backgrounds.

These strain-specific differences are not surprising given the fact that the placenta is an organ affected strongly by natural selection [43,44]. Many imprinted genes play a role in growth and development of the placenta and during the derivation and maintenance of distinct mouse strains, different combinations of alleles that influence placental growth may have been fixed. The unique placental composition and/or expression of genes known to play important roles in trophoblast differentiation observed in standard wildtype laboratory mouse strains is interesting considering the large number of transgenic and mutant models with reported placental defects leading to embryonic lethality [45,46]. For some of these models the embryonic lethal phenotype is dependent on genetic background, suggesting the causative placental defects probably vary by strain. This has been shown to be the case in at

least one model, the *Egfr*^{tm1mag} nullizygous mouse, which has been studied throughout embryogenesis on a number of genetic backgrounds [47]. The inherent strain-specific differences we have observed in wildtype placenta indicate that the response of the placenta to genetic changes may be determined, in part, by strain-specific trophoblast characteristics.

Our study highlights strain dependent variation in placental development as well as the effect of diminished EGFR signaling on placental and embryonic growth. IUGR is a common condition with profound consequences for the fetus including elevated risk for perinatal mortality and increased incidence of reduced cognitive function, diabetes and heart disease later in life [48]. It is known that a large number of IUGR cases are caused by placental defects but the precise developmental mechanisms are not well-understood. *Egfr*^{wa2} homozygous embryos may serve as a model to investigate growth restriction arising from placental dysfunction. We have also demonstrated that the *Egfr*^{Wa5} heterozygote can be used to study levels of EGFR signaling intermediate between wildtype and the *Egfr*^{wa2} homozygote.

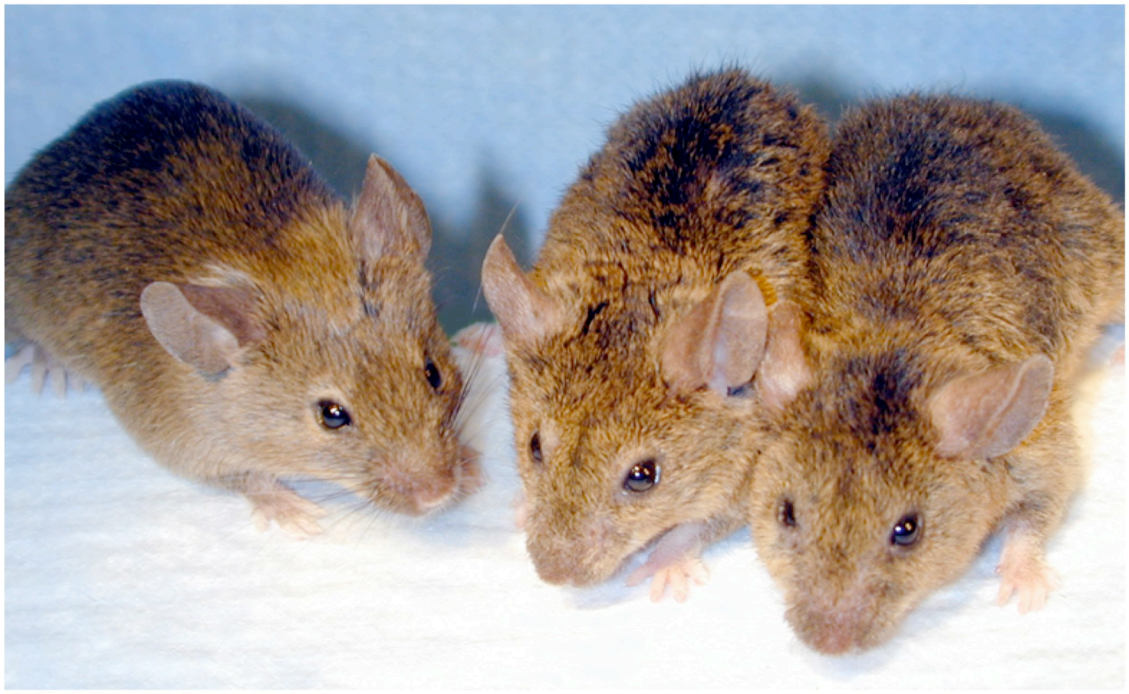

Figure 6. Congenic 129 *Egfr* allelic series: **w**ildtype (left), *Egfr*^{wa2} homozygote (middle) and *Egfr*^{wa5} heterozygote (right). The two *Egfr* mutants shown are born with a curly coat that becomes scruffy as the animals age. As weanlings and adults the *Egfr*^{wa2} homozygotes and *Egfr*^{wa5} heterozygotes are grossly indistinguishable.

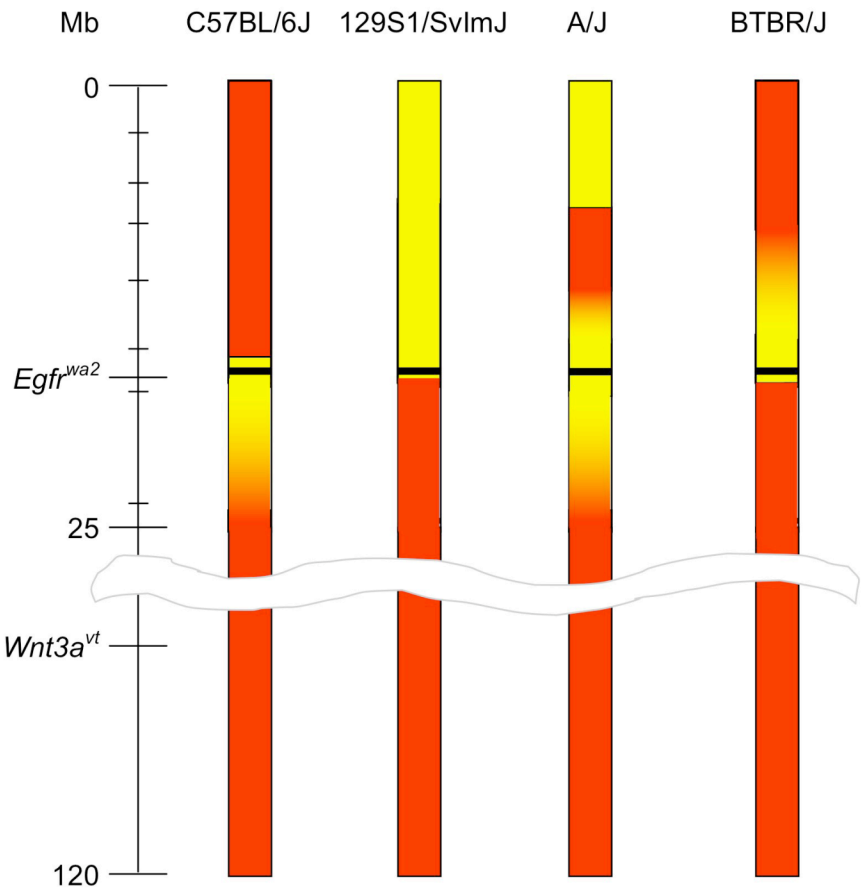

Figure 7. MIT microsatellite markers were used to estimate the size of the donor interval carrying the *Egfr*^{wa2} allele in each congenic line. Yellow, donor genome from original *Egfr*^{wa2} background; red, recipient genome. *Egfr* is located at approximately 16.5 Mb and *Wnt3a* is at 59 Mb. The 0 to 25 Mb region of chromosome 11 around *Egfr* is enlarged to show the location of MIT markers used (hashmarks). Only the B6, 129 and BTBR strain were used in this study.

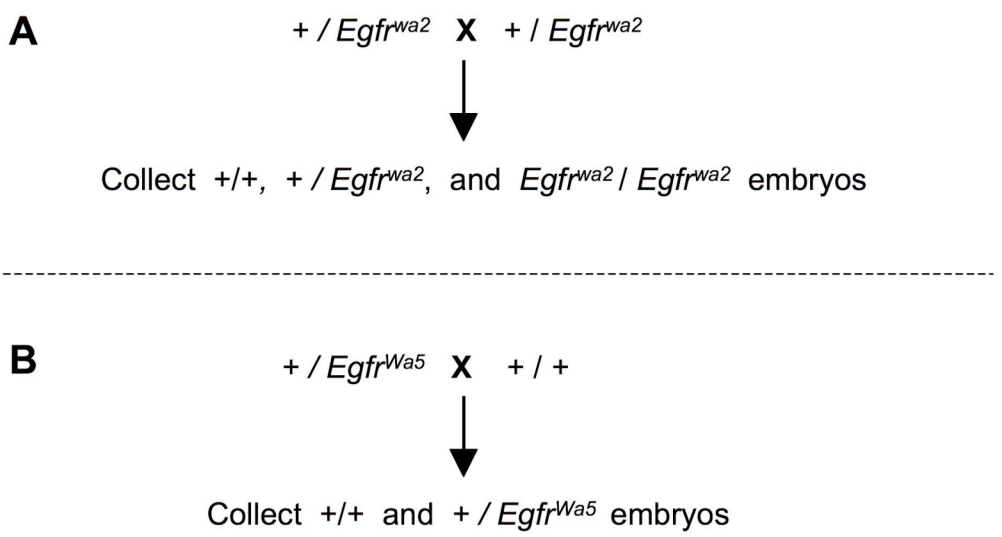

Figure 8. Breeding strategy for the two alleles of *Egfr*. Both crosses were performed with three separate congenic strains; B6, 129, and BTBR. **A.** *Egfr*^{wa2} heterozygous adults were intercrossed to produce litters with wildtype, *Egfr*^{wa2} heterozygous, and *Egfr*^{wa2} homozygous embryos and placentas. **B.** *Egfr*^{Wa5} heterozygous adults were crossed to wildtype to produce litters with wildtype and *Egfr*^{Wa5} heterozygous embryos and placentas.

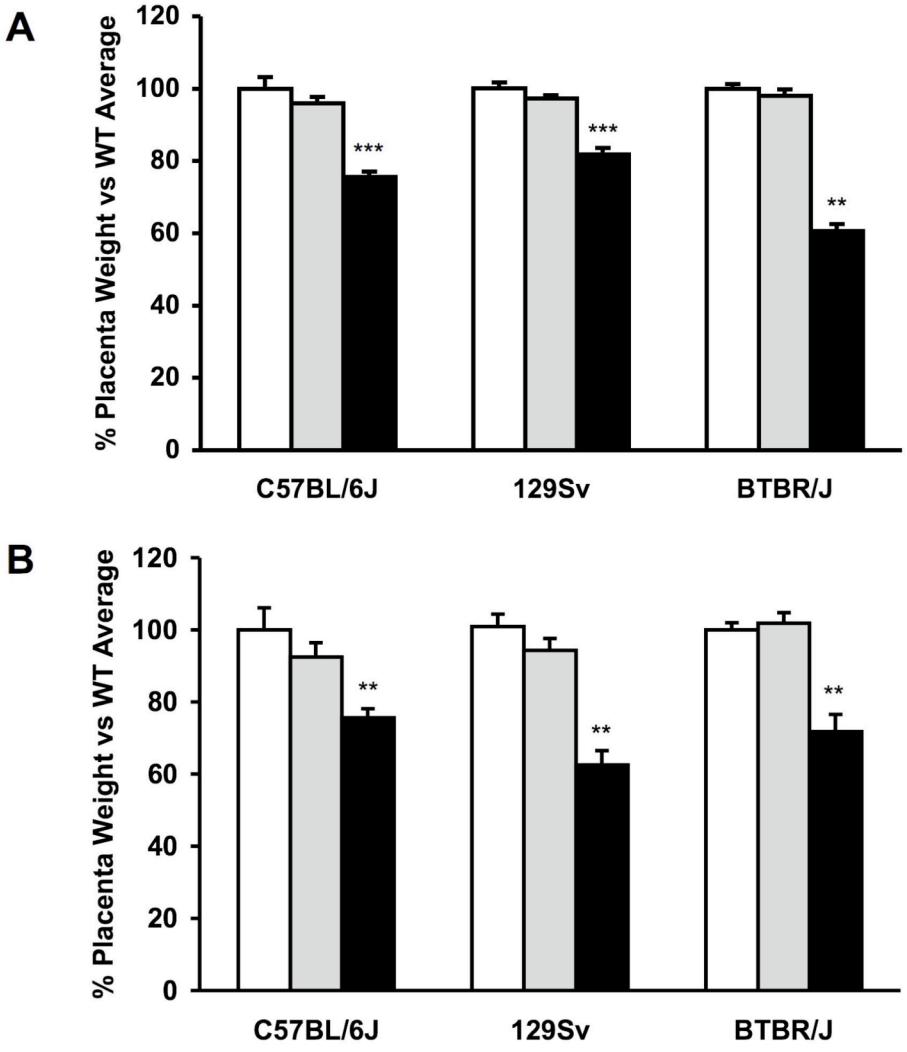

Figure 9. Weights of placentas from wildtype (white bars), *Egfr*^{wa2} heterozygous (gray bars) and homozygous littermates (black bars) measured at 15.5 dpc and 18.5 dpc on three genetic backgrounds. All strains included at least 5 embryos of each genotype. ** indicates $p < 0.01$ compared to wildtype, *** indicates $p < 0.001$ compared to wildtype**. A.** At 15.5 dpc *Egfr*^{wa2} homozygous placentas weighed 24% less than wildtype on B6, 18% less than wildtype on 129, and 39% less than wildtype on BTBR. **B.** At 18.5 dpc *Egfr*^{wa2} homozygous placentas weighed 24% less than wildtype on B6, 37% less than wildtype on 129, and 28% less than wildtype on BTBR.

Figure 10. Weights of embryos from wildtype (white bars), *Egfr*^{wa2} heterozygous (gray bars) and homozygous littermates (black bars) measured at 15.5 dpc and 18.5 dpc on three genetic backgrounds. All strains included at least 5 embryos of each genotype. ** indicates $p < 0.01$ compared to wildtype, *** indicates $p < 0.001$ compared to wildtype**. A.** At 15.5 dpc *Egfr*^{wa2} homozygous embryo weights were not significantly different on B6 and 129 compared to wildtype but homozygous embryos weighed 17% less than wildtype on BTBR. *Egfr*^{wa2} heterozygous embryos on the 129 background weighed 13% more than wildtype embryos ($p < 0.01$). **B.** At 18.5 dpc *Egfr*^{wa2} homozygous embryo weights were not significantly different on B6 compared to wildtype but homozygous embryos weighed 34% less than wildtype on 129 and 32% less than wildype on BTBR. **C.** Growth restricted 129 *Egfr*^{wa2} homozygous embryo at 18.5 dpc (*Egfr*^{wa2} homozygous embryo on right versus wildtype on left). **D.** Correlation between placenta weight and embryo weight in growth-restricted 18.5 dpc *Egfr*^{wa2} homozygous embryo. Red squares are 129 *Egfr*^{wa2} homozygous embryo and black circles are BTBR *Egfr*^{wa2} homozygous embryo. Placenta weight is plotted on the x-axis and embryo weight is plotted on the y-axis.

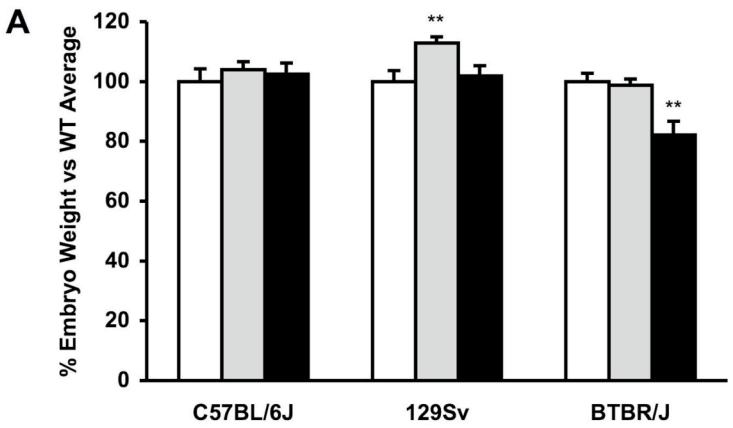
A
% Embryo Weight vs WT Average
120
100
80
60
40
20
0
**
**
C57BL/6J
129Sv
BTBR/J


C

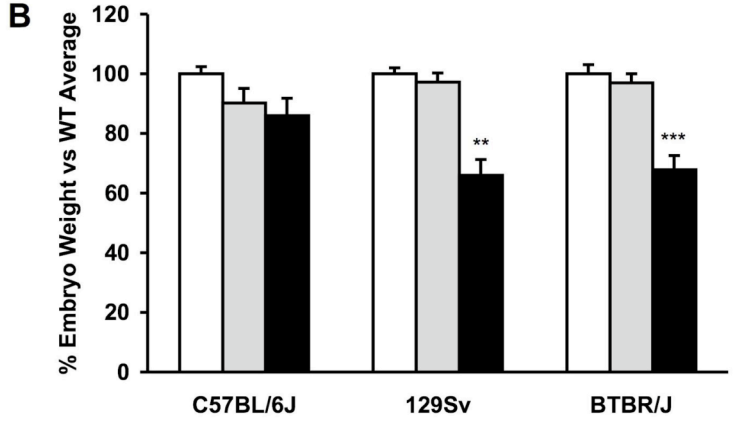
B
% Embryo Weight vs WT Average
120
100
80
60
40
20
0
**
***
C57BL/6J
129Sv
BTBR/J

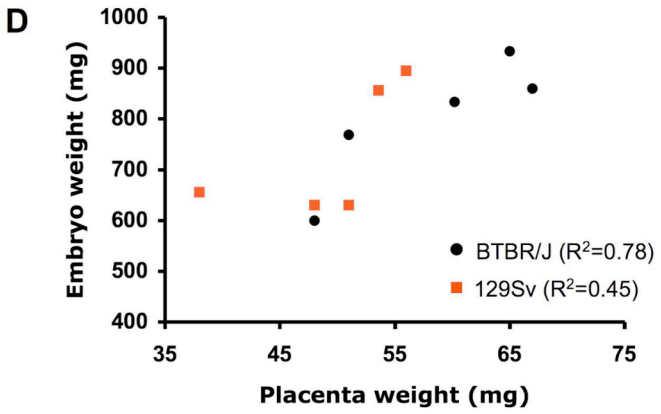
D
Embryo weight (mg)
1000
900
800
700
600
500
400
35
45
55
65
75
Placenta weight (mg)
BTBR/J (R2=0.78)
129Sv (R2=0.45)

Table 5. Survival of *Egfr*^{wa2} homozygotes on three congenic strains

Strain	Age	+ / +	+ / *Egfr*^{wa2}	*Egfr*^{wa2} / *Egfr*^{wa2}	Total viable	*P*
C57BL/6J	15.5 dpc	18 (24%)	33 (44%)	24 (32%)	75	0.361
129/Sv	15.5 dpc	33 (38%)	41 (48%)	12 (14%)	86	0.005
BTBR	15.5 dpc	7 (21%)	19 (58%)	7 (21%)	33[A]	0.678
129/Sv	weaning	38 (30%)	70 (56%)	17 (14%)	125	0.01

[A] 3 out of 3 dead embryos genotyped were *Egfr*^{wa2} / *Egfr*^{wa2}

Figure 11. Weights of placentas and embryos from wildtype (white bars) and *Egfr*^{Wa5} heterozygous littermates (gray bars) measured at 15.5 dpc on three genetic backgrounds. All strains included at least 26 embryos of each genotype for the 15.5 dpc timepoint and 18 embryos of each genotype for 18.5 dpc timepoint. * indicates $p < 0.05$ compared to wildtype, *** indicates $p < 0.001$ compared to wildtype**. A.** *Egfr*^{Wa5} heterozygous placentas weighed 9% less than wildtype on B6, 9% less than wildtype on 129, and 5% less than wildtype on BTBR. **B.** None of the three genetic backgrounds showed significant differences between *Egfr*^{Wa5} heterozygous and wildtype embryo weights. **C.** The 129 *Egfr*^{Wa5} heterozygous placenta and embryo weights did not differ from wildtype at 18.5 dpc.

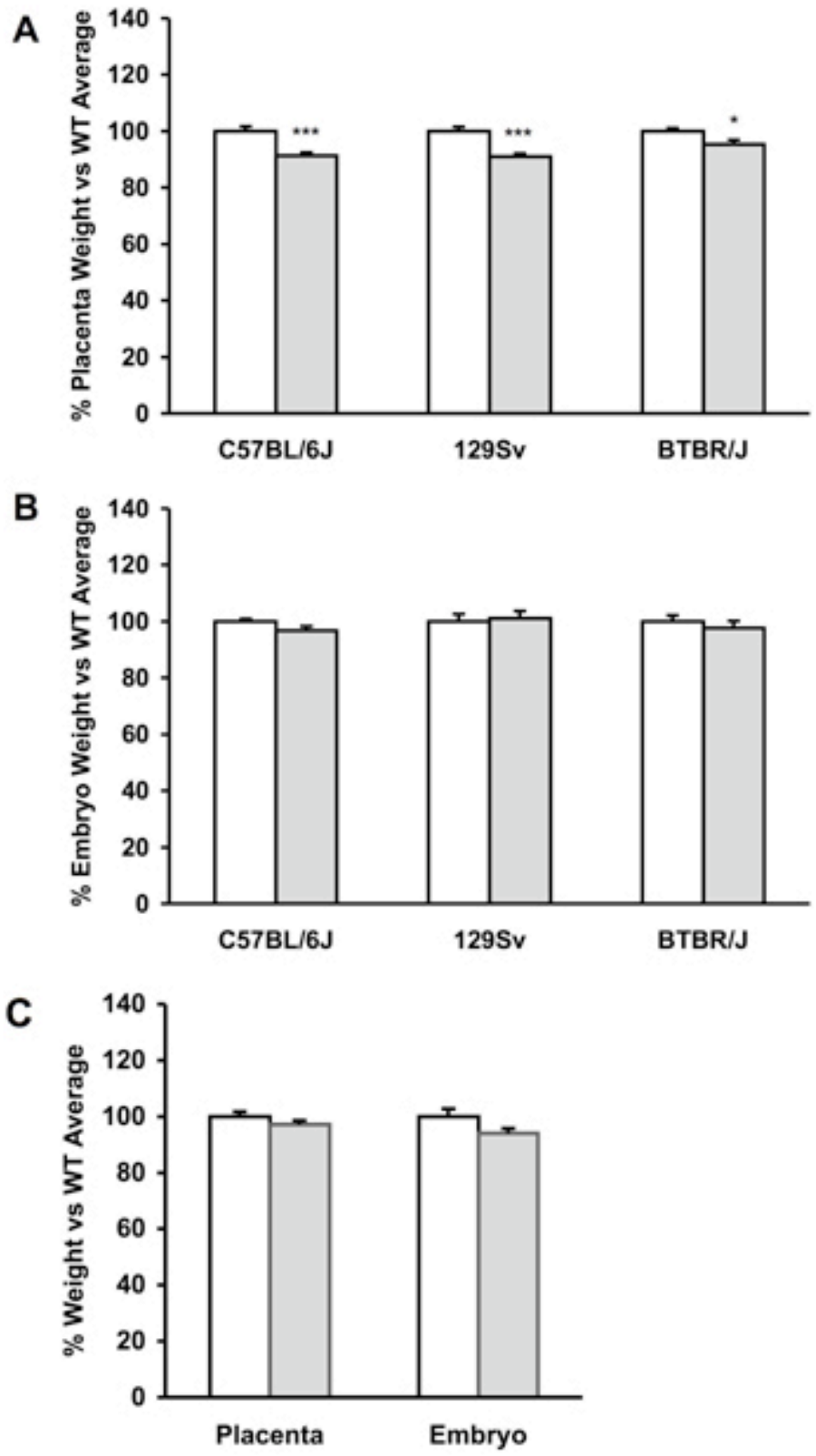
A
% Placenta Weight vs WT Average
140
120
100
80
60
40
20
0
***
***
*
C57BL/6J
129Sv
BTBR/J
B
% Embryo Weight vs WT Average
140
120
100
80
60
40
20
0
C57BL/6J
129Sv
BTBR/J
C
% Weight vs WT Average
140
120
100
80
60
40
20
0
Placenta
Embryo

Table 6. Survival of *Egfr*^{Wa5} heterozygotes on three congenic strains

Strain	Age	+ / +	+ / *Egfr*^{Wa5}	Total viable	*P*
C57BL/6J	15.5 dpc	42 (47%)	48 (53%)	90	0.526
129/Sv	15.5 dpc	32 (49%)	33 (51%)	65	0.901
BTBR	15.5 dpc	61 (60%)	40 (40%)	101	0.036

Figure 12. Placentas from B6, BTBR and 129 at 18.5 dpc. sp: spongiotrophoblast, la: labyrinth. **A.** PAS-stained wildtype B6 placenta (1.25X). **B.** PAS-stained *Egfr*^{wa2} homozygous B6 placenta (1.25X). **C.** Higher magnification of PAS-stained spongiotrophoblasts in *Egfr*^{wa2} homozygous B6 placenta (10X). **D.** PAS-stained wildtype BTBR placenta. **E.** PAS-stained *Egfr*^{wa2} homozygous BTBR placenta. **F.** Higher magnification of very small cluster of PAS-stained spongiotrophoblasts (arrowhead) in *Egfr*^{wa2} homozygous BTBR placenta. **G.** PAS-stained wildtype 129 placenta. **H.** PAS-stained *Egfr*^{wa2} homozygous 129 placenta. **I.** Higher magnification of small cluster of PAS-stained spongiotrophoblasts (arrowhead) in *Egfr*^{wa2} homozygous 129 placenta. **J.** PAS-stained *Egfr*^{Wa5} heterozygous 129 placenta. **K.** Higher magnification of labyrinth region in wildtype 129 placenta (H and E stained, 12X). **L.** Higher magnification of labyrinth region in *Egfr*^{wa2} homozygous 129 placenta (H and E stained).

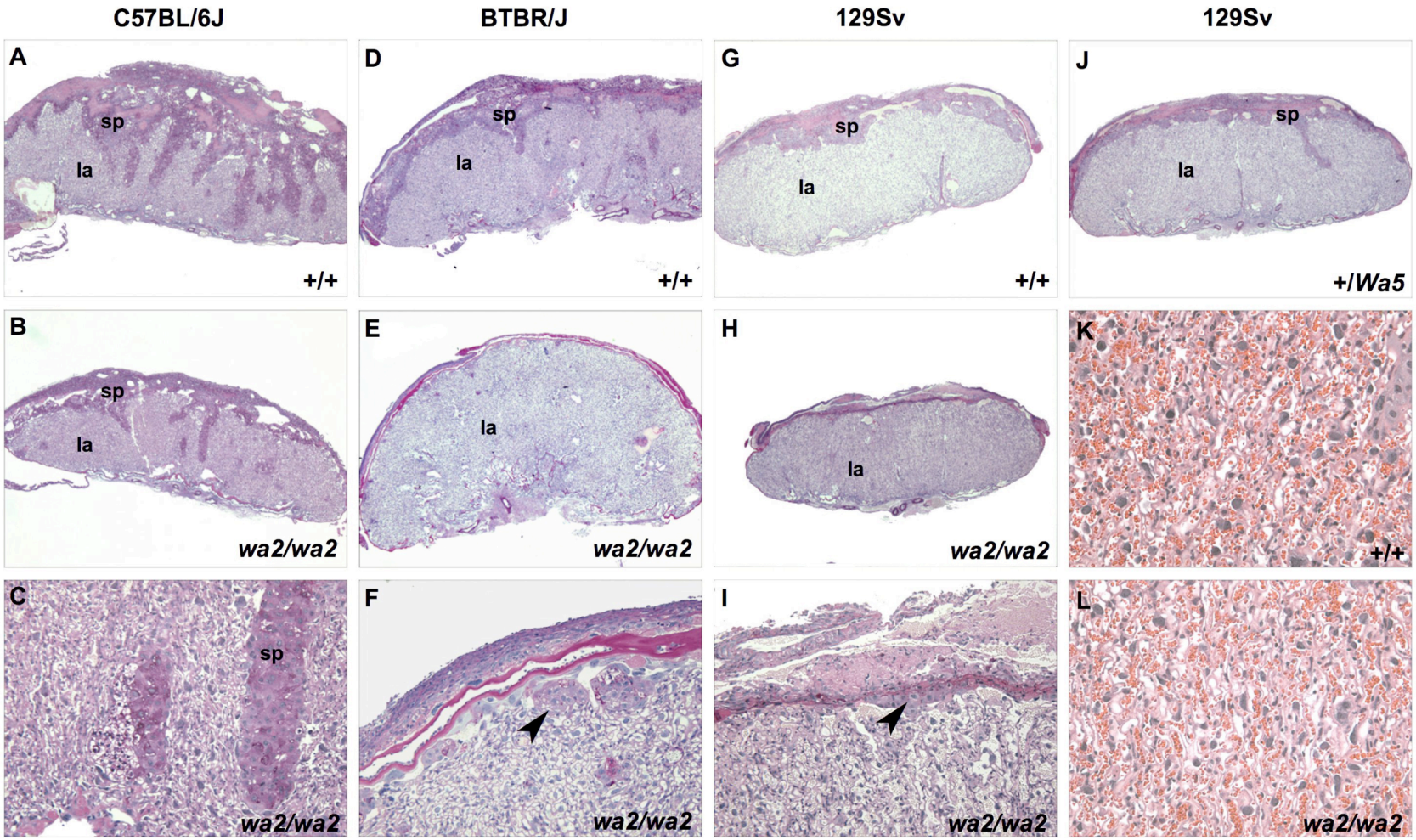
C57BL/6J
BTBR/J
129Sv
129Sv
A
sp
la
+/+
D
sp
la
+/+
G
sp
la
+/+
J
sp
la
+/Wa5
B
sp
la
wa2/wa2
E
la
wa2/wa2
H
la
wa2/wa2
K
+/+
C
sp
wa2/wa2
F
wa2/wa2
I
wa2/wa2
L
wa2/wa2

Table 7. Summary of expression pattern and placental function of genes used to quantify trophoblast cell subtypes

Gene	Function	Expression in Placenta	Function in Placental Development	Reference
Gcm1	Transcription factor	chorionic trophoblast, SynT layer II	labyrinth branching morphogenesis, syncytiotrophoblast differentiation	Basyuk E, 1999
Dlx3	Transcription factor	Lz	labyrinth morphogensis	Morasso MI, 1999
Tcfeb	Transcription factor	Lz	labyrinth branching morphogenesis	Steingrimsson E, 1998
Esx1	Transcription factor	TS cells, Lz	labyrinth morphogenesis, syncytiotrophoblast differentiation	Li Y, 1998
Esrrb1	Nuclear receptor	TS cells	trophoblast pluripotency and proliferation	Luo J, 1997
Eomes	Transcription factor	TS cells, cuboidal Lz trophoblast	trophoblast pluripotency and proliferation	Russ, AP 2000
Gm52	Viral envelope protein	Lz	syncytiotrophoblast fusion	Dupressoir A, 2005
Ctsq	Protease	labyrinth sinusoidal TG	Unknown	Simmons DG, 2007
4311	cytokine	SpT, GT	Unknown	Lescisin KR, 1988
Pdch12	Cell adhesion	GT	Unknown	Bouillot S, 2006
PL-1	cytokine	TG	Unknown	Simmons DG, 2007
Timp2	metalloproteinase inhibitor	decidua	decidual growth and remodeling	Teesalu T, 1999
Glut3	glucose transporter	Lz (rat data only)	nutrient transport	Shin BC, 1997
Cx31	gap junction	GT	cell communication	Coan, PM 2006
Gusb	carbohydrate metabolism	Endogenous control		

SynT- syncytiotrophoblast, Lz- labyrinth, TS- trophoblast stem cells, TG- trophoblast giant cells, SpT- spongiotrophoblast, GT- glycogen trophoblast. Green = labyrinth-specific genes, Red= spongiotrophoblast-specific genes

Table 8. Percent expression of trophoblast cell subtype markers in *Egfr*^{wa2} homozygous and *Egfr*^{Wa5} heterozygous placentas compared to wildtype littermates

	waved-2 homozygous		*Waved-5* heterozygous		
	129Sv	C57BL/6J	129Sv	C57BL/6J	BTBR/J
Gcm1	142% **	129%*	114%	125%*	130%
Dlx3	143% ***	141%***	109%	120%*	123%
Tcfeb	134% **	143%*	95%	110%	135%
Esx1	146%	116%	103%	121%*	114%
Esrrb1	76%	72%	95%	82%	114%
Eomes	114%	94%	104%	105%	119%
Gm52	164% **	135%	115%	104%	133%*
Ctsq	78% **	82%	88%	113%	99%
4311	17% ***	58%***	85%	97%	96%
Pdch12	84%*	71%**	86%	91%	90%
PL-1	105%	116%	97%	80%	130%
Timp2	104%	74%**	106%	94%	109%
Glut3	115%	96%	104%	114%	112%
Cx31	95%	64%***	103%	90%	115%

* $p < 0.05$, ** $p < 0.01$, *** $p < 0.001$

Green = labyrinth-specific genes, Red= spongiotrophoblast-specific genes

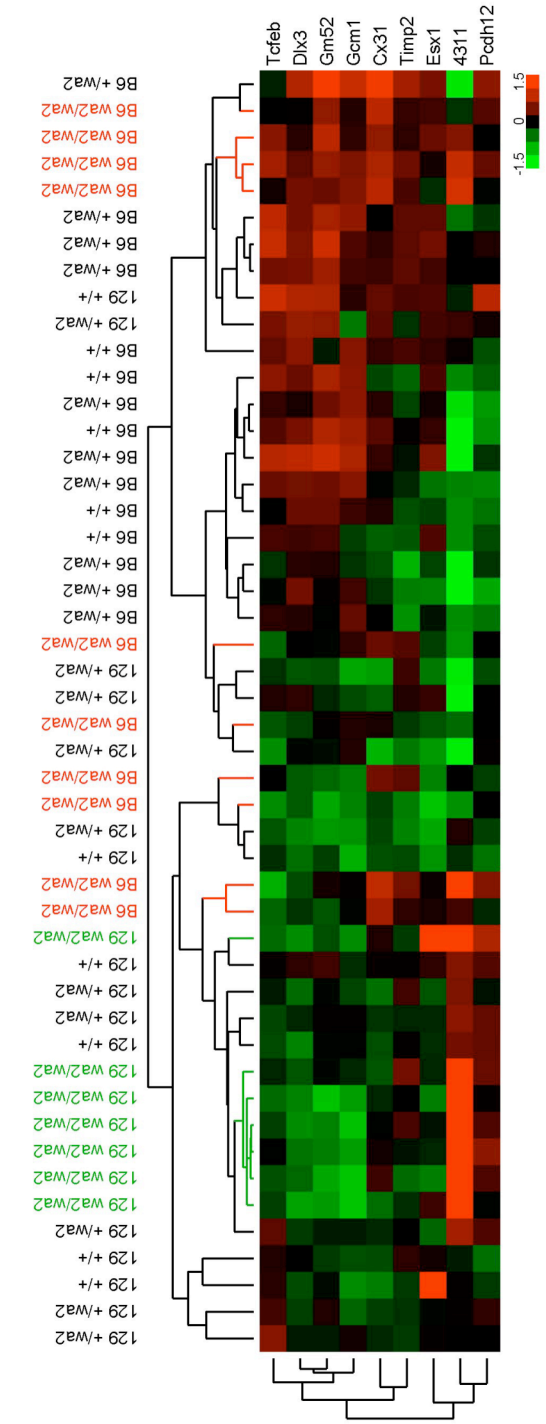

Figure 13. Cluster analysis and dendrogram of ΔCT values for *Egfr*^{wa2} homozygous, heterozygous, and wildtype samples. ΔCT gene expression values were clustered by gene and sample. Red blocks indicate low relative expression and green blocks indicate high relative expression. Cluster analysis included only genes that were significantly different between wildtype and *Egfr*^{wa2} homozygous placenta. *Egfr*^{wa2} homozygous samples are indicated by red (129) and green (B6) bars on dendrogram.

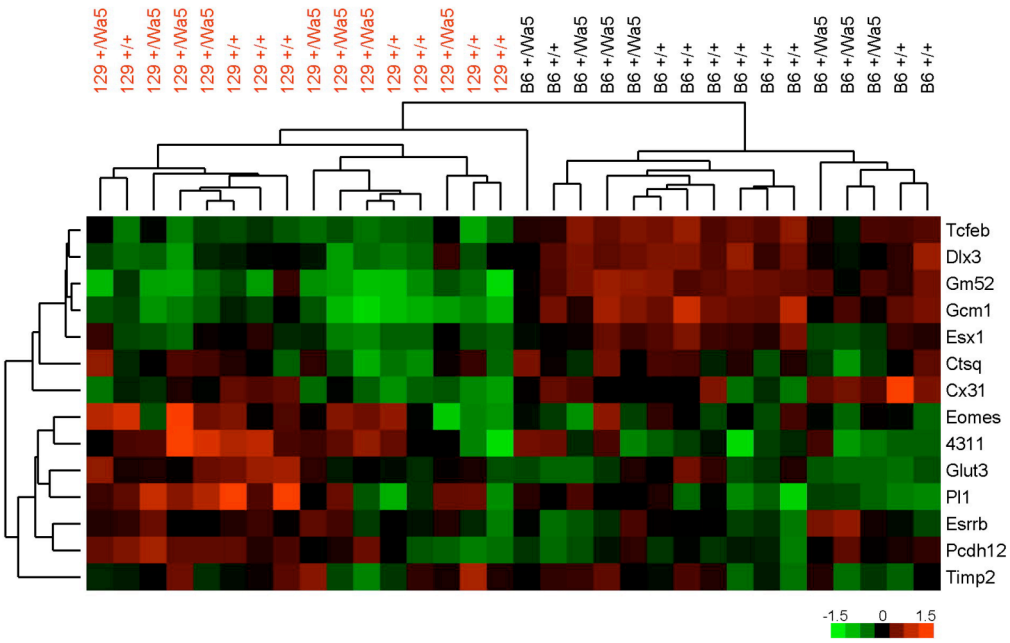

Figure 14. Cluster analysis and dendrogram of ΔCT values for *Egfr*^{wa5} heterozygous and wildtype samples. ΔCT gene expression values were clustered by gene and sample. Red blocks indicate low relative expression and green blocks indicate high relative expression. Analysis included genes that were and were not significantly different between *Egfr*^{wa5} heterozygous and wildtype samples. 129 samples are indicated by red text, B6 samples are indicated by black text.

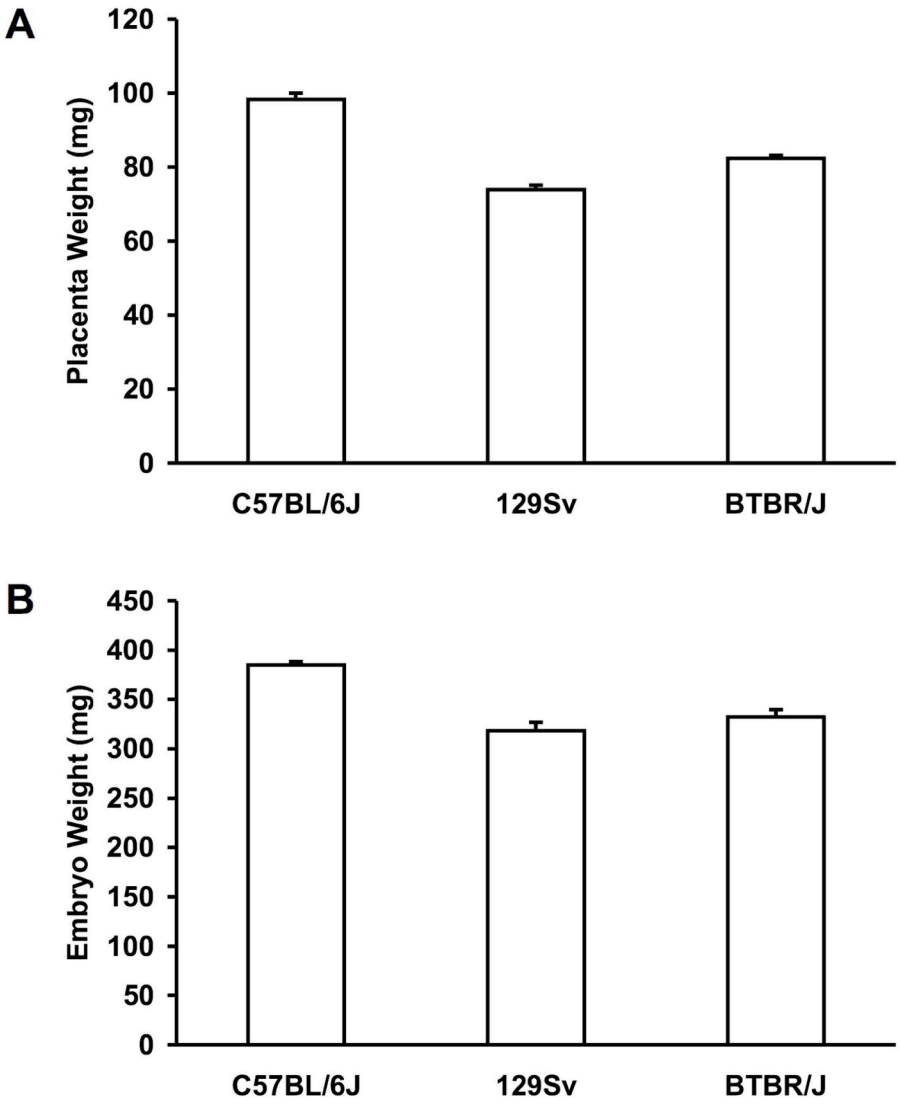

Figure 15. Placenta and embryo weights of three inbred strains measured at 15.5 dpc. **A.** Placenta weight is dependent on genetic background. The average weight of 15.5 dpc placentas was 98.3 mg for B6 (n=42), 73.9 mg for 129 (n=27), and 82.3 mg for BTBR (n=57). Placental weights were significantly different between all three strains ($p<0.001$). **B.** Embryo weight is dependent on genetic background. The average weight of 15.5 dpc embryos was 385.0 mg for B6 (n=29) , 318.6 mg for 129 (n=26), and 332.5 mg for BTBR (n=59). Embryo weights were significantly different between all three strains ($p<0.001$).

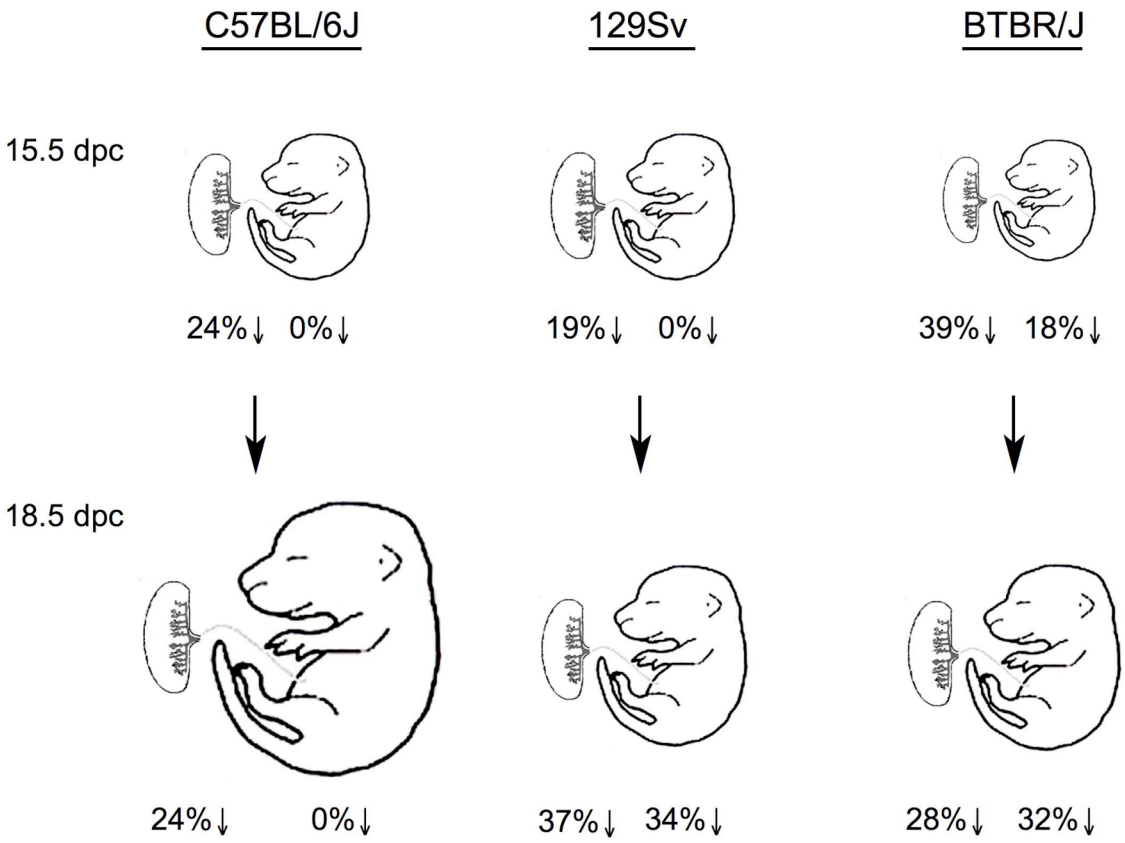

Figure 16. Summary of strain-dependent late gestation growth patterns in *Egfr*^{wa2} homozygous placentas and embryos. Percentages shown are percent reduction in weight compared to wildtype littermates for the placenta and embryo.

References

[1] Yarden Y, Sliwkowski MX. Untangling the ErbB signalling network. Nat Rev Mol Cell Biol 2001; 2:127-137.

[2] Casalini P, Iorio MV, Galmozzi E, Menard S. Role of HER receptors family in development and differentiation. J Cell Physiol 2004; 200:343-350.

[3] Sibilia M, Wagner EF. Strain-dependent epithelial defects in mice lacking the EGF receptor. Science 1995; 269:234-238.

[4] Threadgill DW, Dlugosz AA, Hansen LA, Tennenbaum T, Lichti U, Yee D, LaMantia C, Mourton T, Herrup K, Harris RC, et al. Targeted disruption of mouse EGF receptor: effect of genetic background on mutant phenotype. Science 1995; 269:230-234.

[5] Du X, Tabeta K, Hoebe K, Liu H, Mann N, Mudd S, Crozat K, Sovath S, Gong X, Beutler B. Velvet, a dominant Egfr mutation that causes wavy hair and defective eyelid development in mice. Genetics 2004; 166:331-340.

[6] Fowler KJ, Walker F, Alexander W, Hibbs ML, Nice EC, Bohmer RM, Mann GB, Thumwood C, Maglitto R, Danks JA, et al. A mutation in the epidermal growth factor receptor in waved-2 mice has a profound effect on receptor biochemistry that results in impaired lactation. Proc Natl Acad Sci U S A 1995; 92:1465-1469.

[7] Lee D CS, Strunk KE, Morgan JE, Bailey CL, Jackson IJ, Threadgill DW. Wa5 is a novel ENU-induced antimorphic allele of the epidermal growth factor receptor. Mammalian Genome 2004; in press.

[8] Luetteke NC, Phillips HK, Qiu TH, Copeland NG, Earp HS, Jenkins NA, Lee DC. The mouse waved-2 phenotype results from a point mutation in the EGF receptor tyrosine kinase. Genes Dev 1994; 8:399-413.

[9] Chen B, Bronson RT, Klaman LD, Hampton TG, Wang JF, Green PJ, Magnuson T, Douglas PS, Morgan JP, Neel BG. Mice mutant for Egfr and Shp2 have defective cardiac semilunar valvulogenesis. Nat Genet 2000; 24:296-299.

[10] Egger B, Buchler MW, Lakshmanan J, Moore P, Eysselein VE. Mice harboring a defective epidermal growth factor receptor (waved-2) have an increased susceptibility to acute dextran sulfate-induced colitis. Scand J Gastroenterol 2000; 35:1181-1187.

[11] Helmrath MA, Erwin CR, Warner BW. A defective EGF-receptor in waved-2 mice attenuates intestinal adaptation. J Surg Res 1997; 69:76-80.

[12] Hsieh M, Lee D, Panigone S, Horner K, Chen R, Theologis A, Lee DC, Threadgill DW, Conti M. Luteinizing hormone-dependent activation of the epidermal growth factor network is essential for ovulation. Mol Cell Biol 2007; 27:1914-1924.

[13] O'Brien DP, Nelson LA, Williams JL, Kemp CJ, Erwin CR, Warner BW. Selective inhibition of the epidermal growth factor receptor impairs intestinal adaptation after small bowel resection. J Surg Res 2002; 105:25-30.

[14] Prevot V, Lomniczi A, Corfas G, Ojeda SR. erbB-1 and erbB-4 receptors act in concert to facilitate female sexual development and mature reproductive function. Endocrinology 2005; 146:1465-1472.

[15] Gillgrass A, Cardiff RD, Sharan N, Kannan S, Muller WJ. Epidermal growth factor receptor-dependent activation of Gab1 is involved in ErbB-2-mediated mammary tumor progression. Oncogene 2003; 22:9151-9155.

[16] Ling BC, Wu J, Miller SJ, Monk KR, Shamekh R, Rizvi TA, Decourten-Myers G, Vogel KS, DeClue JE, Ratner N. Role for the epidermal growth factor receptor in neurofibromatosis-related peripheral nerve tumorigenesis. Cancer Cell 2005; 7:65-75.

[17] Roberts RB, Min L, Washington MK, Olsen SJ, Settle SH, Coffey RJ, Threadgill DW. Importance of epidermal growth factor receptor signaling in establishment of adenomas and maintenance of carcinomas during intestinal tumorigenesis. Proc Natl Acad Sci U S A 2002; 99:1521-1526.

[18] Sibilia M, Fleischmann A, Behrens A, Stingl L, Carroll J, Watt FM, Schlessinger J, Wagner EF. The EGF receptor provides an essential survival signal for SOS-dependent skin tumor development. Cell 2000; 102:211-220.

[19] Richards WG, Sweeney WE, Yoder BK, Wilkinson JE, Woychik RP, Avner ED. Epidermal growth factor receptor activity mediates renal cyst formation in polycystic kidney disease. J Clin Invest 1998; 101:935-939.

[20] Livak KJ, Schmittgen TD. Analysis of relative gene expression data using real-time quantitative PCR and the 2(-Delta Delta C(T)) Method. Methods 2001; 25:402-408.

[21] Dissanayake VH, Tower C, Broderick A, Stocker LJ, Seneviratne HR, Jayasekara RW, Kalsheker N, Broughton Pipkin F, Morgan L. Polymorphism in the epidermal growth factor gene is associated with birthweight in Sinhalese and white Western Europeans. Mol Hum Reprod 2007; 13:425-429.

[22] Chan SY, Wong RW. Expression of epidermal growth factor in transgenic mice causes growth retardation. J Biol Chem 2000; 275:38693-38698.

[23] Calvo MT, Romo A, Gutierrez JJ, Relano E, Barrio E, Ferrandez Longas A. Study of genetic expression of intrauterine growth factors IGF-I and EGFR in placental tissue from pregnancies with intrauterine growth retardation. J Pediatr Endocrinol Metab 2004; 17 Suppl 3:445-450.

[24] Faxen M, Nasiell J, Blanck A, Nisell H, Lunell NO. Altered mRNA expression pattern of placental epidermal growth factor receptor (EGFR) in pregnancies complicated by preeclampsia and/or intrauterine growth retardation. Am J Perinatol 1998; 15:9-13.

[25] Fondacci C, Alsat E, Gabriel R, Blot P, Nessmann C, Evain-Brion D. Alterations of human placental epidermal growth factor receptor in intrauterine growth retardation. J Clin Invest 1994; 93:1149-1155.

[26] Fujita Y, Kurachi H, Morishige K, Amemiya K, Terakawa N, Miyake A, Tanizawa O. Decrease in epidermal growth factor receptor and its messenger ribonucleic acid levels in intrauterine growth-retarded and diabetes mellitus-complicated pregnancies. J Clin Endocrinol Metab 1991; 72:1340-1345.

[27] Gabriel R, Alsat E, Evain-Brion D. Alteration of epidermal growth factor receptor in placental membranes of smokers: relationship with intrauterine growth retardation. Am J Obstet Gynecol 1994; 170:1238-1243.

[28] Kamei Y, Tsutsumi O, Yamakawa A, Oka Y, Taketani Y, Imaki J. Maternal epidermal growth factor deficiency causes fetal hypoglycemia and intrauterine growth retardation in mice: possible involvement of placental glucose transporter GLUT3 expression. Endocrinology 1999; 140:4236-4243.

[29] Basyuk E, Cross JC, Corbin J, Nakayama H, Hunter P, Nait-Oumesmar B, Lazzarini RA. Murine Gcm1 gene is expressed in a subset of placental trophoblast cells. Dev Dyn 1999; 214:303-311.

[30] Bouillot S, Rampon C, Tillet E, Huber P. Tracing the glycogen cells with protocadherin 12 during mouse placenta development. Placenta 2006; 27:882-888.

[31] Coan PM, Conroy N, Burton GJ, Ferguson-Smith AC. Origin and characteristics of glycogen cells in the developing murine placenta. Dev Dyn 2006; 235:3280-3294.

[32] Dupressoir A, Marceau G, Vernochet C, Benit L, Kanellopoulos C, Sapin V, Heidmann T. Syncytin-A and syncytin-B, two fusogenic placenta-specific murine envelope genes of retroviral origin conserved in Muridae. Proc Natl Acad Sci U S A 2005; 102:725-730.

[33] Ganguly A, McKnight RA, Raychaudhuri S, Shin BC, Ma Z, Moley K, Devaskar SU. Glucose transporter isoform-3 mutations cause early pregnancy loss and fetal growth restriction. Am J Physiol Endocrinol Metab 2007; 292:E1241-1255.

[34] Lescisin KR, Varmuza S, Rossant J. Isolation and characterization of a novel trophoblast-specific cDNA in the mouse. Genes Dev 1988; 2:1639-1646.

[35] Li Y, Behringer RR. Esx1 is an X-chromosome-imprinted regulator of placental development and fetal growth. Nat Genet 1998; 20:309-311.

[36] Luo J, Sladek R, Bader JA, Matthyssen A, Rossant J, Giguere V. Placental abnormalities in mouse embryos lacking the orphan nuclear receptor ERR-beta. Nature 1997; 388:778-782.

[37] Morasso MI, Grinberg A, Robinson G, Sargent TD, Mahon KA. Placental failure in mice lacking the homeobox gene Dlx3. Proc Natl Acad Sci U S A 1999; 96:162-167.

[38] Russ AP, Wattler S, Colledge WH, Aparicio SA, Carlton MB, Pearce JJ, Barton SC, Surani MA, Ryan K, Nehls MC, Wilson V, Evans MJ. Eomesodermin is required for mouse trophoblast development and mesoderm formation. Nature 2000; 404:95-99.

[39] Simmons DG, Fortier AL, Cross JC. Diverse subtypes and developmental origins of trophoblast giant cells in the mouse placenta. Dev Biol 2007; 304:567-578.

[40] Steingrimsson E, Tessarollo L, Reid SW, Jenkins NA, Copeland NG. The bHLH-Zip transcription factor Tfeb is essential for placental vascularization. Development 1998; 125:4607-4616.

[41] Teesalu T, Masson R, Basset P, Blasi F, Talarico D. Expression of matrix metalloproteinases during murine chorioallantoic placenta maturation. Dev Dyn 1999; 214:248-258.

[42] Zhang X, Gureasko J, Shen K, Cole PA, Kuriyan J. An allosteric mechanism for activation of the kinase domain of epidermal growth factor receptor. Cell 2006; 125:1137-1149.

[43] Angiolini E, Fowden A, Coan P, Sandovici I, Smith P, Dean W, Burton G, Tycko B, Reik W, Sibley C, Constancia M. Regulation of placental efficiency for nutrient transport by imprinted genes. Placenta 2006; 27 Suppl A:S98-102.

[44] Coan PM, Burton GJ, Ferguson-Smith AC. Imprinted genes in the placenta--a review. Placenta 2005; 26 Suppl A:S10-20.

[45] Rossant J, Cross JC. Placental development: lessons from mouse mutants. Nat Rev Genet 2001; 2:538-548.

[46] Watson ED, Cross JC. Development of structures and transport functions in the mouse placenta. Physiology (Bethesda) 2005; 20:180-193.

[47] Strunk KE, Amann V, Threadgill DW. Phenotypic variation resulting from a deficiency of epidermal growth factor receptor in mice is caused by extensive genetic heterogeneity that can be genetically and molecularly partitioned. Genetics 2004; 167:1821-1832.

[48] Barker DJ, Eriksson JG, Forsen T, Osmond C. Fetal origins of adult disease: strength of effects and biological basis. Int J Epidemiol 2002; 31:1235-1239.

Chapter IV

PLACENTAL OVERGROWTH AND FERTILITY DEFECTS IN MICE WITH A HYPERMORPHIC ALLELE OF EPIDERMAL GROWTH FACTOR RECEPTOR

Abstract

Epidermal growth factor receptor (EGFR) is a member of the ERBB family of receptor tyrosine kinases that has been shown to play an important developmental and physiological role in many aspects of pregnancy. We have previously shown in mice that *Egfr*^{tm1mag} nullizygous placentas have fewer proliferative trophoblasts than wildtype and exhibit strain-specific defects in the spongiotrophoblast and labyrinth layers. In this study we used mice with the hypermorphic *Egfr*^{Dsk5} allele to study effects of increased levels of EGFR signaling on placental development. On three genetic backgrounds, heterozygosity for *Egfr*^{Dsk5} resulted in larger placental size with a more prominent spongiotrophoblast layer and increased expression of glycogen cell-specific genes. The C3HeB/FeJ strain showed additional placental enlargement of *Egfr*^{Dsk5} homozygotes with a significant number of homozygous embryos dying prior to 15.5 dpc. We also observed strain-specific sub-fertility in *Egfr*^{Dsk5} heterozygous females and detected higher levels of phospho-EGFR in the uterus of *Egfr*^{Dsk5} heterozygotes. The structure of *Egfr*^{Dsk5} heterozygous non-pregnant uteri appeared similar to wildtype but during pregnancy embryo implantation was deferred beyond the normal window of uterine receptivity in the sub-fertile strains. Collectively, our results

demonstrate that mice with increased levels of EGFR signaling exhibit an extensive level of genetic background-dependent phenotypic variability. In addition, EGFR promotes growth of the placental spongiotrophoblast layer in mice and EGFR expressed in the uterine stroma plays an under-appreciated role in preparation of the uterus for embryo implantation.

Introduction

ERBB family receptor tyrosine kinases are critical mediators of cell signaling in a broad range of developmental and physiological processes. Epidermal growth factor receptor (EGFR), in particular, plays a role in many aspects of female reproduction and pregnancy. Female mice that are homozygous for a hypomorphic allele of *Egfr*, $Egfr^{wa2}$, exhibit impaired lactation as well as delayed puberty, and three ligands that bind EGFR, Epiregulin (EREG), Amphiregulin (AREG), and Betacellulin (BTC) stimulate *in vivo* oocyte maturation and cumulus expansion via EGFR activation in ovarian follicles [1-4]. In addition, EGFR is expressed in the uterine stroma where it regulates not only uterine development but also embryo implantation [5,6]. Uterine grafts derived from $Egfr^{tm1Mag}$ nullizygous pups develop smaller compared to wildtype grafts although differentiation of the uterine luminal and glandular epithelium as well as stroma and myometrium occur normally [7]. Proliferative response to estradiol is diminished in the uterine stroma but not the epithelium of $Egfr^{tm1Mag}$ nullizygous grafts. During implantation expression of EGFR and ligands are observed in the uterus at the site of blastocyst attachment as well as on the surface of the implanting blastocyst [5,6]. Although there is redundancy in uterine expression of EGFR ligands, heparin-binding EGF-like growth factor (HBEGF) may play a unique and essential role since *Hbegf* null female mice are sub-fertile due to partial implantation failure [8]. Finally, EGFR regulates growth and differentiation of the placenta. $Egfr^{tm1Mag}$ nullizygous embryos exhibit strain-dependent placental defects that range from minor reduction of the spongiotrophoblast layer to severe labyrinth dysmorphogenesis [9,10]. The consequences of increased EGFR signaling in placental development and reproduction can now be determined in mice using a hypermorphic EGFR allele, $Egfr^{Dsk5}$ (*Dark skin-5*).

The *Egfr*^{Dsk5} allele was originally discovered during an N-ethyl-N-nitrosourea (ENU)-mutagenesis screen for visible dominant mutations [11]. *Egfr*^{Dsk5} heterozygous and homozygous mice on the C3HeB/FeJ background exhibit hyper-pigmented footpads, long nails, wavy hair, and a thickened epidermis. *Egfr*^{Dsk5} mutants have increased numbers of melanocytes in the epidermis leading to late onset pigment accumulation, apparent in the footpads at approximately 2-3 months of age. The *Egfr*^{Dsk5} mutation was molecularly identified as a Leu863Gln substitution within a region of the kinase domain important for stabilization of the receptor activation loop. When crossed to mice heterozygous for the *Egfr*^{wa2} hypomorphic allele, compound heterozygous mice are wildtype in appearance, suggesting that *Egfr*^{Dsk5} is a gain-of-function allele that causes increased levels of EGFR signaling. Livers from *Egfr*$^{Dsk5/+}$ mice have significantly lower levels of total EGFR, with *Egfr*^{Dsk5} homozygotes having even less, while both a larger proportion of phosphorylated EGFR compared to livers from wildtype mice. This data demonstrates that a negative feedback mechanism limits signaling in *Egfr*^{Dsk5} livers, and possibly other organs, by down-regulating EGFR protein. The hypermorphic *Egfr*^{Dsk5} allele may also be relevant to human cancer since the EGFR L861Q mutation, the human equivalent to mouse L863Q, was identified in gefitinib-responsive non-small-cell lung tumors [12]. When transfected into 32D cells, the L861Q form of EGFR exhibits ligand-independent phosphorylation and escapes ligand-induced receptor down-regulation through a mechanism that involves receptor binding of HSP90 [13]. Although there has been limited physiological characterization of the *Egfr*^{Dsk5} allele, there have been no reports of lung tumors or increased incidence of any other cancers in *Egfr*^{Dsk5} heterozygous or homozygous mice. This is somewhat surprising considering mice homozygous for the hypomorphic *Egfr*^{wa2} allele show a reduction in tumors

when crossed to numerous cancer models including those of the mammary, colon and skin [14-16].

The present study uses *Egfr*^{Dsk5} mice to determine if increased EGFR signaling has an effect on development of the placenta. We utilized three genetic backgrounds to identify strain-dependent phenotypes related to the *Egfr*^{Dsk5} mutation since genetic background influences phenotypes in mice with null or hypomorphic *Egfr* alleles. In addition to the original isogenic C3H strain on which *Egfr*^{Dsk5} was generated, we backcrossed the allele to two additional genetic backgrounds, C57BL/6J (B6) and 129S1/SvImJ (129). We report that placental weight is increased in *Egfr*^{Dsk5} heterozygotes and homozygotes on all three backgrounds. The larger placenta does not affect embryonic growth but is accompanied by strain-specific embryonic lethality of some *Egfr*^{Dsk5} homozygotes before 15.5 days post-coitus (dpc). Additionally, we identified a strain-specific fertility defect in *Egfr*^{Dsk5} heterozygous females that may be related to delayed implantation timing, and we found that older female *Egfr*^{Dsk5} heterozygotes frequently exhibited additional reproductive phenotypes of the uterus and ovary.

Materials and Methods

Mice and genetic crosses

The *Egfr*^{Dsk5} allele was generated by random mutagensis with ENU as previously described and maintained isogenic on the C3H background [11]. B6 and 129-*Egfr*^{Dsk5} congenic mice were generated by backcrossing C3H-*Egfr*^{Dsk5} heterozygous stocks to B6 and 129 wildtype strains for ten or more generations. Congenic *Egfr*^{Dsk5} heterozygous mice were then intercrossed to produce litters from each background containing wildtype, *Egfr*^{Dsk5}

heterozygous and homozygous congenic embryos and pups. Mice were fed Purina Mills Lab Diet 5058 or 5010 and water *ad libitum* under specific pathogen free conditions in an American Association for the Accreditation of Lab Animal Care approved facility. All experiments were approved by an Institutional Animal Care and Use Committee.

Genotyping

DNA was extracted from adult ear punches or embryo tail biopsies for genotyping by incubating at 95°C in 100 *u*L of 25mM NaOH/0.2mM EDTA for 20 minutes and then neutralizing with 100 *u*L 40mM TrisHCl pH 5.0. For the subsequent genotyping reactions, 1 *u*L of lysed tissue sample was used per reaction.

Egfr^{Dsk5} allele was amplified by PCR with the following primers: DskF, 5'-AGATGGTTCACTCCCTCACG-3' and DskR, 5'-ATGCTTCCTGATCTACTCCC-3' (Qiagen). PCR conditions were 40 cycles at 94°C for 20 seconds, 62°C for 20 seconds and 72°C for 60 seconds. PCR products were digested for 3 hours at 37°C with *Alu* I and Restriction Enzyme Buffer 2 (NEB) and run on a 3% agarose gel to separate a 220-bp product corresponding to wildtype *Egfr* and a 150 and 70-bp set of products corresponding to the digested *Egfr*^{Dsk5} allele.

Collection of placenta and uterus samples

Noon on the day that copulation plugs were observed was designated as 0.5 dpc. Pregnant females were euthanized by exposure to a lethal dose of isoflourane and embryos with their corresponding placentas dissected from the uterine horns on the morning of 15.5 dpc or 18.5 dpc into phosphate buffered saline (PBS). The placenta and extra-embryonic tissues were separated from the embryo by mechanical dissection and a tail biopsy collected for DNA extraction to determine the genotype of each embryo. Wet weights of embryos and

placentas were recorded at the time of dissection. Placentas were preserved in RNAlater (Ambion) for extraction of RNA or fixed in 10% NBF (neutral buffered formalin) for histological analysis. Uteri were collected from non-pregnant virgin mice approximately 3 months of age and fixed in 10% NBF.

Histology

After fixing placentas and uteri in 10% neutral buffered formalin overnight, tissues were washed in PBS, dehydrated in a grade series of ethanols and xylenes, and embedded in paraffin. Seven-micron sections were cut using a Leica RM2165 microtome. Sections were deparaffinized, rehydrated in a graded series of ethanols, and stained with hematoxylin and eosin (H&E) or Periodic acid-Schiff (PAS). Stained sections were dehydrated in a series of ethanols and mounted using permount. Representative histological images were photographed on a Nikon FXA microscope at a magnification of 1X, 2X, or 10X using a CCD digital camera.

Real time PCR

Placentas were homogenized in 1.2 mLs Trizol using a bead mill (Eppendorf) and RNA was isolated according to manufacturer's protocol (Invitrogen). For each sample, 15 ug of RNA was DNAse-treated, followed by a phenol-chloroform extraction. RNA was quantified (Nanodrop) and 1 ug of each sample was reverse transcribed using the cDNA Archive kit (Applied Biosystems). The amount of cDNA corresponding to 20 ng of RNA was used for each 20 uL real-time PCR reaction on an MXP-3000 instrument (Stratagene). Primer and probe sets for *Gusb*, *Eomes*, *Esrrb*, *Esx1*, *Dlx3*, *Gm52*, *Tcfeb*, *Ctsq*, *Timp2*, *Glut3*, *Cx31* and *Pdch12* were run according to manufacturer's protocol with 2X Taqman Universal Mastermix (ABI). Probes for *4311*, *Gcm1* and *Pl1* were designed and manufactured in-house

(Dr. Kathleen Caron, UNC). *Gusb* was used as an endogenous control and fold change of each gene of interest was calculated using the ΔΔCt method. The average ΔCT of wildtype animals for each strain/allele combination was used as the control value to calculate ΔΔCt values for samples of the same strain and allele. Fold-change values were computed from the ΔΔCt for each sample and converted to a percent increase over the wildtype average fold change for $Egfr^{Dsk5}$ heterozygous and homozygous samples.

For clustering analysis, ΔCT values for each sample and probe were uploaded into Cluster and median-centered. Data was visualized using TreeView.

Implantation site visualization

Tail vein injections were performed on pregnant wildtype and $Egfr^{Dsk5}$ heterozygous C3H and B6 females at 4.5 and 5.5 dpc. Approximately 1 mL 0.5% Evan's blue dye was injected into the tail vein of anesthetized mice and 5 minutes later mice were asphyxiated using CO_2. Mice were dissected and implantation sites were scored for each genotype.

Western blot

Three-month-old females were treated with 10μL per gram body weight phosphotase inhibitor (5mM Na_3VO_4, 50mM H_2O_2) by intraperitoneal injection and sacrificed by CO_2 after five minutes. Whole uteri were collected and snap frozen in liquid nitrogen. Frozen tissue was minced in 5 volumes lysis buffer (10 mM Tris-HCl pH 7.4, 100 mM NaCl, 1mM EDTA, 1 mM EGTA, 1% NP-40, 10% glycerol, 0.1% SDS, 0.5% Sodium deoxycholate, 1mM PMSF, 10 μg/mL Leupeptin, 10 μg/mL Aprotinin, 1mM Na_3VO_4, 1mM NaF) and homogenized in 2 mL tubes for 4 minutes using a bead mill. Samples were then sonicated for 30 seconds and incubated for 1 hour on ice. Lysates were cleared by centrifugation for 10

minutes at 13,000 rpm and protein quantified using the Bradford-based Protein Assay (Biorad).

Samples were diluted with 2X sample buffer and boiled for 5 minutes. 18 μg of each sample was separated by denaturing 7.5% sodium dodecylsulfate polyacrylamide gel electrophoresis (SDS-PAGE) for 1 hour at 200 V and transferred to a PVDF membrane for 1.5 hours at 100 V. The membranes were blocked for 1 hour in 5% BSA/TBST (10 mM Tris pH 7.5, 150 mM NaCl, 0.1% Tween 20) for phospho-EGFR detection and 5% milk/TBST for total EGFR and β-actin detection. Primary antibody incubations were overnight at 4°C followed by five TBST washes and secondary antibody incubations were 1 hour at room temperature. The phospho-EGFR antibody (Cell signaling) was diluted 1:1,000 in 5 % BSA /TBST and the total EGFR antibody (Upstate) was diluted 1:1,000 in 5% milk /TBST. The β-actin antibody (Sigma) was diluted 1:10,000 in 5% milk /TBST. HRP-conjugated secondary antibodies were diluted 1:10,000 in 5% blocking agent /TBST. Following the secondary antibody incubation blots were washed five times in TBST and protein detected by an enhanced chemiluminescence system (Amersham).

Statistical analysis

All placenta and embryo weights were analyzed using the Mann Whitney test. A χ^2 goodness of fit test was performed to determine if the genotype distribution deviated from expected Mendelian ratios. Real-time fold change values were analyzed using the student's T-test.

Results

$Egfr^{Dsk5}$ heterozygous and homozygous placentas weigh more than wildtype littermates at 15.5 dpc

Strain-dependent phenotypes were evident when the $Egfr^{Dsk5}$ allele was backcrossed to 129 and B6 and compared to the original C3H background. $Egfr^{Dsk5}$ heterozygotes and homozygotes exhibited slightly wavy coats on all three backgrounds, with the phenotype being most pronounced on the B6 background (Figure 17A and 17B). The C3H and 129-$Egfr^{Dsk5}$ heterozygotes exhibited pigmented footpads at 3 months of age, a phenotype not manifested by B6-$Egfr^{Dsk5}$ heterozygotes (Figure 17C and 17D). However, some B6-$Egfr^{Dsk5}$ heterozygotes showed very slight footpad pigmentation by 6 to 8 months of age. We also observed long toenails in the C3H and 129-$Egfr^{Dsk5}$ heterozygotes that were frequently dark-colored on the 129 background (Figure 17E).

Since reduced EGFR signaling has a detrimental effect on proper development of the placenta, we investigated whether an increased level of EGFR signaling affects placental growth. At 15.5 dpc placenta weight was increased 18% in B6-$Egfr^{Dsk5}$ heterozygotes ($p < 0.001$) and homozygotes ($p < 0.001$) compared to placentas from wildtype littermates (Figure 18A). On the C3H background, $Egfr^{Dsk5}$ heterozygotes had placenta weights that were increased 17% over wildtype ($p < 0.01$) and $Egfr^{Dsk5}$ homozygotes 55% more than wildtype ($p < 0.001$; Figure 18A). The difference in placenta weight between $Egfr^{Dsk5}$ heterozygotes and homozygotes on the C3H background was significant; placentas from $Egfr^{Dsk5}$ homozygotes weighted 28% more than placentas from $Egfr^{Dsk5}$ heterozygotes ($p < 0.001$). Placenta weight was increased 12% in 129-$Egfr^{Dsk5}$ heterozygotes ($p < 0.01$) and homozygotes ($p < 0.01$) compared to wildtype (Figure 18A). None of the strains examined

showed differences in embryo weight between the three genotypes suggesting that increased placental weight did not affect growth of the embryo (Figure 18B).

Altered expression of trophoblast cell subtype markers in Egfr^{Dsk5} heterozygous and homozygous placentas

In order to determine the effect of the *Egfr^{Dsk5}* allele on differentiation of the placental trophoblast, we measured transcript levels for a panel of specific trophoblast cell subtype markers (Table 7). Significant differences were observed in the expression of several genes in *Egfr^{Dsk5}* heterozygous and homozygous when compared wildtype placentas at 15.5 dpc (Table 9). On the B6 background labyrinth-expressed genes *Gcm1 and Dlx3* were significantly reduced in *Egfr^{Dsk5}* heterozygous (n = 7) and homozygous placentas (n = 4) while *4311*, a marker of spongiotrophoblast, was elevated in *Egfr^{Dsk5}* heterozygotes and homozygotes compared to wildtype controls (n = 7). *Pdch12*, a marker of glycogen cells, and *Pl-1*, a marker of trophoblast giant cells, were significantly elevated in *Egfr^{Dsk5}* heterozygotes and homozygotes when data from the two genotypes was combined and compared to wildtype. In addition, expression of the trophoblast stem cell marker, Eomes, was significantly elevated in B6 *Egfr^{Dsk5}* homozygotes but not heerozygotes. There were no significant changes in the expression of *Tcfeb*, *Esx1*, *Esrrb1*, *Gm52*, *Ctsq*, *Timp2*, *Glut3* and *Cx31*.

On the C3H background expression of *Dlx3* was reduced in *Egfr^{Dsk5}* heterozygotes (n = 5) and homozygotes (n = 5) compared to wildtype (n = 5). *Tcfeb* and *Gm52*, both labyrinth-specific genes, were reduced in *Egfr^{Dsk5}* homozygous placentas, while *4311* expression was increased in both *Egfr^{Dsk5}* heterozygotes and homozygotes compared to

wildtype but the data did not reach significance. *Pdch12* was significantly elevated in *Egfr*^{Dsk5} homozygotes and increased in *Egfr*^{Dsk5} heterozygotes.

The 129 strain also exhibited genotype-associated changes in gene expression. Overall, the labyrinth-specific genes were reduced in *Egfr*^{Dsk5} heterozygotes and homozygotes but the reduction was not significant for any probe alone. *Esrrb1* was elevated in *Egfr*^{Dsk5} heterozygotes (n = 6) and homozygotes (n = 6) compared to wildtype (n = 4). Similar to B6 and C3H, the expression of *4311* and *Pdch12* were increased in 129-*Egfr*^{Dsk5} heterozygotes and homozygotes but the changes were not significant.

ΔCT expression values for significant and non-significant genes were also median-entered and clustered by sample and gene to visualize strain and genotype patterns within the data (Figure 19). Clustering analysis showed strain-specific clustering for B6, C3H and 129. The C3H strain showed relatively low expression of *Eomes*, *Glut3* and *Gcm1*, while 129 showed relatively low expression of *4311* and *Pcdh12* and B6 showed highest expression of *Ctsq*, *4311* and *Timp2* compared to the other strains. The B6 strain showed the strongest genotype clustering with relatively low expression of *Gcm1* and high expression of *4311* in *Egfr*^{Dsk5} heterozygotes and homozygotes (red bars) versus wildtype placenta (green bars).

Egfr^{Dsk5} *heterozygous and homozygous placentas have an expanded spongiotrophoblast layer*

We examined H & E and PAS-stained tissue sections to further characterize the over-growth phenotype observed in *Egfr*^{Dsk5} heterozygous and homozygous placentas. Consistent with the real-time data, we observed an increased layer of spongiotrophoblast in *Egfr*^{Dsk5} heterozygotes and homozygotes compared to wildtype (Figure 20). There was also increased

numbers of PAS-positive cells suggesting that the population of glycogen trophoblasts was larger in the *Egfr*^{Dsk5} placentas (Figure 20G-I). We did not observe any obvious changes in the size or structure of the labyrinth layer for any of the genotypes. The decreased expression of labyrinth markers was probably due to the disproportionate increase in the size of the spongiotrophoblast layer.

Reduced fertility observed in 129 and C3H Egfr^{Dsk5} *heterozygous females*

During collection of 15.5 dpc placentas, we observed a large number of dead embryos in litters from C3H and 129, but not B6-*Egfr*^{Dsk5} heterozygous females. In the B6 strain, 93% of embryos were viable, while in C3H and 129, 39% and 21% of embryos were viable, respectively (Figure 21A). Viable embryos from each strain were genotyped to determine if the genotype distribution deviated from expected Mendelian ratios (Table 10). Neither B6 nor 129 had numbers of viable *Egfr*^{Dsk5} heterozygous and *Egfr*^{Dsk5} homozygous embryos that were different than the expected ratios, although data for 129 approached significance with a higher number of *Egfr*^{Dsk5} homozygotes than expected. However, for C3H only 11% of viable embryos were *Egfr*^{Dsk5} homozygous, which is significantly different from the expected 25% ($p < 0.05$). The viability of *Egfr*^{Dsk5} heterozygous embryos was not affected in the C3H cross and the lethality of the *Egfr*^{Dsk5} homozygotes did not fully account for the 50 – 60% reduction in live embryos observed at 15.5 dpc in C3H.

Since genotype alone did not explain the lethality of C3H embryos at 15.5 dpc, additional matings were set up for C3H and 129 to investigate the origin of reduced embryonic viability. When wildtype C3H and 129 females were mated to *Egfr*^{Dsk5} heterozygous males from their respective strains, a significant increase in the number of

viable embryos was observed compared to results from the *Egfr*^{Dsk5} heterozygous intercrosses (Figure 21B). For C3H embryo viability was 86% versus the 39% observed in *Egfr*^{Dsk5} heterozygous intercrosses. For 129, embryo viability was 88% when the female was wildtype versus 36% viability in *Egfr*^{Dsk5} heterozygous intercrosses. To confirm that the embryonic lethality was due to uterine environment, reciprocal crosses were performed for the 129 strain (Figure 21B). When *Egfr*^{Dsk5} heterozygous females were mated to wildtype males, embryo viability was 21%, similar to the number observed in *Egfr*^{Dsk5} heterozygous intercrosses (39%).

Levels of phospho-EGFR are higher in Egfr^{Dsk5} *heterozygous uteri*

Since the fertility defect observed seemed to be dependent on maternal, but not embryonic, genotype, we measured the levels of total and phosphorylated EGFR in uteri from *Egfr*^{Dsk5} heterozygous mice to evaluate whether there is a similar down-regulation of EGFR in the uterus compared to that previously reported for the *Egfr*^{Dsk5} liver. Uteri were collected from phosphatase inhibitor-treated 3-month-old wildtype and B6 and C3H-*Egfr*^{Dsk5} heterozygotes and their wildtype littermates. Analysis using western blots revealed that the levels of total EGFR were similar in samples from wildtype and *Egfr*^{Dsk5} heterozygous placentas but phospho-EGFR was significantly higher in the *Egfr*^{Dsk5} heterozygous placental samples (Figure 22). Additionally, phospho- and total EGFR were detected at higher levels in the C3H strain versus B6.

Non-pregnant Egfr^{Dsk5} heterozygous and wildtype uteri are similar at the histological level

Next we examined from uteri from virgin, random cycling Egfr^{Dsk5} heterozygous and wildtype female littermates at approximately three months of age. In all four pairs of B6 and C3H littermates examined *Egfr^{Dsk5}* heterozygous uteri weighed more than wildtype. H & E stained tissue sections revealed no obvious defects in *Egfr^{Dsk5}* heterozygous uterine morphology (Figure 23A-D). Uteri from B6 and C3H-*Egfr^{Dsk5}* heterozygotes had clearly differentiated luminal and glandular epithelium, stroma and myometrium that appeared similar to wildtype tissue. In our B6 breeding colony *Egfr^{Dsk5}* heterozygous female fertility declined at a relatively young age compared to wildtype females (data not shown). We dissected several five to nine month old B6 *Egfr^{Dsk5}* heterozygous females and frequently noted the appearance of fluid-filled cysts on one or both ovaries (Figure 23E). The aged *Egfr^{Dsk5}* heterozygous females exhibited additional sporadic uterine abnormalities not observed in younger animals but these defects have not been fully characterized.

Implantation is delayed in Egfr^{Dsk5} heterozygous females

Since high levels of embryonic lethality within a litter has been previously associated with a delay in the timing of implantation we examined the timing of implantation in *Egfr^{Dsk5}* heterozygous versus wildtype females [17]. Evan's blue dye tail vein injections were performed at 4.5 and 5.5 dpc to visualize implantation sites in C3H and B6 uteri (Figure 24). At 4.5 dpc we consistently observed implantation sites in wildtype C3H females (8/10) but not C3H-*Egfr^{Dsk5}* heterozygous females (2/9) (Figure 24A-C). However, implantation did eventually occur in C3H-*Egfr^{Dsk5}* heterozygous females since all C3H females (3/3 for

wildtype, 5/5 for *Egfr*^{Dsk5} heterozygous) examined at 5.5 dpc regardless of genotype had implantation sites present in both uterine horns (Figure 24A and 24D). This data suggest that embryos in the C3H-*Egfr*^{Dsk5} heterozygous uterus implant beyond the normal window of uterine receptivity. In B6-*Egfr*^{Dsk5} heterozygous females implantation sites were evident at 4.5 dpc (4/6) suggesting that implantation timing is normal in this strain (Figure 24A and 24E).

Discussion

Similar to mouse models in which EGFR signaling is reduced or abolished, we have shown here that phenotypes resulting from increased EGFR signaling vary by genetic background. Mice that are heterozygous or homozygous for the hypermorphic *Egfr*^{Dsk5} allele display strain-dependent hair, skin, and nail phenotypes. EGFR is known to be involved in progression of several types of cancer, but our initial characterization of B6, 129 and C3H-*Egfr*^{Dsk5} heterozygotes did not reveal an obvious increase in tumor susceptibility in mice younger than nine months of age. However, we found *Egfr*^{Dsk5} heterozygous and homozygous placentas enlarged and *Egfr*^{Dsk5} heterozygotes sub-fertile due to several strain-specific defects in the female reproduction.

EGFR in the placenta

Our examination of placentas from mice with at least one hypermorphic allele of EGFR demonstrates that increased activation of EGFR can result in strain-specific effects on placental growth. In the B6 and 129 strains heterozygosity and homozygosity for *Egfr*^{Dsk5} resulted in the same increase in placental weight, suggesting that placental growth does not

continue beyond a threshold reached with one *Egfr*^{Dsk5} allele. However, it is unkonwn whether this limitation on growth is a property of the trophoblast population or general negative feedback inhibition of EGFR signaling. There is evidence from studies using *Egfr*^{Dsk5} mouse livers that total EGFR is down-regulated, particularly in the homozygote, and a similar mechanism could limit the increase in trophoblasts observed in B6 and 129-*Egfr*^{Dsk5} strains. If there is a threshold in growth-promoting effects of *Egfr*^{Dsk5}, it is not reached in C3H *Egfr*^{Dsk5} heterozygotes since placentas from *Egfr*^{Dsk5} homozygous mice are larger than heterozygous placentas. The weight differences were highly significant between *Egfr*^{Dsk5} genotypes, and we observed some embryonic lethality of C3H-*Egfr*^{Dsk5} homozygotes that could be related to the placental overgrowth.

Although placental weights were altered, no significant effects of the *Egfr*^{Dsk5} allele on embryo weights were observed at 15.5 dpc in any of the three strains. Both molecular and histological analyses showed that the increased placental weights are due to an increase in spongtiotrophoblast and glycogen cell populations. Overall, expression of spongiotrophoblast and glycogen trophoblast markers *4311* and *Pdch12* were significantly increased in placentas from *Egfr*^{Dsk5} heterozygous and homozygous embryos. Expression of several labyrinth markers was decreased in *Egfr*^{Dsk5} heterozygous and *Egfr*^{Dsk5} homozygous placentas but this was probably due to a disproportionate amount of RNA coming from the abundant spongiotrophoblasts rather than an actual reduction in labyrinth trophoblast. Histological examination of B6 placentas revealed an enlarged layer of spongiotrophoblast and glycogen cells in the *Egfr*^{Dsk5} heterozygotes and homozygotes. Placentas homozygous for the *Egfr*^{tm1Mag} null allele have fewer numbers of proliferating trophoblasts and this phenotype does not correlate with severity of labyrinth defects. Therefore, the increased layer of

spongiotrophoblast observed in *Egfr*^{Dsk5} heterozygous and *Egfr*^{Dsk5} homozygous placentas is probably a result of greater trophoblast proliferation and suggest that EGFR plays a major role in promoting cell cycle progression in spongiotrophoblast and glycogen cell precursors.

EGFR in uterine preparation for implantation

Our data indicate that 129 and C3H female mice heterozygous for the dominant *Egfr*^{Dsk5} hypermorphic mutation may exhibit uterine defects that significantly reduce fertility. In litters from *Egfr*^{Dsk5} pregnant females, embryos of all genotypes showed reduced survival suggesting that the maternal uterine environment has a detrimental effect on litter viability. The maternal origin of embryo loss was verified in crosses between *Egfr*^{Dsk5} heterozygous females and wildtype males, which resulted in significant embryo loss while crosses between wildtype females and *Egfr*^{Dsk5} heterozygous males did not. This phenotype was strain-specific since embryo viability was normal in litters from B6- *Egfr*^{Dsk5} heterozygous females. The precise timing of implantation is mediated by molecular crosstalk between the uterus and blastocyst, and a delay in implantation can result in pregnancy loss [18]. An examination of early implantation sites revealed that in C3H-*Egfr*^{Dsk5} heterozygous females, implantation is deferred beyond the normal window of uterine receptivity, which occurs on the evening of 3.5 dpc in wildtype females. In B6- *Egfr*^{Dsk5} heterozygous females, implantation timing was normal suggesting that the implantation timing defect in C3H-*Egfr*^{Dsk5} heterozygous may be related to the high levels of embryonic lethality.

Implantation normally occurs during a defined window of time in which the uterus is receptive to the implanting, activated blastocyst [19]. This window of uterine receptivity occurs on the evening of day 3 in mice and is controlled by a low dose surge of ovarian

estrogen that acts upon the already progesterone-primed uterus [20]. By late day 5 the uterus proceeds to a refractory state and no longer supports implantation of embryos. Several mouse models have been described with blastocyst implantation beyond the normal window of uterine receptivity and characterization of the phenotype has revealed that production of prostaglandins is essential for the process. In mice deficient for prostaglandin endoperoxide synthase 2 (COX2) or cytosolic phospholipase A2 (CPLA2), a provider of arachidonic acid for prostaglandin synthesis, implantation sites are not apparent until day 5.5 and they are fewer in number with poor permeability compared to implantation sites in wildtype females [17,21]. The implantation delay in these mice has been shown to lead to a later wave of embryonic lethality resulting in smaller litter sizes for both models. Wildtype blastocyst that are transferred into a pseudopregnant uterus on day 5.5 also exhibit this wave of lethality suggesting that embryonic lethality observed in the COX2 and CPLA2 deficient mice is a result of the delay in implantation rather than a direct consequence of the gene deletion [17]. Mice that are null for lysophosphatidic acid G-protein-coupled receptor 7 (*Lpa3*) also exhibit a similar phenotype that is probably due to a reduction in uterine prostaglandin levels observed in the model [22].

The $Egfr^{Dsk5}$ heterozygous females exhibit a phenotype that appears similar to the deferred implantation observed in COX2, CPLA2, and LPA3-deficient females. We observed embryonic lethality that is independent of embryo genotype and probably a direct result of implantation beyond the normal window of uterine receptivity. Although it has been proposed that uterine EGFR may play a role in implantation, few studies have used genetic models to investigate the function of EGFR in this process. In fact, the majority of studies to date have focused on the consequences of reduced EGFR signaling in the embryo during

implantation. EGFR and ERBB4 are expressed on the surface of implanting blastocysts and are thought to mediate adhesion to the uterus via interactions with the trans-membrane form of HBEGF expressed on the uterine luminal epithelium [23,24]. ERBB receptors are also expressed in the uterus before, during and following implantation suggesting that receptor expression is important in the uterus as well as the implanting embryo [5,6]. Full length EGFR is strongly expressed in uterine stroma underlying implantation sites but is absent in the luminal epithelium, where a truncated secreted form of EGFR is expressed instead that is hypothesized to negatively regulate ERBB signaling [6,25]. ERBB2 is expressed in the luminal epithelium throughout the uterus with a peak in expression on day 1 and then again on day 5, when both the epithelium and decidualizing stroma surrounding the embryo express ERBB2 [26]. ERBB3 and ERBB4 are also present throughout the uterus but their expression is less dynamic during pregnancy. ERBB3 expression is primarily in the luminal and glandular epithelium of the uterus, while ERBB4 is expressed in the submyometrial stroma and myometrial connective tissue [27].

A majority of the eleven ERBB ligands have been reported as expressed in the mouse uterus during implantation [28-33]. Most important is HBEGF, which is the most extensively studied ligand since it is expressed in the uterine luminal epithelium on the evening of day 3 specifically at the site of blastocyst apposition [32]. HBEGF-deficient female mice are subfertile suggesting that HBEGF plays an essential role in the process of embryo apposition and attachment [8]. Leukemia Inhibitory Factor (LIF) deficient mice that have a complete failure of implantation do not exhibit the normal upregulation of HBEGF, nor the normal up-regulation of the other EGFR ligands AREG and EREG [34]. There are no fertility defects reported for females that are null for *Btc*, *Ereg* or triple null for *Areg, Egf*,

and *Tgfa* [35-37]. However, injection of EGF antibody into the uterine horn on day 3 of pregnancy decreases the number of implantation sites [29].

Previous studies suggested that EGFR signaling is involved in uterine receptivity and implantation timing. Transgenic mice that over-express either *Tgfa* or *Btc* display delayed implantation similar to the $Egfr^{Dsk5}$ heterozygous females [38,39]. However it is unclear whether embryonic lethality is associated with the phenotype in these models. In addition, expression of the *Tgfa* and *Btc* trangenes may be controlled in a manner not spatially or temporally similiar to expression of the endogenous genes making it difficult to determine if these particular ligands are involved in implantation timing under normal circumstances. Our data demonstrates that hyper-activation of endogenous EGFR in the uterine stroma does result in delayed implantation of blastocysts and suggests that EGFR signaling is important for coordinating uterine receptivity and blastocyst activation.

Conjoined placentas and aberrant embryo spacing are also observed in litters from *Cpla2* and *Lpa3* null females [17,22]. This phenotype is probably unrelated to the delay in implantation timing since prostaglandin supplementation corrects implantation timing and embryonic lethality defects but has no effect on embryo crowding. Although the $Egfr^{Dsk5}$ heterozygous females exhibit the same delay in implantation there is no evidence from our results to suggest that EGFR is involved in embryo spacing.

EGFR in female reproductive tract pathology

In addition to abnormal implantation timing, we also noticed other reproductive system anomalies in $Egfr^{Dsk5}$ heterozygous females. $Egfr^{Dsk5}$ heterozygous uteri weighed more than uteri from wildtype littermates, however differentiation of the tissue appeared

similar to wildtype at the histological level. At a young age B6-*Egfr*^{Dsk5} heterozygous exhibited normal reproductive capacity but we did notice that following their first pregnancy B6 *Egfr*^{Dsk5} heterozygous female fertility declined (data not shown). In B6-*Egfr*^{Dsk5} heterozygous females, particularly those older than five months we frequently observed sporadic uterine abnormalities as well as fluid-filled cysts on one or both ovaries, similar to the phenotype of *Inhibin alpha* (*Inha*) transgenic mice [40]. Uterine and/or ovarian defects may render older *Egfr*^{Dsk5} heterozygous females unable to ovulate and/or support implantation of embryos but more extensive characterization of these phenotypes is needed. Several recent studies suggest that increased levels of EGFR activity in female mice may result in uterine hyperplasia. Transgenic mice with mouse mammary tumor virus (MMTV)-regulated over-expression of human EGFR exhibit cystic hyperplasia of uterine glands at nine months of age [41]. Nine month-old mice deficient for Mitogen-inducible gene-6 (MIG6), an endogenous inhibitor of EGFR signaling, have enlarged uteri with an increased numbers of uterine glands and hyperplastic glandular and luminal epithelium [42]. In humans, *Mig-6* is over-expressed in moderate to severe cases of endometriosis [43].

In summary our study emphasizes extensive strain-dependent phenotypic variation evident in mice with increased levels of EGFR signaling. The same modifiers that influence variability observed in mice with null and hypomorphic alleles of EGFR are probably involved but there may be an additional class of modifiers that control down-regulation of activated EGFR. Our data also indicates that EGFR plays a previously under-appreciated role in the uterus during pregnancy. The fertility defects we have described in *Egfr*^{Dsk5} heterozygous mice suggest that in humans an increased level of uterine EGFR signaling may be a cause of infertility.

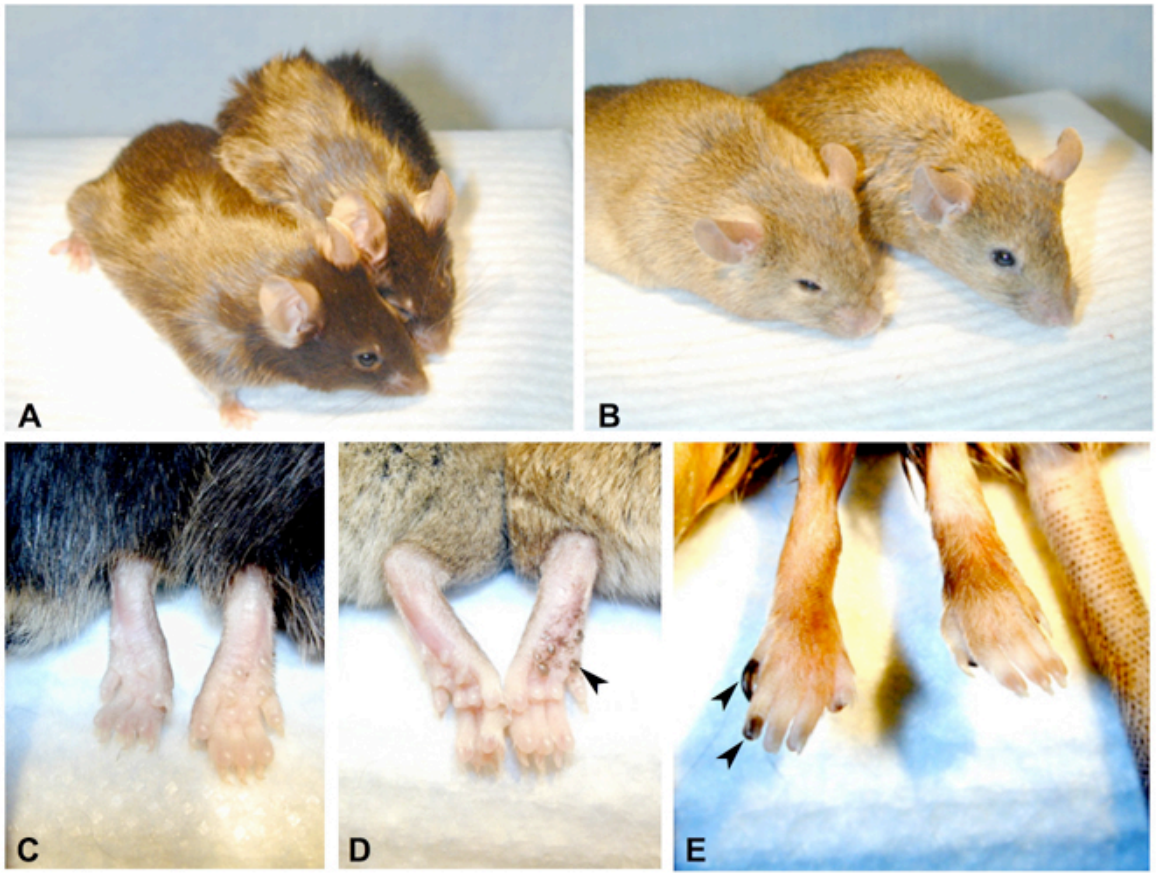

Figure 17. Strain-specific coat and skin phenotypes observed in *Egfr*^{Dsk5} heterozygotes. **A.** Wildtype (left) and *Egfr*^{Dsk5} heterozygote (right) on C57BL/6J (B6) background. **B.** Wildtype (left) and *Egfr*^{Dsk5} heterozygote (right) on C3HEB/FeJ (C3H) background. **C.** Footpads from 3 month old B6 wildtype (left) and *Egfr*^{Dsk5} heterozygote (right). **D.** Footpads from 3 month old C3H wildtype (left) and *Egfr*^{Dsk5} heterozygote (right). Arrowhead indicates excess pigmentation on footpad from *Egfr*^{Dsk5} heterozygote. **E.** Pigmented nails (arrowheads) in 129- *Egfr*^{Dsk5} heterozygote (left) but not C3H- *Egfr*^{Dsk5} heterozygote (right). Pigmentation visible on C3H is from footpad.

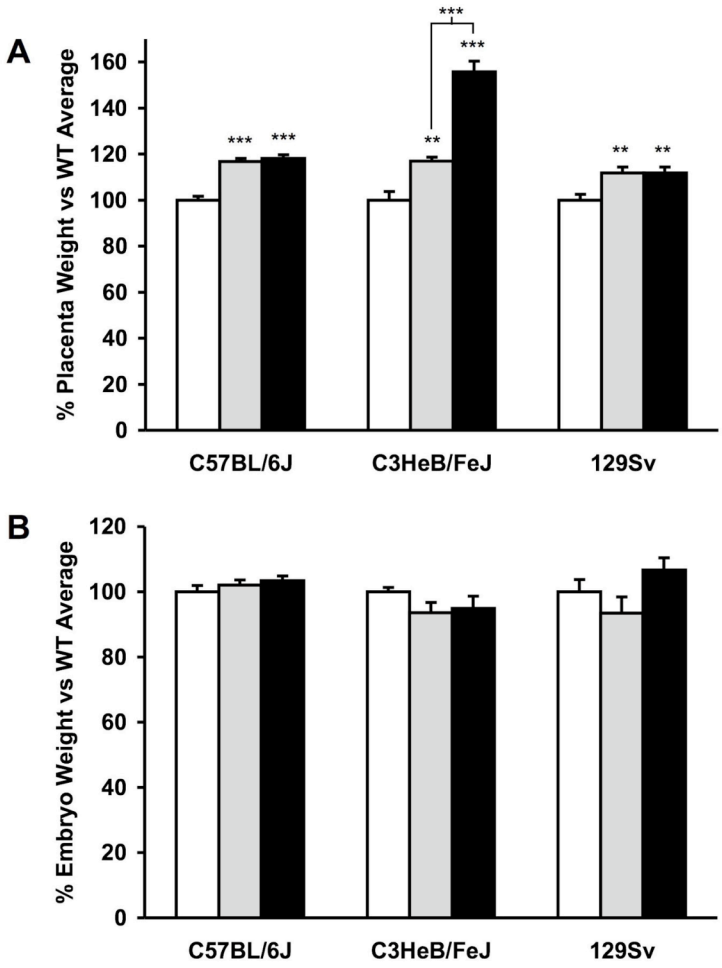

Figure 18. Weights of placentas and embryos from wildtype (white bars), *Egfr*^{Dsk5} heterozygous (gray bars) and homozygous littermates (black bars) measured at 15.5 dpc on three genetic backgrounds. ** indicates $p < 0.01$ compared to wildtype, *** indicates $p < 0.001$ compared to wildtype unless a different comparison is designated by horizontal bars. **A.** *Egfr*^{Dsk5} heterozygous (n=37) and homozygous (n= 24) placentas weighed 18% more than wildtype (n=29) on B6. C3H-*Egfr*^{Dsk5} heterozygous (n=20) placentas weighed 17% more than wildtype (n=15) and homozygous placentas (n=4) showed a 55% increase in weight compared to wildtype. *Egfr*^{Dsk5} heterozygous (n=20) and homozygous (n= 15) placentas weighed 12% more than wildtype (n=9) on 129. **B.** There were no significant differences observed in weight when *Egfr*^{Dsk5} heterozygous and homozygous embryos were compared to wildtype in any of the three strains.

Table 9. Percent expression of trophoblast cell subtype markers in *Egfr*^{Dsk5} heterozygous and homozygous placentas compared to wildtype littermates

	C57BL/6J		C3HeB/FeJ		129Sv	
	+ / Dsk5	*Dsk5/Dsk5*	*+ / Dsk5*	*Dsk5/Dsk5*	*+ / Dsk5*	*Dsk5/Dsk5*
Gcm1	58% ***	73%[1]	97%	83%	80%	90%
Dlx3	77% **	79%**	74%[1]	65%*	89%	84%
Tcfeb	97%	94%	83%	78%*	93%	90%
Esx1	94%	96%	95%	98%	81%	85%
Esrrb1	109%	108%	106%	136%	117%[1]	148%*
Eomes	103%	118%*	86%	89%	100%	109%
Gm52	103%	100%	79%[1]	73%*	85%	79%
Ctsq	113%	122%	80%	96%	94%	124%
4311	120%[1]	127%**	132%	123%	137%	171%
Pdch12	126%[1]	138%[1]	142%[1]	150%*	117%	144%
PL-1	135%[1]	148%[1]	69%	87%	81%	101%
Timp2	98%	116%	101%	91%	91%	98%
Glut3	94%	95%	96%	111%	89%	87%
Cx31	90%	90%	91%	94%	99%	115%

* $p < 0.05$, ** $p < 0.01$, *** $p < 0.001$, [1] $p < 0.05$ when +/*Dsk5* and *Dsk5/Dsk5* data were combined

Green = labyrinth-specific genes, Red= spongiotrophoblast-specific genes

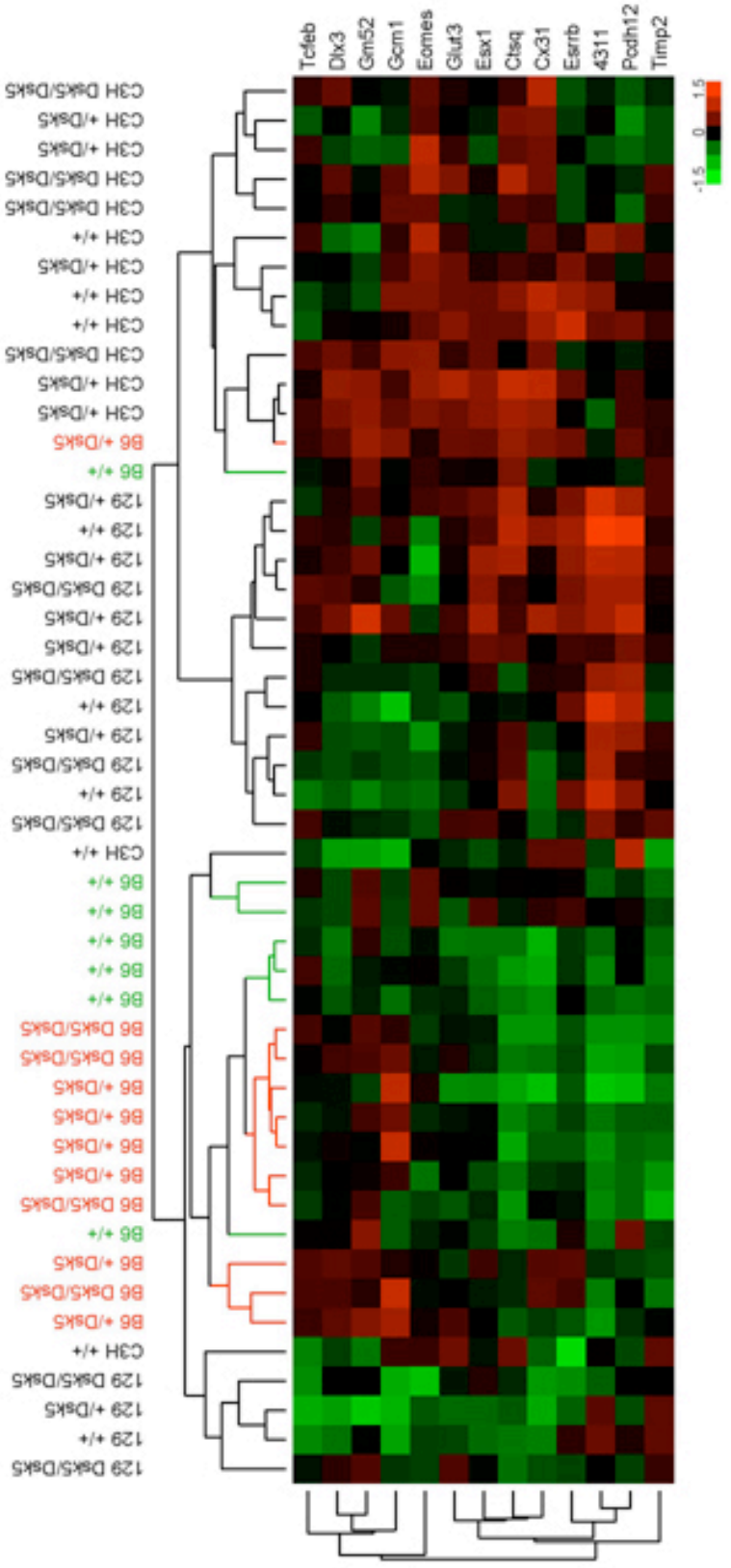

Figure 19. Cluster analysis and dendrogram of ΔCT values for *Egfr*^{Dsk5} homozygous, heterozygous, and wildtype samples. ΔCT gene expression values clustered by gene and sample. Red blocks indicate low relative expression and green blocks indicate high relative expression. Cluster analysis included genes that were and were not significantly changed in *Egfr*^{Dsk5} heterozygous and homozygous versus wildtype placenta. B6 *Egfr*^{Dsk5} heterozygous and homozygous samples are indicated by red and wildtype by green bars on dendrogram.

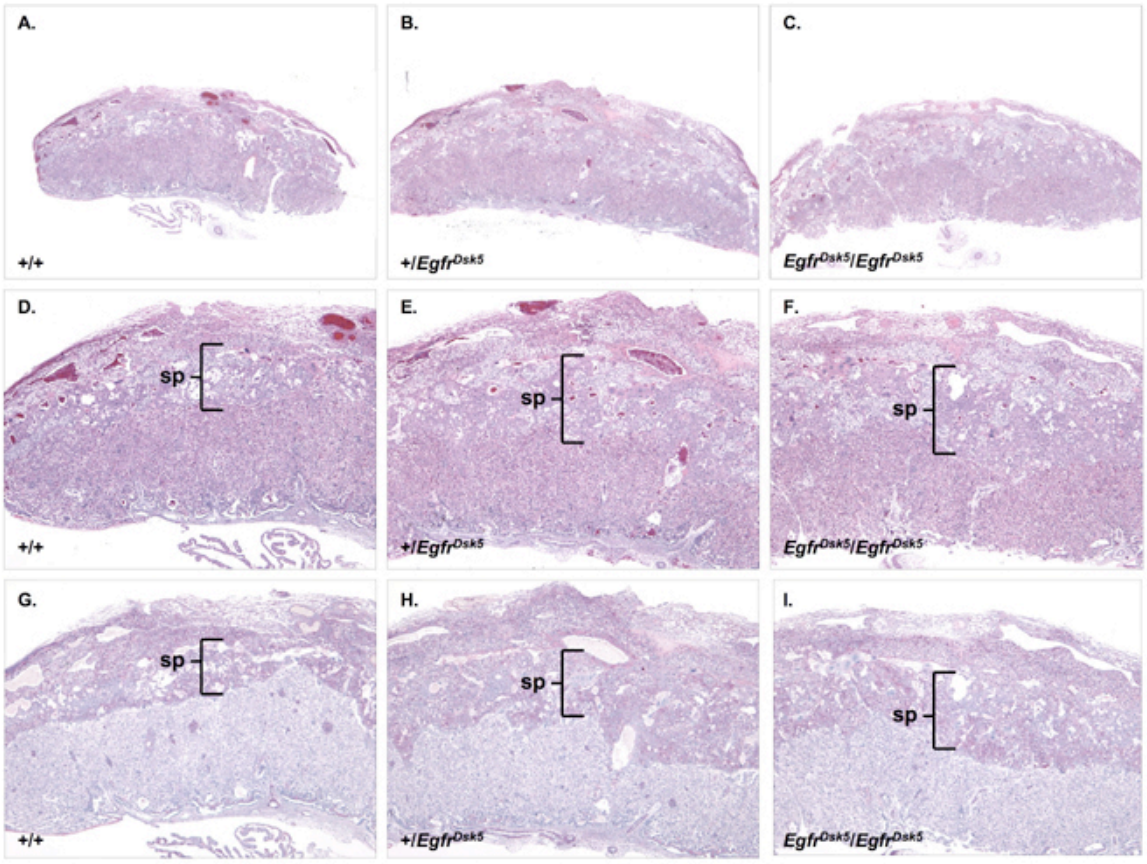

Figure 20. *Egfr*^{Dsk5} heterozygous and homozygous placentas have an expanded spongiotrophoblast layer compared to wildtype. **A, B, C.** H&E staining of 15.5 dpc placentas from B6 wildtype (A), *Egfr*^{Dsk5} heterozygote (B), and *Egfr*^{Dsk5} homozygote (C). **D, E, F.** Close-up of placentas from A. – C. **G, H, I.** PAS staining of 15.5 dpc placentas from B6 wildtype (G), *Egfr*^{Dsk5} heterozygote (H), and *Egfr*^{Dsk5} homozygote (I). The spongiotrophoblast (**sp**) compartment is bracketed in each section.

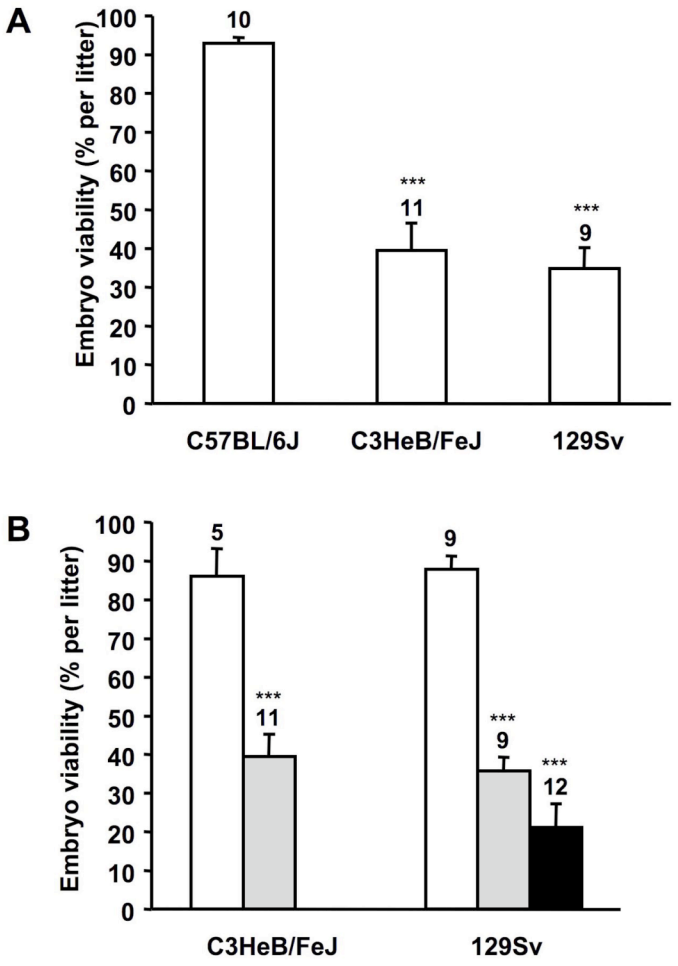

Figure 21. Embryo viability in C3H and 129 litters depends on maternal genotype. The number of litters used for each group is indicated above the error bars. *** indicates $p < 0.001$ compared to wildtype female X *Egfr*^{Dsk5} heterozygous male breeding. **A.** Overall embryo viability (all genotypes) in litters from *Egfr*^{Dsk5} heterozygous intercrosses using three genetic backgrounds. 93% of embryos were viable in litters from B6 intercrosses versus 39 % in C3H and 36% in 129 intercrosses. *** indicates $p < 0.001$ compared to B6. **B.** Embryo viability in C3H crosses between wildtype females and *Egfr*^{Dsk5} heterozygous males (white bar) was 86% versus 39% for *Egfr*^{Dsk5} heterozygous intercrosses (gray bar). Embryo viability in 129Sv crosses between wildtype females and *Egfr*^{Dsk5} heterozygous males (white bar) was 88% versus 36% for *Egfr*^{Dsk5} heterozygous intercrosses (gray bar) and 21% for *Egfr*^{Dsk5} heterozygous females crossed to wildtype males (black bar).

Table 10. Survival of 15.5 dpc embryos from *Egfr*^{Dsk5} intercrosses on three congenic strains

Strain	+ / +	+ / *Egfr*^{Dsk5}	*Egfr*^{Dsk5} / *Egfr*^{Dsk5}	Total viable	*P*
C57BL/6J	31 (30.5%)	44 (44%)	26 (25.5%)	101	0.338
C3HeB/FeJ	16 (26%)	39 (63%)	7 (11%)	62	0.034
129/Sv	10 (20%)	21 (42%)	19 (38%)	50	0.104

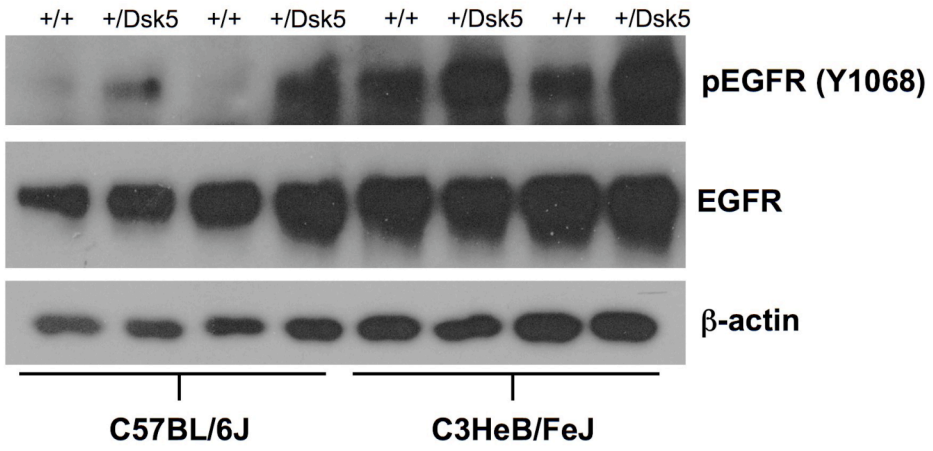

Figure 22. Western blot for phospho-EGFR and total EGFR in uteri extracts from B6 and C3H females. Samples are B6 in Lanes 1 -4 and C3H in lanes 5 -8. Even numbered lanes are wildtype animals and odd numbered lanes are their *Egfr*^{Dsk5} heterozygous littermates. The top panel shows protein levels of phospho-EGFR, the middle panel shows levels of total EGFR and the bottom panel shows β-actin as a loading control.

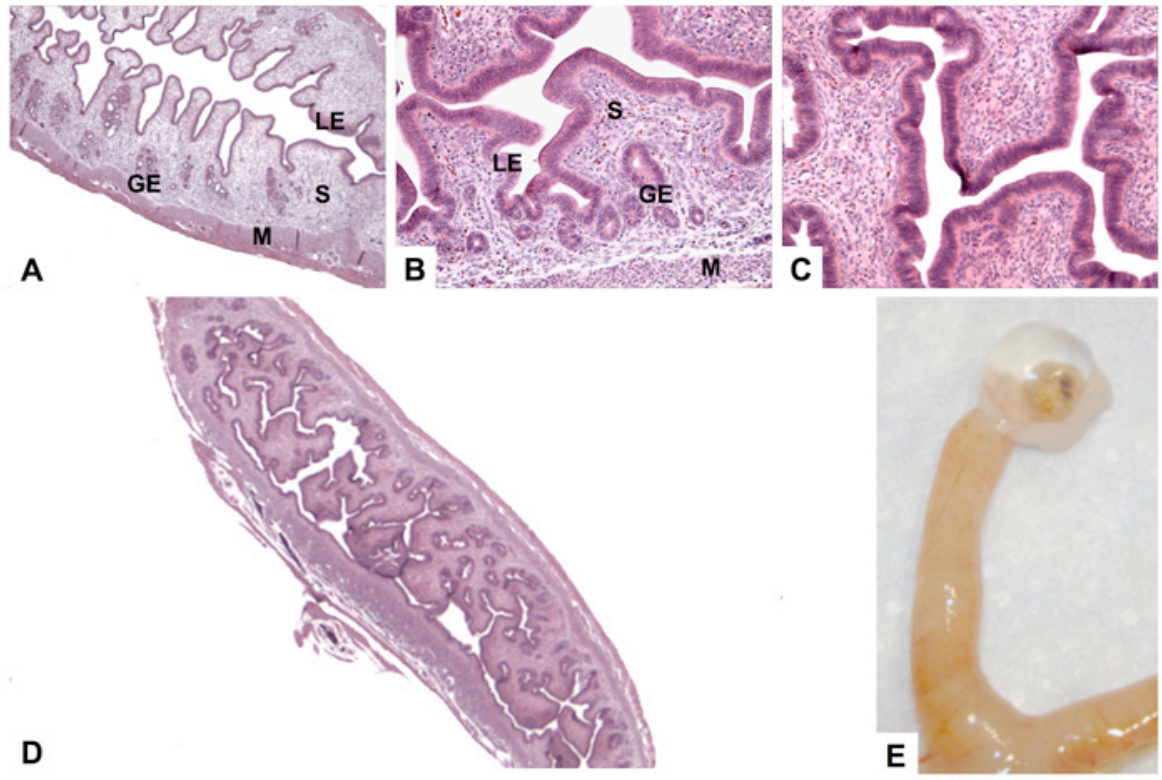

Figure 23. Reproductive system phenotypes in *Egfr*^{Dsk5} heterozygous females. **A.** Wildtype B6 non-pregnant uterus with myometrium (M), glandular epithelium (GE), stroma (S) and luminal epithelium (LE) labeled (2X). **B.** Wildtype C3H non-pregnant uterus (10X). **C.** *Egfr*^{Dsk5} heterozygous C3H uterus. No obvious histological differences were observed. **D.** *Egfr*^{Dsk5} heterozygous uterus (1X). **E.** *Egfr*^{Dsk5} heterozygous B6 ovary. Bursal sac is filled with fluid.

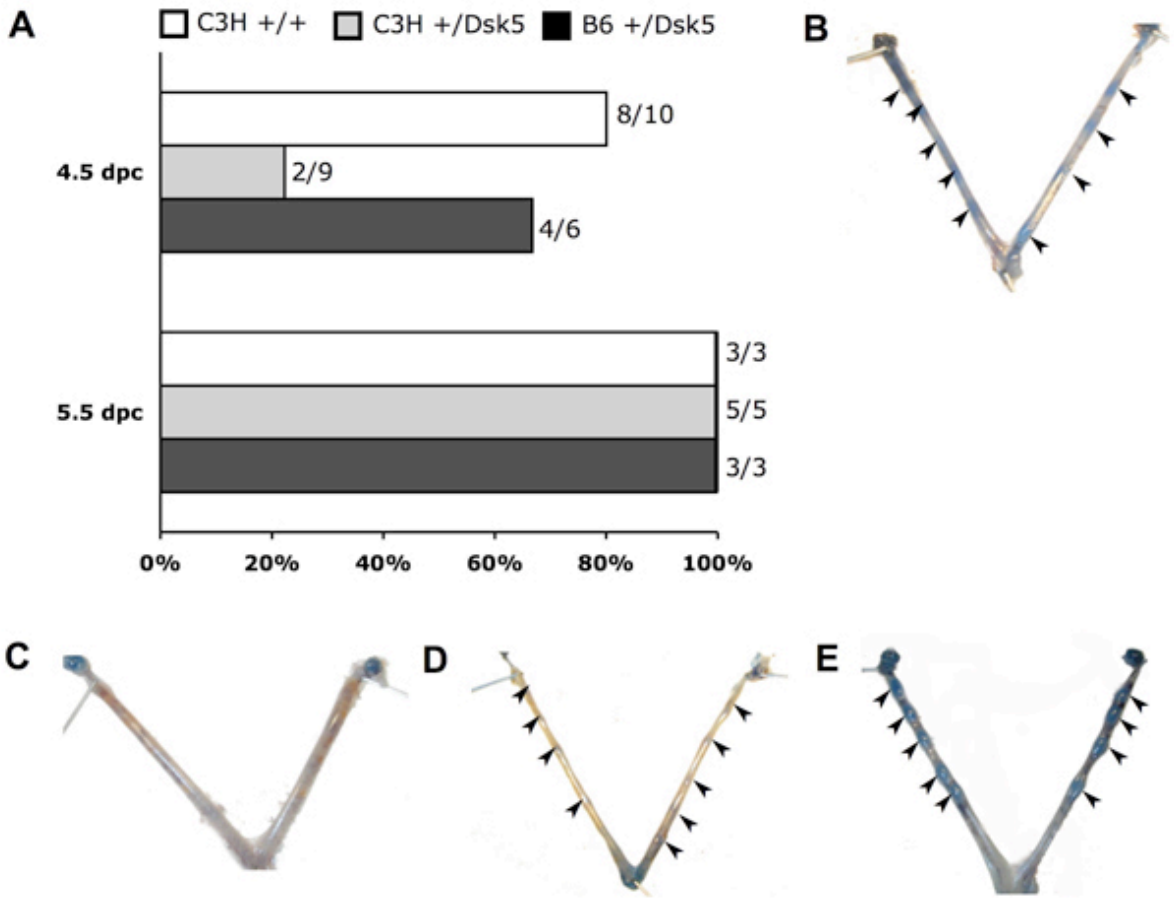

Figure 24. Implantation timing may be altered in C3H *Egfr*^{Dsk5} heterozygous females. **A.** Percent females with implantation sites visible at 4.5 and 5.5 dpc. White bars are wildtype C3H females, gray bars are *Egfr*^{Dsk5} heterozygous C3H females and black bars are *Egfr*^{Dsk5} heterozygous B6 females. **B.** Wildtype C3H 4.5 dpc pregnant uterus. **C.** *Egfr*^{Dsk5} heterozygous C3H 4.5 dpc pregnant uterus.. **D.** *Egfr*^{Dsk5} heterozygous B6 4.5 dpc pregnant uterus. **E.** *Egfr*^{Dsk5} heterozygous C3H 5.5 dpc pregnant uterus.

References

[1] Fowler KJ, Walker F, Alexander W, Hibbs ML, Nice EC, Bohmer RM, Mann GB, Thumwood C, Maglitto R, Danks JA, et al. A mutation in the epidermal growth factor receptor in waved-2 mice has a profound effect on receptor biochemistry that results in impaired lactation. Proc Natl Acad Sci U S A 1995; 92:1465-1469.

[2] Hsieh M, Lee D, Panigone S, Horner K, Chen R, Theologis A, Lee DC, Threadgill DW, Conti M. Luteinizing hormone-dependent activation of the epidermal growth factor network is essential for ovulation. Mol Cell Biol 2007; 27:1914-1924.

[3] Park JY, Su YQ, Ariga M, Law E, Jin SL, Conti M. EGF-like growth factors as mediators of LH action in the ovulatory follicle. Science 2004; 303:682-684.

[4] Prevot V, Lomniczi A, Corfas G, Ojeda SR. erbB-1 and erbB-4 receptors act in concert to facilitate female sexual development and mature reproductive function. Endocrinology 2005; 146:1465-1472.

[5] Das SK, Tsukamura H, Paria BC, Andrews GK, Dey SK. Differential expression of epidermal growth factor receptor (EGF-R) gene and regulation of EGF-R bioactivity by progesterone and estrogen in the adult mouse uterus. Endocrinology 1994; 134:971-981.

[6] Tong BJ, Das SK, Threadgill D, Magnuson T, Dey SK. Differential expression of the full-length and truncated forms of the epidermal growth factor receptor in the preimplantation mouse uterus and blastocyst. Endocrinology 1996; 137:1492-1496.

[7] Hom YK, Young P, Wiesen JF, Miettinen PJ, Derynck R, Werb Z, Cunha GR. Uterine and vaginal organ growth requires epidermal growth factor receptor signaling from stroma. Endocrinology 1998; 139:913-921.

[8] Xie H, Wang H, Tranguch S, Iwamoto R, Mekada E, Demayo FJ, Lydon JP, Das SK, Dey SK. Maternal heparin-binding-EGF deficiency limits pregnancy success in mice. Proc Natl Acad Sci U S A 2007; 104:18315-18320.

[9] Sibilia M, Wagner EF. Strain-dependent epithelial defects in mice lacking the EGF receptor. Science 1995; 269:234-238.

[10] Threadgill DW, Yee D, Matin A, Nadeau JH, Magnuson T. Genealogy of the 129 inbred strains: 129/SvJ is a contaminated inbred strain. Mamm Genome 1997; 8:390-393.

[11] Fitch KR, McGowan KA, van Raamsdonk CD, Fuchs H, Lee D, Puech A, Herault Y, Threadgill DW, Hrabe de Angelis M, Barsh GS. Genetics of dark skin in mice. Genes Dev 2003; 17:214-228.

[12] Lynch TJ, Bell DW, Sordella R, Gurubhagavatula S, Okimoto RA, Brannigan BW, Harris PL, Haserlat SM, Supko JG, Haluska FG, Louis DN, Christiani DC, Settleman J, Haber DA. Activating mutations in the epidermal growth factor receptor underlying responsiveness of non-small-cell lung cancer to gefitinib. N Engl J Med 2004; 350:2129-2139.

[13] Yang S, Qu S, Perez-Tores M, Sawai A, Rosen N, Solit DB, Arteaga CL. Association with HSP90 inhibits Cbl-mediated down-regulation of mutant epidermal growth factor receptors. Cancer Res 2006; 66:6990-6997.

[14] Gillgrass A, Cardiff RD, Sharan N, Kannan S, Muller WJ. Epidermal growth factor receptor-dependent activation of Gab1 is involved in ErbB-2-mediated mammary tumor progression. Oncogene 2003; 22:9151-9155.

[15] Roberts RB, Min L, Washington MK, Olsen SJ, Settle SH, Coffey RJ, Threadgill DW. Importance of epidermal growth factor receptor signaling in establishment of adenomas and maintenance of carcinomas during intestinal tumorigenesis. Proc Natl Acad Sci U S A 2002; 99:1521-1526.

[16] Sibilia M, Fleischmann A, Behrens A, Stingl L, Carroll J, Watt FM, Schlessinger J, Wagner EF. The EGF receptor provides an essential survival signal for SOS-dependent skin tumor development. Cell 2000; 102:211-220.

[17] Song H, Lim H, Paria BC, Matsumoto H, Swift LL, Morrow J, Bonventre JV, Dey SK. Cytosolic phospholipase A2alpha is crucial [correction of A2alpha deficiency is crucial] for 'on-time' embryo implantation that directs subsequent development. Development 2002; 129:2879-2889.

[18] Wang H, Dey SK. Roadmap to embryo implantation: clues from mouse models. Nat Rev Genet 2006; 7:185-199.

[19] Paria BC, Huet-Hudson YM, Dey SK. Blastocyst's state of activity determines the "window" of implantation in the receptive mouse uterus. Proc Natl Acad Sci U S A 1993; 90:10159-10162.

[20] Ma WG, Song H, Das SK, Paria BC, Dey SK. Estrogen is a critical determinant that specifies the duration of the window of uterine receptivity for implantation. Proc Natl Acad Sci U S A 2003; 100:2963-2968.

[21] Wang H, Ma WG, Tejada L, Zhang H, Morrow JD, Das SK, Dey SK. Rescue of female infertility from the loss of cyclooxygenase-2 by compensatory up-regulation of cyclooxygenase-1 is a function of genetic makeup. J Biol Chem 2004; 279:10649-10658.

[22] Ye X, Hama K, Contos JJ, Anliker B, Inoue A, Skinner MK, Suzuki H, Amano T, Kennedy G, Arai H, Aoki J, Chun J. LPA3-mediated lysophosphatidic acid signalling in embryo implantation and spacing. Nature 2005; 435:104-108.

[23] Paria BC, Elenius K, Klagsbrun M, Dey SK. Heparin-binding EGF-like growth factor interacts with mouse blastocysts independently of ErbB1: a possible role for heparan sulfate proteoglycans and ErbB4 in blastocyst implantation. Development 1999; 126:1997-2005.

[24] Raab G, Kover K, Paria BC, Dey SK, Ezzell RM, Klagsbrun M. Mouse preimplantation blastocysts adhere to cells expressing the transmembrane form of heparin-binding EGF-like growth factor. Development 1996; 122:637-645.

[25] Basu A, Raghunath M, Bishayee S, Das M. Inhibition of tyrosine kinase activity of the epidermal growth factor (EGF) receptor by a truncated receptor form that binds to EGF: role for interreceptor interaction in kinase regulation. Mol Cell Biol 1989; 9:671-677.

[26] Lim H, Dey SK, Das SK. Differential expression of the erbB2 gene in the periimplantation mouse uterus: potential mediator of signaling by epidermal growth factor-like growth factors. Endocrinology 1997; 138:1328-1337.

[27] Lim H, Das SK, Dey SK. erbB genes in the mouse uterus: cell-specific signaling by epidermal growth factor (EGF) family of growth factors during implantation. Dev Biol 1998; 204:97-110.

[28] Brown N, Deb K, Paria BC, Das SK, Reese J. Embryo-uterine interactions via the neuregulin family of growth factors during implantation in the mouse. Biol Reprod 2004; 71:2003-2011.

[29] Cai L, Zhang J, Duan E. Dynamic distribution of epidermal growth factor during mouse embryo peri-implantation. Cytokine 2003; 23:170-178.

[30] Das SK, Chakraborty I, Paria BC, Wang XN, Plowman G, Dey SK. Amphiregulin is an implantation-specific and progesterone-regulated gene in the mouse uterus. Mol Endocrinol 1995; 9:691-705.

[31] Das SK, Das N, Wang J, Lim H, Schryver B, Plowman GD, Dey SK. Expression of betacellulin and epiregulin genes in the mouse uterus temporally by the blastocyst solely at the site of its apposition is coincident with the "window" of implantation. Dev Biol 1997; 190:178-190.

[32] Das SK, Wang XN, Paria BC, Damm D, Abraham JA, Klagsbrun M, Andrews GK, Dey SK. Heparin-binding EGF-like growth factor gene is induced in the mouse uterus temporally by the blastocyst solely at the site of its apposition: a possible ligand for interaction with blastocyst EGF-receptor in implantation. Development 1994; 120:1071-1083.

[33] Paria BC, Das SK, Huet-Hudson YM, Dey SK. Distribution of transforming growth factor alpha precursors in the mouse uterus during the periimplantation period and after steroid hormone treatments. Biol Reprod 1994; 50:481-491.

[34] Song H, Lim H, Das SK, Paria BC, Dey SK. Dysregulation of EGF family of growth factors and COX-2 in the uterus during the preattachment and attachment reactions of the blastocyst with the luminal epithelium correlates with implantation failure in LIF-deficient mice. Mol Endocrinol 2000; 14:1147-1161.

[35] Jackson LF, Qiu TH, Sunnarborg SW, Chang A, Zhang C, Patterson C, Lee DC. Defective valvulogenesis in HB-EGF and TACE-null mice is associated with aberrant BMP signaling. Embo J 2003; 22:2704-2716.

[36] Lee D, Pearsall RS, Das S, Dey SK, Godfrey VL, Threadgill DW. Epiregulin is not essential for development of intestinal tumors but is required for protection from intestinal damage. Mol Cell Biol 2004; 24:8907-8916.

[37] Troyer KL, Luetteke NC, Saxon ML, Qiu TH, Xian CJ, Lee DC. Growth retardation, duodenal lesions, and aberrant ileum architecture in triple null mice lacking EGF, amphiregulin, and TGF-alpha. Gastroenterology 2001; 121:68-78.

[38] Das SK, Lim H, Wang J, Paria BC, BazDresch M, Dey SK. Inappropriate expression of human transforming growth factor (TGF)-alpha in the uterus of transgenic mouse causes downregulation of TGF-beta receptors and delays the blastocyst-attachment reaction. J Mol Endocrinol 1997; 18:243-257.

[39] Gratao AA, Dahlhoff M, Sinowatz F, Wolf E, Schneider MR. Betacellulin overexpression in the mouse ovary leads to MAPK3/MAPK1 hyperactivation and reduces litter size by impairing fertilization. Biol Reprod 2008; 78:43-52.

[40] McMullen ML, Cho BN, Yates CJ, Mayo KE. Gonadal pathologies in transgenic mice expressing the rat inhibin alpha-subunit. Endocrinology 2001; 142:5005-5014.

[41] Marozkina NV, Stiefel SM, Frierson HF, Jr., Parsons SJ. MMTV-EGF receptor transgene promotes preneoplastic conversion of multiple steroid hormone-responsive tissues. J Cell Biochem 2007.

[42] Jin N, Gilbert JL, Broaddus RR, Demayo FJ, Jeong JW. Generation of a Mig-6 conditional null allele. Genesis 2007; 45:716-721.

[43] Burney RO, Talbi S, Hamilton AE, Vo KC, Nyegaard M, Nezhat CR, Lessey BA, Giudice LC. Gene expression analysis of endometrium reveals progesterone resistance and candidate susceptibility genes in women with endometriosis. Endocrinology 2007; 148:3814-3826.

CHAPTER V

FUTURE EXPERIMENTS AND GENERAL DISCUSSION

Introduction

This thesis has described the use of an allelic series in mice to determine the role of *Egfr* during pregnancy, with a particular focus on placental development. We showed that $Egfr^{tm1Mag}$ nullizygous placentas have fewer proliferating trophoblasts compared to wildtype and that $Egfr^{tm1Mag}$ nullizygous embryonic lethality is not rescued by ablation of genes that negatively regulate the cell cycle. We also described growth restriction of placentas and embryos homozygous for the hypomorphic $Egfr^{wa2}$ allele. A less severe placental phenotype in mice heterozygous for the antimorphic $Egfr^{Wa5}$ allele led us to conclude that higher levels of EGFR signaling occur in $Egfr^{Wa5}$ heterozygotes versus $Egfr^{wa2}$ homozygotes. Our characterization of embryos heterozygous and homozygous for the hypermorphic $Egfr^{Dsk5}$ allele reiterated the important role of EGFR in placentation since these embryos exhibited enlarged placentas. We have also begun to uncover unexpected defects in the female reproductive system of $Egfr^{Dsk5}$ heterozygous adults. Since most of our experiments included several genetic backgrounds, our results reveal striking strain-dependent variation in many of the phenotypes examined. This chapter outlines a strategy to map modifying loci that influence the strain-dependent $Egfr^{tm1Mag}$ nullizygous placental phenotype. In addition, the

significance of our results will be discussed as they pertain to genetic background specific phenotypes, spongiotrophoblast development and intrauterine growth restriction (IUGR).

Mapping modifiers of the *Egfr*^{tm1Mag} homozygous placental phenotype

Mice homozygous for a null allele of *Egfr*, *Egfr*^{tm1Mag}, display a strain-dependent placental phenotype that results in embryonic lethality on many genetic backgrounds [1,2]. Most strains examined to date, including Swiss-derived outbred CD-1, exhibit a reduced spongiotrophoblast layer. Strains dying before mid-gestation, such as inbred 129S6, are also distinguished by a disorganized labyrinth layer. Our lab has made several attempts to map genes that contribute to the strain differences in *Egfr*^{tm1Mag} homozygous placental development. In *Egfr*^{tm1Mag} homozygous F2 progeny from a cross between CD-1, which survives to term, and the non-surviving 129S1 strain carrying *Egfr*^{tm1Mag}, no QTL were identified that are associated with embryonic survival. CD-1 is an outbred strain and due to the strain's genetic heterogeneity, there may have been a number of modifiers segregating that rescued the placental phenotype. To eliminate genetic heterogeneity as a confounding factor, we set up a cross between 129S1- *Egfr*^{tm1Mag} and a surviving inbred strain, ALR/LtJ [3]. Unfortunately we were unable to map modifiers in this cross because N2 animals created by backcrossing ALS.129 F1- *Egfr*^{tm1Mag} mice to 129S1- *Egfr*^{tm1Mag} did not segregate the embryonic lethality phenotype. The fact that most N2 *Egfr*^{tm1Mag} homozygous embryos survived in this experiment suggests that the ALR genome contributed numerous dominant modifiers that rescued the placental phenotype.

We have also extensively investigated genetic heterogeneity affecting placental development of *Egfr* nullizygous animals by measuring embryonic survival on selected

backgrounds [3]. Intercrosses between *Egfr*^{tm1Mag} 129S1 and a panel of Swiss-derived inbred strains related to CD-1 showed a full range of placental phenotypes that were genetic background dependent. Some strains such as ALS/LtJ and ALR/LtJ supported robust *Egfr*^{tm1Mag} nullizygous survival when crossed to 129S1 while other strains such as ICR/HaROS did not support development of *Egfr*^{tm1Mag} nullizygous embryos past mid-gestation. Most strains exhibited a moderate placental phenotype that allowed some embryonic survival past mid-gestation when intercrossed with 129S1. The variable survival observed in the panel of Swiss-derived strains suggest that different combinations of *Egfr* modifiers were captured from CD-1 by each of the inbred backgrounds. We have obtained similar results when more diverse congenic *Egfr*^{tm1Mag} lines are intercrossed. Some strains complement each other to allow robust survival of *Egfr*^{tm1Mag} nullizygous embryos while other strain combinations do not. Taken together, all of these studies reveal that the strain-specific *Egfr* placental phenotype is not modified by a single locus but is determined instead by a number of interacting loci in various combinations. The genomes of inbred mouse strains contain unique sets of *Egfr* modifying loci giving rise to the variation in embryonic survival observed between genetic backgrounds.

The lack of success our lab has encountered while attempting to map *Egfr* modifiers suggest that traditional mapping strategies may not be sufficient to dissect the genetic complexity associated with the *Egfr*^{tm1Mag} homozygous placental phenotype. An approach that may allow us to map QTL is the genetic partitioning of dominant modifiers through a serial-backcross breeding scheme. This approach was used successfully to map genes in B10.D2 mice that confer resistance to the parasite *Leishmania major* [4]. The breeding scheme involved backcrossing F1 mice to an *L. major* susceptible strain, BALB/c and then

selecting N2 animals resistant to *L. major* to establish a subsequent BALB/c backcross. The selection of resistant animals and backcrossing to susceptible BALB/c continued for three more generations (N5) resulting in isolation of a minimum number of dominant modifiers required for *L. major* resistance on an otherwise susceptible BALB/c background. Results from the experiment demonstrated that the trait is genetically complex with no single locus required for *L. major* resistance. Six QTL were found to be significantly associated with resistance and various combinations of these loci were present in the N5 resistant animals.

In order to map QTL associated with normal development of EGFR-deficient placentas, we utilized a similar backcrossing strategy designed to isolate dominant modifiers from the ALS strain, which supports survival of a majority of *Egfr*^{tm1Mag} nullizygous embryos. F1 strains were generated by crossing the ALS strain to 129S1 and FVB/NJ, two strains exhibiting embryonic lethality at or before mid-gestation (Figure 25). The ALS.129 and ALS.FVB hybrids were then backcrossed for four generations to 129 and FVB, respectively. Only animals that produced viable *Egfr*^{tm1Mag} homozygous pups were used to establish each subsequent backcross. Selection and backcrossing of heterozygous adults with *Egfr*^{tm1Mag} homozygous progeny continued up to N6 in the ALS.129 background and up to N5 in the ALS.FVB background.

Data from these crosses indicates that dominant loci from the ALS strain were better able to support placentation in combination with the 129S1 genome compared to FVB. From 15 original ALS.129 N2 animals, we were able to establish nine independent lines of N4-*Egfr*^{tm1Mag} mice in which ALS placental modifiers were isolated. We were able to establish only two lines of N4-*Egfr*^{tm1Mag} mice from 16 original ALS.FVB N2 animals. We consistently observed a higher percentage of ALS.129 lines supporting viability of *Egfr*^{tm1Mag}

nullizygous embryos than ALS.FVB lines (Figure 26). We observed 53% of ALS.129 N2 lines supporting survival of *Egfr*^{tm1Mag} nullizygous embryos compared to 25% of ALS.FVB N2 lines. *Egfr*^{tm1Mag} nullizygous pups represented approximately 5% of all pups born in the ALS.129 N2 and only 3% of pups born in ALS.FVB N2. For the subsequent backcross 24% of ALS.129 N3 lines rescued *Egfr*^{tm1Mag} homozygous embryos versus 8% of ALS.FVB N3. From the ALS.129 N3 lines approximately 3% of embryos were nullizygous versus 1% of ALS.FVB embryos. Table 11 shows the number of surviving *Egfr*^{tm1Mag} homozygous pups expected within an established rescuing line based on the number of ALS loci required to modify the placental phenotype. We predict that three dominant ALS modifiers are required to rescue placental development of *Egfr* -/- embryos on the 129 background since 4.9% surviving N4 pups and 4.3 % surviving N5 pups were *Egfr*^{tm1Mag} homozygous. Approximately three to four modifiers are required on the FVB background since 2.3 % of surviving N4 pups collected from N3 rescuing lines were *Egfr*^{tm1Mag} homozygous.

We have completed collection of samples from seven original N2 lines for 129 and four N2 lines for FVB (Table 12). We have performed preliminary genotyping using a panel of 672 SNP originally designed for another project. Genotyping with this panel was performed on 63 ALS.129 and 21 ALS.FVB *Egfr*^{tm1Mag} homozygous pups and their parents. Because of a small sample number and technical difficulties with SNP genotyping of ALS.FVB samples we have focused on the ALS.129 cross. From the SNP panel, 347 assays spread throughout the genome were found to be informative between ALS and 129 (Figure 27). There were several large gaps in our genome coverage particularly for chromosomes 4, 7, 8, 9, 10, and 16 and additional genotyping will be required to adequately cover the entire genome. The data we have analyzed so far shows that as expected, ALS.129 N5 animals

retain only small portions of the ALS genome. We have not identified any single QTL required for embryonic survival but further analysis will most likely reveal multiple combinations of ALS genomic segments associated with *Egfr*^{tm1Mag} homozygous embryo survival. Candidate genes in ALS intervals are predicted to include gene products downstream of EGFR and/or genes involved in cell signaling and placentation.

EGFR and genetic background dependent phenotypes

In addition to placental phenotypes, we have also observed that other phenotypes associated with changes in the level of EGFR signaling are strain-dependent (summarized in Table 13). Mice homozygous for a hypomorphic allele of *Egfr*, *Egfr*^{wa2}, exhibit strain-dependent differences in percent tumor reduction when crossed to the *Apc*^{min} model of intestinal tumorogenesis (unpublished data). *Egfr*^{wa2} homozygotes also exhibit pronounced cardiac hypertrophy on the B6 but not the 129 background (CJ Barrick, in press). Chapter 3 of this dissertation describes strain differences in *Egfr*^{wa2} homozygous placental and embryonic growth restriction with the 129 strain being more severely affected than B6. We also reported strain-dependent embryonic lethality of 129 and BTBR-*Egfr*^{wa2} homozygotes and BTBR embryos heterozygous for an antimorphic allele of *Egfr*, *Egfr*^{Wa5}.

In addition to phenotypes resulting from reduced or abolished EGFR signaling, we described strain-dependent phenotypes in mice with a hypermorphic allele of *Egfr*, *Egfr*^{Dsk5}. We observed differences in *Egfr*^{Dsk5} hair, skin and nail phenotypes, which is interesting considering that the hair phenotype in *Egfr*^{wa2} homozygotes does not vary obviously by strain. The placental overgrowth phenotype observed in *Egfr*^{Dsk5} heterozygotes is similar in the three strains examined but only one strain, C3H, shows a more severe phenotype in

Egfr^{Dsk5} homozygotes. We also reported in Chapter 4 a strain-dependent sub-fertility phenotype in 129 and C3H-*Egfr*^{Dsk5} heterozygous females. The origin of the fertility defect remains to be determined but an initial examination of uteri and ovaries suggest that there may be multiple reproductive phenotypes in the *Egfr*^{Dsk5} heterozygotes that may or may not vary by strain. The genetic modifiers that give rise to the variability in the phenotypes we described have not been identified, although two known genes have been found to enhance phenotypes in *Egfr*^{wa2} homozygotes Heterozygosity for a null allele of the guanine nucleotide exchange factor, *Sos1*, increases the penetrance of delayed eyelid closure during embryonic development and neonatal mortality in *Egfr*^{wa2} homozygotes [5]. Heterozygosity for a null allele of the protein-tyrosine-phosphatase, *Ptpn11,* also increases penetrance of defective eyelid closure and enhances severity of semilunar valves enlargement and electrocardiographic abnormalities in *Egfr*^{wa2} homozygotes [6]. Genetic variation in *Sos1*, *Ptpn11* or in many other genes could underlie strain-dependent variability of phenotypes observed in the *Egfr* allelic series.

EGFR and spongiotrophoblast

Previous studies have shown that *Egfr* nullizygous placentas from most genetic backgrounds examined to date exhibit a reduction in the spongiotrophoblast layer [2,7]. The data presented in Chapters 3 and 4 confirm that spongiotrophoblasts are very sensitive to levels of EGFR signaling compared to other trophoblast cell types. We have shown that a decrease in EGFR signaling, such as in the *Egfr*^{wa2} homozygous and *Egfr*^{Wa5} heterozygous placentas causes a reduction in the thickness of the spongiotrophoblast layer. Conversely, if EGFR signaling is increased, such as in the *Egfr*^{Dsk5} heterozygote and homozygote,

spongiotrophoblast layer is enlarged. Based on data from Chapter 1 showing reduced proliferation in *Egfr*^{tm1Mag} homozygous placentas, the changes we saw in the *Egfr*^{wa2}, *Egfr*^{Wa5} and *Egfr*^{Dsk5} placentas are probably due to the effect of EGFR on spongiotrophoblast proliferation. The level of EGFR signaling is correlated with spongiotrophoblast proliferation but the threshold required may vary by strain since some strains are more severely affected by changes in the level of signaling than others. An additional experiment that should be performed to test this hypothesis is BrdU labeling of cells in *Egfr*^{wa2} homozygous and *Egfr*^{Dsk5} heterozygous placentas to quantify proliferative spongiotrophoblasts.

Based on studies using a chimera between *Mash2* null and wildtype cells, it was hypothesized that spongiotrophoblasts are required for proper morphogenesis of the labyrinth [8]. MASH2 is necessary for spongiotrophoblast differentiation, and chimeras with a MASH2-deficient placenta fail to develop a layer of spongiotrophoblast and also exhibit defects in formation of the labyrinth. However, MASH2 seems to be required only in the spongiotrophoblast and not labyrinth trophoblasts for normal placental development. Chimeric placentas with *Mash2* wildtype spongiotrophoblasts and a labyrinth composed of *Mash2* null trophoblasts develop normally and fully support embryonic growth. The spongiotrophoblast layer may provide necessary structural support for labyrinth development and/or spongiotrophoblasts may secrete signals required for proper labyrinth formation. Interestingly, we observed normal development of the placental labyrinth in two homozygous *Egfr*^{wa2} strains almost entirely lacking spongiotrophoblasts, 129 and BTBR. Our results suggest that only a very small number of spongiotrophoblast are sufficient for labyrinth morphogenesis, that the *Mash2* phenotype is strain-specific and not all strains require

spongiotrophoblasts for proper labyrinth formation, or that another cell trophoblast cell type present in *Egfr* null placentas is absent or non-functional in *Mash2* null placentas.

EGFR signaling and intrauterine growth restriction

Data from human and mouse studies have suggested that ERBB signaling regulates fetal growth through multiple mechanisms. In mouse, maternal EGF-deficiency by sialoadenectomy causes fetal, but not placental growth restriction, that is rescued by exogenous EGF supplementation [9]. Fetal liver but not brain weights are significantly reduced in litters from sialoadenectomized females, which is probably due to compromised transplacental transfer of glucose. Over-expression of EGF has also been shown to result in fetal growth restriction. Transgenic mouse embryos that over-express human EGF are born at half the weight of non-transgenic littermates and have reduced serum levels of IGFBP3 [10]. Since EGF transgenic placental weight and nutrient transfer was not measured in this study, embryonic growth restriction due to placental defects cannot be ruled out. Mice that over-express TGFA are also smaller at birth than their non-transgenic littermates, but further characterization of this phenotype has not been reported [11].

In humans reduced placental *EGFR* mRNA and protein, as well as receptor phosphorylation, are associated with fetal growth restriction [12-15]. Low levels of EGF in maternal urine, maternal and fetal plasma, and amniotic fluid have also been associated with IUGR [16-19]. In contrast, a recent study showed that a polymorphism (c.61G) in the 5' untranslated region of EGF, previously shown to increase EGF expression, is associated with lower birthweight in healthy pregnancies [20]. Also, babies affected by IUGR are more likely to have inherited the c.61G polymorphism in combination with c.2566A, another EGF

polymorphism that by itself is associated with low birth weight of normal babies. Together, mouse and human studies demonstrate that regulation of fetal growth by EGFR signaling is complex and is modulated by both maternal and fetal components. The various *Egfr* alleles our lab maintains as congenic mouse strains can be used to better understand the genetics of IUGR. In support of placental and embryonic EGFR phosphorylation being required for normal fetal growth, we have shown that 18.5 dpc $Egfr^{wa2}$ homozygous embryos exhibit severe growth restriction. The growth characteristics of these animals following birth remain to be determined. The $Egfr^{Dsk5}$ heterozygous and homozygous embryos do not exhibit growth restriction at 15.5 dpc. However, considering the reported effects of increased EGF and TGFA expression on birth weight, growth patterns of $Egfr^{Dsk5}$ heterozygotes and homozygotes should be examined later in gestation and following birth. Preliminary observations suggest that $Egfr^{Dsk5}$ homozygotes are smaller than their littermates at weaning (data not shown). Additionally, adult females null for EGF could be used to genetically test the requirement of maternal EGF in fetal growth.

Conclusions

Experiments presented in this dissertation have focused primarily on the role of EGFR in placental development and pregnancy. We showed that EGFR is essential for normal growth of placenta and embryo and that increased EGFR signaling has detrimental effects on female fertility. Our finding that EGFR is particularly important in driving proliferation of placental spongiotrophoblast may help broaden our understanding of how EGFR functions in human placental development. In addition, we have generated a number of mouse lines congenic for mutant *Egfr* alleles that will be useful genetic models for

studying the origins of fetal growth restriction. Through examination of our EGFR allelic series on multiple genetic backgrounds, our studies have emphasized the strain-dependent variation in phenotypes due to perturbations in EGFR signaling. Thus far we have been unable to identify genetic modifiers that contribute to strain variation in EGFR placental and reproductive phenotypes. Extensive genetic characterization of the *Egfr*^{tm1Mag} homozygous strain-dependent placental phenotype has led us to conclude that the phenotype is modified by numerous interacting loci. To simplify QTL mapping for this multigenic phenotype we are currently exploring the use of a serial backcross strategy designed to isolate a minimum set of modifiers required. The identity of genetic modifiers of EGFR signaling could provide additional insight into biology and treatment of numerous human diseases and conditions in which EGFR is involved.

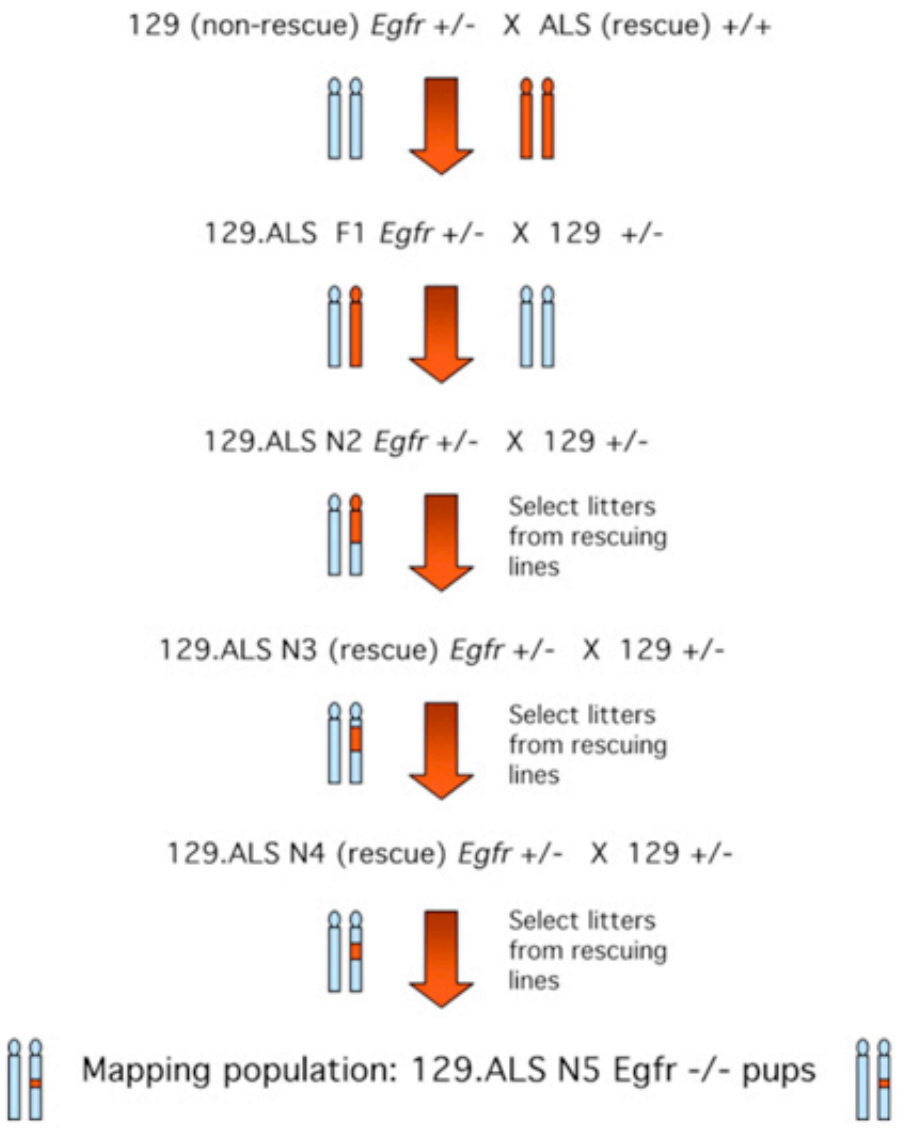

Figure 25. Breeding scheme for serial backcross mapping strategy. ALS/LtJ animals were backcrossed to 129S6 or FVB/NJ for five generations. Dominant modifying loci from the ALS genome were isolated by establishing each subsequent generation with only lines supporting survival of *Egfr* null embryos ("rescue" of placental development). Genome scans were performed on N5 *Egfr* nullizygous pups to reveal the unique sets of modifiers captured from the ALS genome in the individual lines derived.

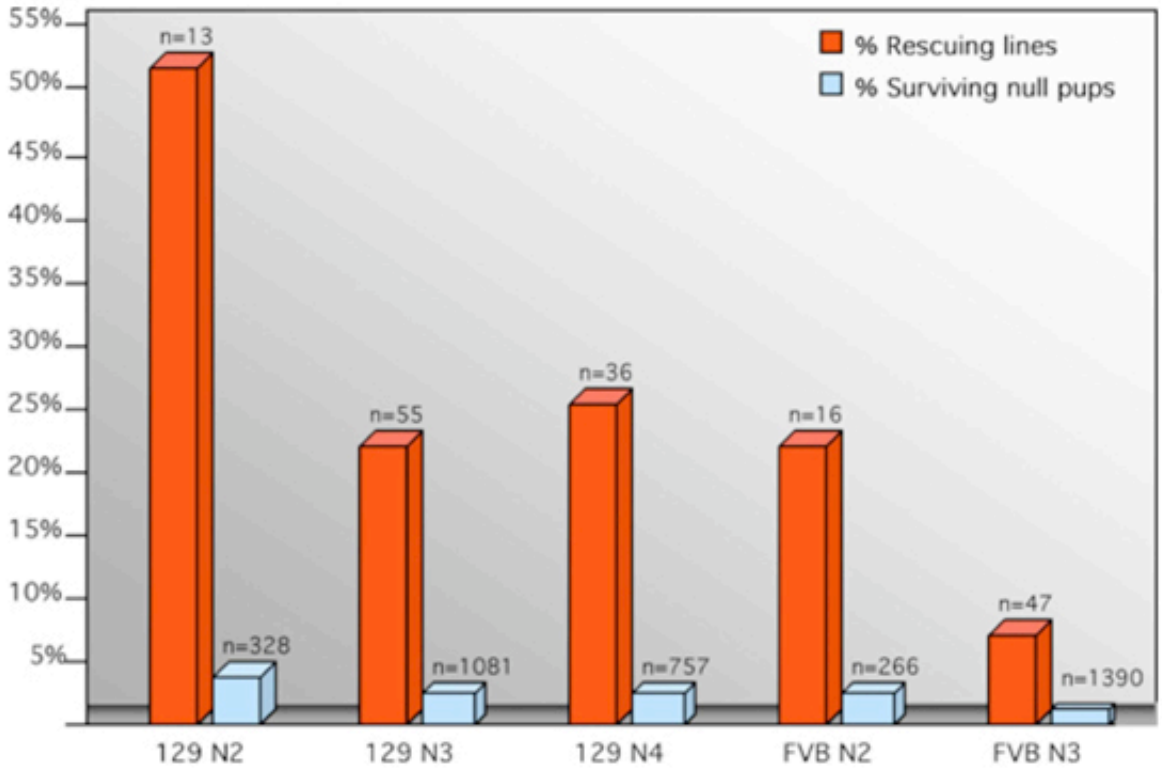

Figure 26. To assess the effect of ALS modifiers in the 129 versus FVB genome the percentage of lines supporting survival of *Egfr* null embryos ("rescuing") and percentage surviving null pups were calculated for each generation of backcrossing. ALS modifiers in combination with the 129 background supported more robust survival in every generation compared to FVB.

Table 11. Percent live *Egfr* -/- pups expected based on number of ALS modifiers to rescue embryonic lethality

# ALS modifiers required	Live *Egfr* - / - expected (%)
1	14.3
2	7.7
3	4.0
4	2.0
5	1.0

Table 12. Number of samples with ALS rescuing modifiers collected from each generation

ALS.129	N2	N3	N4	N5	N6	Total
Line 2	1	1	1	0	0	3
Line 3	1	1	5	5	3	15
Line 4	1	7	9	4	0	21
Line 5	1	9	3	2	0	15
Line 9	1	1	1	0	0	3
Line 11	1	2	3	0	0	6
Line 13	1	2	6	5	0	14

ALS.FVB	N2	N3	N4	N5	N6	Total
Line 1	1	5	6	2	0	14
Line 12	1	1	0	0	0	2
Line 15	1	2	2	0	0	5
Line 16	1	0	0	0	0	1

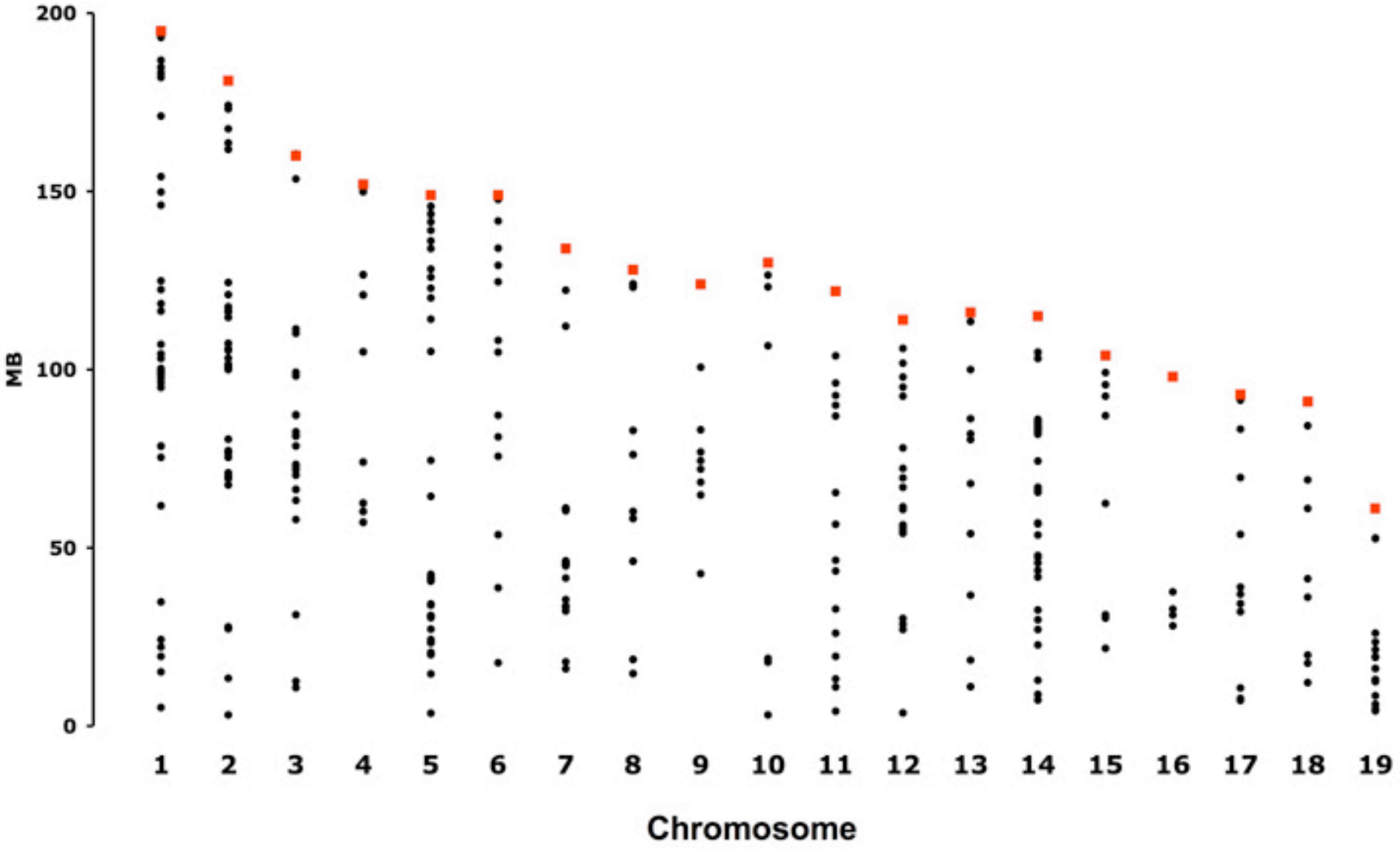

Figure 27. Location of SNP genotyping assays that were informative between ALS and 129 strains (black circles). Chromosome number is indicated on x-axis and Megabase (Mb) location is shown on y-axis. Centromeres are located at 0 Mb and telomere location is indicated by red squares.

Table 13. Summary of strain-dependent phenotypic variation observed in mouse *Egfr* allelic series

Egfr Allele		strains	strain-dependent phenotype	strain-independent phenotype
$Egfr^{tm1Mag}$	null	C57BL/6 129 BTBR BALB/c FVB/NJ others	placental labyrinth and spongiotrophoblast, peri-implantation embryonic lethality	hair, whiskers, skin, neurodegeneration
$Egfr^{wa2}$	hypomorph	C57BL/6 129 BTBR A/J	placental spongiotrophoblast, embryonic growth restriction, embryonic lethality, Apc^{min} intestinal tumor reduction, cardiac hypertrophy	hair, whiskers
$Egfr^{Wa5}$	antimorph	C57BL/6 129 BTBR BALB/c	embryonic lethality, uncharacterized eye phenotype	hair, whiskers
$Egfr^{Dsk5}$	hypermorph	C57BL/6 129 C3HeB/FeJ FVB/NJ	hair, nails, skin pigmentation, embryonic lethality, fertility	heterozygous placental overgrowth

References

[1] Sibilia M, Steinbach JP, Stingl L, Aguzzi A, Wagner EF. A strain-independent postnatal neurodegeneration in mice lacking the EGF receptor. Embo J 1998; 17:719-731.

[2] Threadgill DW, Dlugosz AA, Hansen LA, Tennenbaum T, Lichti U, Yee D, LaMantia C, Mourton T, Herrup K, Harris RC, et al. Targeted disruption of mouse EGF receptor: effect of genetic background on mutant phenotype. Science 1995; 269:230-234.

[3] Strunk KE, Amann V, Threadgill DW. Phenotypic variation resulting from a deficiency of epidermal growth factor receptor in mice is caused by extensive genetic heterogeneity that can be genetically and molecularly partitioned. Genetics 2004; 167:1821-1832.

[4] Beebe AM, Mauze S, Schork NJ, Coffman RL. Serial backcross mapping of multiple loci associated with resistance to Leishmania major in mice. Immunity 1997; 6:551-557.

[5] Wang DZ, Hammond VE, Abud HE, Bertoncello I, McAvoy JW, Bowtell DD. Mutation in Sos1 dominantly enhances a weak allele of the EGFR, demonstrating a requirement for Sos1 in EGFR signaling and development. Genes Dev 1997; 11:309-320.

[6] Chen B, Bronson RT, Klaman LD, Hampton TG, Wang JF, Green PJ, Magnuson T, Douglas PS, Morgan JP, Neel BG. Mice mutant for Egfr and Shp2 have defective cardiac semilunar valvulogenesis. Nat Genet 2000; 24:296-299.

[7] Sibilia M, Wagner EF. Strain-dependent epithelial defects in mice lacking the EGF receptor. Science 1995; 269:234-238.

[8] Tanaka M, Gertsenstein M, Rossant J, Nagy A. Mash2 acts cell autonomously in mouse spongiotrophoblast development. Dev Biol 1997; 190:55-65.

[9] Kamei Y, Tsutsumi O, Yamakawa A, Oka Y, Taketani Y, Imaki J. Maternal epidermal growth factor deficiency causes fetal hypoglycemia and intrauterine growth retardation in mice: possible involvement of placental glucose transporter GLUT3 expression. Endocrinology 1999; 140:4236-4243.

[10] Chan SY, Wong RW. Expression of epidermal growth factor in transgenic mice causes growth retardation. J Biol Chem 2000; 275:38693-38698.

[11] Sandgren EP, Luetteke NC, Palmiter RD, Brinster RL, Lee DC. Overexpression of TGF alpha in transgenic mice: induction of epithelial hyperplasia, pancreatic metaplasia, and carcinoma of the breast. Cell 1990; 61:1121-1135.

[12] Faxen M, Nasiell J, Blanck A, Nisell H, Lunell NO. Altered mRNA expression pattern of placental epidermal growth factor receptor (EGFR) in pregnancies complicated by preeclampsia and/or intrauterine growth retardation. Am J Perinatol 1998; 15:9-13.

[13] Fondacci C, Alsat E, Gabriel R, Blot P, Nessmann C, Evain-Brion D. Alterations of human placental epidermal growth factor receptor in intrauterine growth retardation. J Clin Invest 1994; 93:1149-1155.

[14] Gabriel R, Alsat E, Evain-Brion D. Alteration of epidermal growth factor receptor in placental membranes of smokers: relationship with intrauterine growth retardation. Am J Obstet Gynecol 1994; 170:1238-1243.

[15] Calvo MT, Romo A, Gutierrez JJ, Relano E, Barrio E, Ferrandez Longas A. Study of genetic expression of intrauterine growth factors IGF-I and EGFR in placental tissue from pregnancies with intrauterine growth retardation. J Pediatr Endocrinol Metab 2004; 17 Suppl 3:445-450.

[16] Lindqvist P, Grennert L, Marsal K. Epidermal growth factor in maternal urine--a predictor of intrauterine growth restriction? Early Hum Dev 1999; 56:143-150.

[17] Moharam A, Aleem F, Farmakides G, Schulman H, Maghzangy M, Rashed A, Konstantinou E. Urinary and amniotic epidermal growth factor during normal and abnormal pregnancies. A comparison based upon umbilical Doppler velocimetry. Gynecol Endocrinol 1992; 6:287-292.

[18] Shigeta K, Hiramatsu Y, Eguchi K, Sekiba K. Urinary and plasma epidermal growth factor levels are decreased in neonates with intrauterine growth retardation and in their mothers. Biol Neonate 1992; 62:76-82.

[19] Varner MW, Dildy GA, Hunter C, Dudley DJ, Clark SL, Mitchell MD. Amniotic fluid epidermal growth factor levels in normal and abnormal pregnancies. J Soc Gynecol Investig 1996; 3:17-19.

[20] Dissanayake VH, Tower C, Broderick A, Stocker LJ, Seneviratne HR, Jayasekara RW, Kalsheker N, Broughton Pipkin F, Morgan L. Polymorphism in the epidermal growth factor

gene is associated with birthweight in Sinhalese and white Western Europeans. Mol Hum Reprod 2007; 13:425-429.